

Spatiotemporal Analysis of Streamflow Drought in the Mediterranean

Flowing through dry times: Understanding
streamflow droughts in the Mediterranean

Master Thesis: Environmental Engineering
Thomas Poort

Spatiotemporal Analysis of Streamflow Drought in the Mediterranean

Flowing through dry times: Understanding
streamflow droughts in the Mediterranean

by

Thomas Poort

<u>Student Name</u>	<u>Student Number</u>
---------------------	-----------------------

Thomas Poort	4715500
--------------	---------

to obtain the degree of Master of Science

at the Delft University of Technology,

to be defended publicly on (Monday November 4, 2024 at 11:00 AM).

Main supervisor:	Dr. M. Hrachowitz
Secondary supervisor:	Dr.ir. A.M. Droste
Project Duration:	March, 2024 - November, 2024
Faculty:	Faculty of Civil Engineering and Geosciences, Delft

Abstract

Driven by global temperature increase and changing precipitation patterns, the intensifying hydrological cycle is expected to introduce more frequent and severe streamflow droughts. These changes will have a profound impact on agriculture, ecosystems and water management. This study analysed the spatial and temporal changes in streamflow droughts across 386 Mediterranean river basin from 1970 to 2019, focusing on their drought characteristics: duration, severity, intensity, maximum deficit, inter-arrival time, recovery rate and decline rate. The river basins were categorized into seven climatic regimes, and each was analysed for changes in these drought characteristics. Streamflow droughts were quantified using the Threshold Level Method, defining drought events as periods in which daily streamflow is below a set threshold. To identify patterns, trends were assessed across four fixed time periods, along with multi-temporal analyses for both annual and seasonal changes. The analysis showed that annual streamflow droughts, although becoming longer, are getting slightly less severe and intense across the majority of river basins. However, distinct seasonal and regional variations were found. Between 1988 and 2019, winter and spring streamflow droughts experienced a decrease in duration and severity (up to -30% for winter) across the entire study area. On the other hand, regional differences were observed for summer and fall. During this same time period, summer and fall streamflow droughts in the Pyrenees, Southern France, Italy and Croatia have become much longer, more severe and more intense (20-40% for summer), whereas Central and Southern Spain experienced decreasing duration and drought deficit volumes. The implications of increasing streamflow drought conditions on the water availability in Mediterranean river basins is severe, which highlights the need for better understanding and water management of streamflow droughts.

Contents

Abstract	i
List of Figures	iv
List of Tables	x
1 Introduction	1
1.1 Climate change in the Mediterranean	1
1.2 Streamflow drought in the Mediterranean	2
1.3 Problem Statement	5
1.4 Research Question	6
2 Methodology	7
2.1 Data	7
2.2 Study area	8
2.2.1 Climate classification	9
2.3 Streamflow drought quantification	13
2.3.1 Drought characteristics	15
2.4 Trend analysis	16
2.5 Multi-temporal analysis	18
3 Results	20
3.1 Trend analysis: Fixed time periods	20
3.1.1 Main observations	34
3.2 Multi-Temporal Analysis	34
3.2.1 Annual Trends	35
3.2.2 Winter Trends	38
3.2.3 Summer Trends	43
3.2.4 Spring & Fall Trends	53
3.2.5 Summary	53
4 Discussion	54
4.1 Fixed vs. Multi-temporal trend analysis	54
4.2 Spatiotemporal changes in streamflow drought characteristics	54
4.3 Relationship between streamflow drought characteristics	56
4.4 Implications & Significance	57
4.5 Limitations & Uncertainties	58
5 Conclusion	61
Bibliography	66
A Spring & Fall trends	67
A.1 Spring	67
A.2 Fall	71

B Additional Figures	75
B.1 Trend Analysis	76
B.2 Multi-Temporal Analysis	77
B.2.1 Annual Trends	77
B.2.2 Annual-interval trends	85
C Additional Tables	88

List of Figures

1.1	Scheme of drought categories and their relationship (Van Loon, 2015)	2
1.2	Propagation of meteorological drought to streamflow drought (a) and the change in streamflow across the Mediterranean (b).	3
1.3	Streamflow droughts in Mediterranean river basins	4
2.1	Study area including the elevation profile, the 386 selected river basins and their corresponding gauging stations.	8
2.2	The river basins and gauging stations corresponding to the four different study periods, including the number of basins for each study period.	9
2.3	Conceptual description of the climate classification according to the framework devised by Berghuijs and Woods (2016)	10
2.4	Climatic indices for each individual river basins (part 1).	10
2.4	Climatic indices for each selected river basins (part 2).	11
2.5	Climate classification applied to study area, classes are notated based on the values of the five indices using the notation: $(\bar{P}, \bar{T}, \delta_P, \Delta T, s_d)$	12
2.6	Derivation of monthly threshold from monthly flow duration curves (Van Loon, 2013)	14
2.7	Example: streamflow drought quantification based on smoothed monthly threshold, including the pooling of drought events and the exclusion of minor droughts	15
2.8	Overview of the determined streamflow drought characteristics.	16
2.9	Example of the change in TSA trends in streamflow drought duration over four time periods: 1970-2019 (blue), 1980-2019 (orange), 1990-2019 (green), 2000-2019 (red).	17
2.10	(a) Julian Dates for starting time of most severe droughts, divided into four seasons; (b) Polar plot of starting time of most severe droughts, divided into four seasons, and indicating the meaning of positive and negative trends.	18
2.11	(a) Example of Multi-temporal analysis illustrated in a heatmap showing the median trend magnitude across all combinations of time periods; the x-axis represents the starting year and the y-axis represents the end year of the time period, (b) trends corresponding to the four highlighted grid cells in the green ellipse in the upper row of the heatmap, (c) trends corresponding to the four highlighted grid cells in the violet ellipse on the diagonal of the heatmap.	19
3.1	Trend results for four fixed time periods for drought duration. The heatmaps on the left side show the spatial distribution of the trends across the study area. Red shapes indicate an increasing trend and blue shapes indicate a decreasing trend. The boxplots on the right side display the distribution of trends for each specific region.	21
3.2	Trend results for four fixed time periods for drought severity. The heatmaps on the left side show the spatial distribution of the trends across the study area. Red shapes indicate an increasing trend and blue shapes indicate a decreasing trend. The boxplots on the right side display the distribution of trends for each specific region.	23
3.3	Trend results for four fixed time periods for drought intensity. The heatmaps on the left side show the spatial distribution of the trends across the study area. Red shapes indicate an increasing trend and blue shapes indicate a decreasing trend. The boxplots on the right side display the distribution of trends for each specific region.	25

3.4	Trend results for four fixed time periods for maximum drought deficit. The heatmaps on the left side show the spatial distribution of the trends across the study area. Red shapes indicate an increasing trend and blue shapes indicate a decreasing trend. The boxplots on the right side display the distribution of trends for each specific region.	27
3.5	Trend results for four fixed time periods for drought inter-arrival time. The heatmaps on the left side show the spatial distribution of the trends across the study area. Red shapes indicate an increasing trend and blue shapes indicate a decreasing trend. The boxplots on the right side display the distribution of trends for each specific region.	29
3.6	Trend results for drought recovery rate. The heatmaps on the left side show the spatial distribution of the trends across the study area. Red shapes indicate an increasing trend and blue shapes indicate a decreasing trend. The boxplots on the right side display the distribution of trends for each specific region.	31
3.7	Trend results for drought decline rate. The heatmaps on the left side show the spatial distribution of the trends across the study area. Red shapes indicate an increasing trend and blue shapes indicate a decreasing trend. The boxplots on the right side display the distribution of trends for each specific region.	33
3.8	Multi-temporal analysis of annual median trends for each drought characteristic, expressed as a percentage, across all river basins. The heatmap illustrates the magnitude of trends for all combinations of time periods between 1970-2019, with the x-axis representing the start year and the y-axis representing the end year of each time period. Red indicates increasing trends, while blue represents decreasing trends.	35
3.9	Multi-temporal analysis of annual median trends for drought duration and severity, expressed as a percentage, across river basins of class 4. The heatmap illustrates the magnitude of trends for all combinations of time periods between 1970-2019, with the x-axis representing the start year and the y-axis representing the end year of each time period. Red indicates increasing trends, while blue represents decreasing trends.	37
3.10	Multi-temporal analysis of winter median trends for each drought characteristic, expressed as a percentage, across all river basins. The heatmap illustrates the magnitude of trends for all combinations of time periods between 1970-2019, with the x-axis representing the start year and the y-axis representing the end year of each time period. Red indicates increasing trends, while blue represents decreasing trends.	38
3.11	Multi-temporal analysis of median trends in winter drought timing, expressed in day/year, across all river basins. The heatmap illustrates the magnitude of trends for all combinations of time periods between 1970-2019, with the x-axis representing the start year and the y-axis representing the end year of each time period. Red indicates droughts occurring later in the season, while blue represents droughts occurring earlier in the season.	39
3.12	Multi-temporal analysis of median trends, expressed as percentage, in winter drought characteristics for river basins of class 4 (location shown in bottom right corner). The heatmap illustrates the magnitude of trends for all combinations of time periods between 1970-2019, with the x-axis representing the start year and the y-axis representing the end year of each time period. Red indicates increasing trends, while blue represents decreasing trends.	40
3.13	Multi-temporal analysis of median trends, expressed as percentage, in winter drought characteristics for river basins of class 6 (location shown in bottom right corner). The heatmap illustrates the magnitude of trends for all combinations of time periods between 1970-2019, with the x-axis representing the start year and the y-axis representing the end year of each time period. Red indicates increasing trends, while blue represents decreasing trends.	42

- 3.14 Multi-temporal analysis of summer median trends for each drought characteristic, expressed as a percentage, across all river basins. The heatmap illustrates the magnitude of trends for all combinations of time periods between 1970-2019, with the x-axis representing the start year and the y-axis representing the end year of each time period. Red indicates increasing trends, while blue represents decreasing trends. 44
- 3.15 Multi-temporal analysis of median trends in summer drought timing, expressed in day/year, across all river basins. The heatmap illustrates the magnitude of trends for all combinations of time periods between 1970-2019, with the x-axis representing the start year and the y-axis representing the end year of each time period. Red indicates droughts occurring later in the season, while blue represents droughts occurring earlier in the season. 45
- 3.16 Multi-temporal analysis of median trends, expressed as percentage, in summer drought characteristics (duration, severity, intensity, and maximum deficit) for river basins of class 1 (location shown in bottom right corner). The heatmap illustrates the magnitude of trends for all combinations of time periods between 1970-2019, with the x-axis representing the start year and the y-axis representing the end year of each time period. Red indicates increasing trends, while blue represents decreasing trends. 45
- 3.17 Multi-temporal analysis of median trends, expressed as percentage, in summer drought characteristics (duration, severity, intensity, and maximum deficit) for river basins of class 2 (location shown in bottom right corner). The heatmap illustrates the magnitude of trends for all combinations of time periods between 1970-2019, with the x-axis representing the start year and the y-axis representing the end year of each time period. Red indicates increasing trends, while blue represents decreasing trends. 46
- 3.18 Multi-temporal analysis of median trends, expressed as percentage, in summer drought characteristics (duration, severity, intensity, and maximum deficit) for river basins of class 4 (location shown in bottom right corner). The heatmap illustrates the magnitude of trends for all combinations of time periods between 1970-2019, with the x-axis representing the start year and the y-axis representing the end year of each time period. Red indicates increasing trends, while blue represents decreasing trends. 48
- 3.19 Multi-temporal analysis of median trends, expressed as percentage, in summer drought characteristics for river basins of class 7 (location shown in bottom right corner). The heatmap illustrates the magnitude of trends for all combinations of time periods between 1970-2019, with the x-axis representing the start year and the y-axis representing the end year of each time period. Red indicates increasing trends, while blue represents decreasing trends. 49
- 3.20 Multi-temporal analysis of median trends, expressed as percentage, in summer drought characteristics for river basins of class 3 (location shown in bottom right corner). The heatmap illustrates the magnitude of trends for all combinations of time periods between 1970-2019, with the x-axis representing the start year and the y-axis representing the end year of each time period. Red indicates increasing trends, while blue represents decreasing trends. 50
- 3.21 Multi-temporal analysis of median trends, expressed as percentage, in summer drought characteristics for river basins of class 5 (location shown in bottom right corner). The heatmap illustrates the magnitude of trends for all combinations of time periods between 1970-2019, with the x-axis representing the start year and the y-axis representing the end year of each time period. Red indicates increasing trends, while blue represents decreasing trends. 52

A.1	Multi-temporal analysis of spring median trends for each drought characteristic, expressed as a percentage, across all river basins. The heatmap illustrates the magnitude of trends for all combinations of time periods between 1970-2019, with the x-axis representing the start year and the y-axis representing the end year of each time period. Red indicates increasing trends, while blue represents decreasing trends.	68
A.2	Multi-temporal analysis of median trends in spring drought timing, expressed in day/year, across all river basins. The heatmap illustrates the magnitude of trends for all combinations of time periods between 1970-2019, with the x-axis representing the start year and the y-axis representing the end year of each time period. Red indicates increasing trends, while blue represents decreasing trends.	69
A.3	Multi-temporal analysis of median trends, expressed as percentage, in spring drought characteristics for river basins of class 2. The heatmap illustrates the magnitude of trends for all combinations of time periods between 1970-2019, with the x-axis representing the start year and the y-axis representing the end year of each time period. Red indicates increasing trends, while blue represents decreasing trends.	70
A.4	Multi-temporal analysis of fall median trends for each drought characteristic, expressed as a percentage, across all river basins. The heatmap illustrates the magnitude of trends for all combinations of time periods between 1970-2019, with the x-axis representing the start year and the y-axis representing the end year of each time period. Red indicates increasing trends, while blue represents decreasing trends.	71
A.5	Multi-temporal analysis of median trends in fall drought timing, expressed in day/year, across all river basins. The heatmap illustrates the magnitude of trends for all combinations of time periods between 1970-2019, with the x-axis representing the start year and the y-axis representing the end year of each time period. Red indicates droughts occurring later in the season, while blue represents droughts occurring earlier in the season.	72
A.6	Multi-temporal analysis of median trends, expressed as percentage, in fall drought characteristics (duration, severity, intensity and maximum deficit) for river basins of class 3. The heatmap illustrates the magnitude of trends for all combinations of time periods between 1970-2019, with the x-axis representing the start year and the y-axis representing the end year of each time period. Red indicates increasing trends, while blue represents decreasing trends.	73
A.7	Multi-temporal analysis of median trends, expressed as percentage, in fall drought characteristics (duration, severity, intensity and maximum deficit) for river basins of class 5. The heatmap illustrates the magnitude of trends for all combinations of time periods between 1970-2019, with the x-axis representing the start year and the y-axis representing the end year of each time period. Red indicates increasing trends, while blue represents decreasing trends.	74
B.1	Trend results for the basins with data in period 1. These were used as validation of the overall trends in the entire study area.	76
B.2	Multi-temporal analysis of median trends, expressed as percentage, in annual drought characteristics for river basins of period 1 (1970-2019). The heatmap illustrates the magnitude of trends for all combinations of time periods between 1970-2019, with the x-axis representing the start year and the y-axis representing the end year of each time period. Warmer colors indicate increasing trends, while cooler colors represent decreasing trends.	77

- B.3 Multi-temporal analysis of median trends, expressed as percentage, in annual drought characteristics for river basins of class 1. The heatmap illustrates the magnitude of trends for all combinations of time periods between 1970-2019, with the x-axis representing the start year and the y-axis representing the end year of each time period. Warmer colors indicate increasing trends, while cooler colors represent decreasing trends. 78
- B.4 Multi-temporal analysis of median trends, expressed as percentage, in annual drought characteristics for river basins of class 2. The heatmap illustrates the magnitude of trends for all combinations of time periods between 1970-2019, with the x-axis representing the start year and the y-axis representing the end year of each time period. Warmer colors indicate increasing trends, while cooler colors represent decreasing trends. 79
- B.5 Multi-temporal analysis of median trends, expressed as percentage, in annual drought characteristics for river basins of class 3. The heatmap illustrates the magnitude of trends for all combinations of time periods between 1970-2019, with the x-axis representing the start year and the y-axis representing the end year of each time period. Warmer colors indicate increasing trends, while cooler colors represent decreasing trends. 80
- B.6 Multi-temporal analysis of median trends, expressed as percentage, in annual drought characteristics for river basins of class 4. The heatmap illustrates the magnitude of trends for all combinations of time periods between 1970-2019, with the x-axis representing the start year and the y-axis representing the end year of each time period. Warmer colors indicate increasing trends, while cooler colors represent decreasing trends. 81
- B.7 Multi-temporal analysis of median trends, expressed as percentage, in annual drought characteristics for river basins of class 5. The heatmap illustrates the magnitude of trends for all combinations of time periods between 1970-2019, with the x-axis representing the start year and the y-axis representing the end year of each time period. Warmer colors indicate increasing trends, while cooler colors represent decreasing trends. 82
- B.8 Multi-temporal analysis of median trends, expressed as percentage, in annual drought characteristics for river basins of class 6. The heatmap illustrates the magnitude of trends for all combinations of time periods between 1970-2019, with the x-axis representing the start year and the y-axis representing the end year of each time period. Warmer colors indicate increasing trends, while cooler colors represent decreasing trends. 83
- B.9 Multi-temporal analysis of median trends, expressed as percentage, in annual drought characteristics for river basins of class 7. The heatmap illustrates the magnitude of trends for all combinations of time periods between 1970-2019, with the x-axis representing the start year and the y-axis representing the end year of each time period. Warmer colors indicate increasing trends, while cooler colors represent decreasing trends. 84
- B.10 Multi-temporal analysis of median trends, expressed as percentage, in mean annual drought characteristics for all river basins. The heatmap illustrates the magnitude of trends for all combinations of time periods between 1970-2019, with the x-axis representing the start year and the y-axis representing the end year of each time period. Warmer colors indicate increasing trends, while cooler colors represent decreasing trends. 85
- B.11 Multi-temporal analysis of median trends, expressed as percentage, in mean annual drought characteristics for all river basins, including years with no drought events as a value of zero. The heatmap illustrates the magnitude of trends for all combinations of time periods between 1970-2019, with the x-axis representing the start year and the y-axis representing the end year of each time period. Warmer colors indicate increasing trends, while cooler colors represent decreasing trends. 85

B.12 Multi-temporal analysis of median trends, expressed as percentage, in mean annual drought characteristics for river basins of class 3, including years with no drought events as a value of zero. The heatmap illustrates the magnitude of trends for all combinations of time periods between 1970-2019, with the x-axis representing the start year and the y-axis representing the end year of each time period. Warmer colors indicate increasing trends, while cooler colors represent decreasing trends. 86

B.13 Multi-temporal analysis of median trends, expressed as percentage, in mean winter drought characteristics for all river basins. The heatmap illustrates the magnitude of trends for all combinations of time periods between 1970-2019, with the x-axis representing the start year and the y-axis representing the end year of each time period. Warmer colors indicate increasing trends, while cooler colors represent decreasing trends. 86

B.14 Multi-temporal analysis of median trends, expressed as percentage, in mean summer drought characteristics for all river basins. The heatmap illustrates the magnitude of trends for all combinations of time periods between 1970-2019, with the x-axis representing the start year and the y-axis representing the end year of each time period. Warmer colors indicate increasing trends, while cooler colors represent decreasing trends. 87

List of Tables

2.1	The seven climatic classes with: their climatic features, the number of river basins per climatic class and their location.	13
C.1	Number of river basins for each country in each study period	88
C.2	Climate classification boundaries based on Berghuijs and Woods (2016)'s framework. . .	88

1

Introduction

1.1. Climate change in the Mediterranean

The Mediterranean climate is characterized by a high variability in precipitation, seasonal rainfall patterns, intense rainfall events and droughts during summer (Merheb et al., 2016). Due to these characteristics of the climate in this region, the Mediterranean areas have always had an issue with water availability (Morán-Tejeda et al., 2010). However, due to the change in climate this issue has become even more worrying. Predictions from Milly et al. (2005) and IPCC (2014) show that due to climate change and the increasing water demands of economic and societal sectors the water availability will become even scarcer in the future.

The main causes of these circumstances are the changes in precipitation and temperature in the Mediterranean region over recent decades. It is important to understand these historical trends, as they provide insight into the evolution of climate change in the future. Studying past climate behaviour will lead to better anticipation of future climate patterns. Precipitation, a principal component of the hydrological cycle, is the main source of water for river systems and changes in the amount of precipitation or its variability can directly affect the water availability. For this reason many scientific articles have focused on determining the spatial and temporal evolution of precipitation (e.g. López-Moreno et al. (2009)), as well as predicting future climate scenarios (e.g. Giorgi (2006)). The consensus from most of this research is that the total annual precipitation in the Mediterranean is decreasing and that seasonal changes in precipitation patterns are significant. López-Moreno et al. (2009) assessed whether monthly precipitation in the Mediterranean basin had changed since 1950 and concluded that especially the spring and summer months experienced a decrease in precipitation whereas during the other months precipitation tends to increase. Similar results were found by Cramer et al. (2018) who predict that Southern Europe will experience a decrease in summer precipitation up to 30% by 2080 compared to the current average summer precipitation. As the water availability during summer always was a big issue for the Mediterranean, this shift in precipitation variability will lead to an even bigger mismatch between available water resources and the water demand.

Apart from the precipitation, temperature is another main impacting factor for the Mediterranean water resources. Compared to the global average temperature change, the temperature in the Mediterranean is increasing at a faster pace (Orlowsky and Seneviratne, 2012). According to Seneviratne et al. (2016), the daily maximum temperature in the Mediterranean basin is expected to increase between 2.2-3°C, compared to a global increase of 1.5-2°C. And this difference becomes even more noticeable in summer, as warming rates across the Mediterranean are expected to be 50% higher than the global increase in temperature (Vogel et al., 2021; Lionello and Scarascia, 2018).

1.2. Streamflow drought in the Mediterranean

Droughts are a natural phenomenon that cover several meteorological, biophysical and hydrological processes which can impact both the society as well as the economy (Tramblay et al., 2020; de Dios Gomez-Gomez et al., 2022). They are recurring global events with varying temporal and spatial characteristics depending on the region (Stahl et al., 2010) and tend to have a devastating impact on the affected area. An increase in either the duration, severity, intensity or timing of droughts can create negative consequences and complications for water management. Given the changes in the previously mentioned climatic drivers, many future climate projections indicate that there will be a potential decrease in precipitation accompanied by a temperature increase, which consequently may lead to more frequent and severe droughts in the future.

As droughts are complex, many definitions of this natural phenomenon exist. Tallaksen and van Lanen (2023); Sheffield et al. (2012) reviewed some of these definitions and the most used definition is a period of 'below-normal' water availability. However, the definition of normal conditions is not universal and also depends on what part of the hydrological cycle is being studied. There are different forms of droughts which can be classified into four categories depending on their position in the hydrological cycle (see Figure 1.1): meteorological, soil moisture, hydrological and socio-economic drought. A period of precipitation deficiency, at times combined with intensified potential evaporation, is often defined as a meteorological drought. Soil moisture droughts are due to a deficit in soil moisture. This reduces the amount of moisture supplied to vegetation and, as it causes crop failure, it is often called agricultural drought. A hydrological drought relates to the lack of water in a hydrological system, which can be observed by low discharge in rivers or low water levels in lakes, reservoirs and groundwater storage (Van Loon, 2015). Hydrological droughts which are defined as below-normal streamflow in a river system are often called streamflow droughts. The final form of drought is the socio-economic drought, which is a period of time during which the human water demand cannot be met.

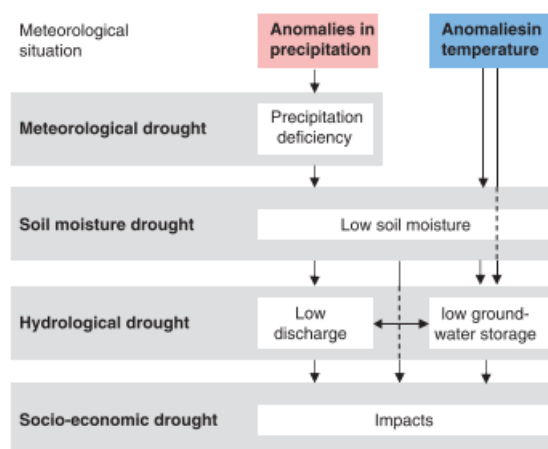


Figure 1.1: Scheme of drought categories and their relationship (Van Loon, 2015)

Streamflow droughts are the topic of this study due to their direct and profound impact on water availability. These types of drought are particularly critical in regions where water resources are already under pressure. Looking at the total impact streamflow droughts have on the surrounding environment and society, streamflow droughts can be seen as natural disasters with damage that is in the same order of magnitude as floods or earthquakes (Van Loon and Van Lanen, 2012). They have the ability to cover large areas and can persist for months or in some cases even years. Due to their large spatial extent and prolonged duration, streamflow droughts can result in severe consequences for the ecosystem and economic sectors, which all depend on the water levels in the river system to be sufficient. Economic

sectors that can be affected are agriculture (irrigation), drinking water availability, shipping, recreation and electricity production by hydropower. The impacts of drought on ecosystems can be seen through plant mortality and the disruption of aquatic ecosystems through reduced habitat connectivity, altered population density and lower food availability (Van Loon, 2015).

Streamflow droughts are driven particularly by the combined effects of reduced precipitation, increased evaporation and rising human water demand. The lack of precipitation is often associated with being the most significant factor in the onset of droughts. The streamflow present in a river system is directly affected by the presence of precipitation or absence of precipitation, with extended periods of insufficient precipitation causing reduced streamflow, which can ultimately propagate to a streamflow drought (Figure 1.2a) (Behrangi et al., 2016; Van Loon, 2013). Apart from the hydrological factors impacting the river streamflow, temperature is another critical impacting factor affecting streamflow. Temperature, along solar radiation, humidity and wind speed, is one of the drivers of potential evaporation, which leads to water leaving the river system. An increase in temperature elevates evaporation rates, depleting river water levels. Additionally, changes in temperature patterns highly affect snowmelt, which is a crucial source of water in many regions (Behrangi et al., 2016; Herrero et al., 2009). Higher temperatures can cause the snowmelt to occur earlier and faster, which leads to an altering of the timing and water volume entering a river system. The changes in these climatic drivers all contribute to a decrease in streamflow. Research on the changes in the streamflow was performed by Masseroni et al. (2021) who observed a decreasing trend in annual streamflow for the main Mediterranean river basins (Figure 1.2b). This reduction in streamflow in Mediterranean river basins is expected to lead to an increase in streamflow droughts.

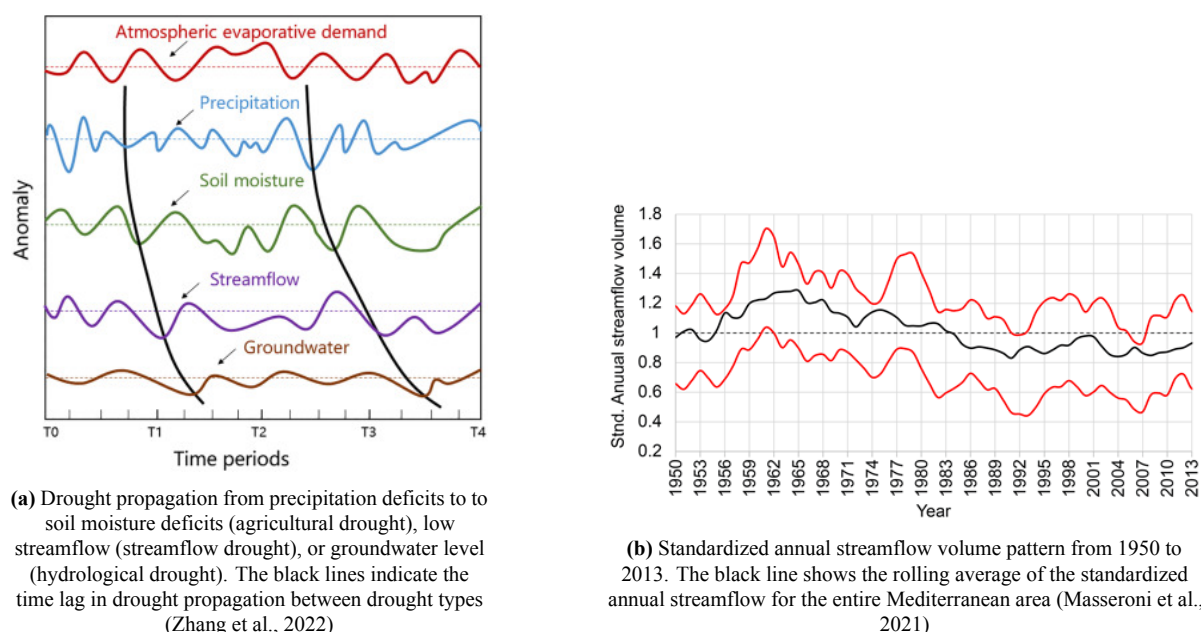


Figure 1.2: Propagation of meteorological drought to streamflow drought (a) and the change in streamflow across the Mediterranean (b).

The Mediterranean basin, consisting of 21 countries with a combined population of around 520 million, of which around 205 million live in the European part (UN, 2022), is particularly vulnerable to streamflow droughts. Due to its high population and the limited water availability, the Mediterranean is considered to be one of the regions with the highest socioeconomic risk due to droughts, which will likely worsen even more in the future (Tramblay et al., 2020). Many Mediterranean countries experienced drought in the last twenty years leading to many areas having a problem with water availability

(Merheb et al., 2016) and the area is therefore often described as one of the climate change hotspots of the twenty-first century (Lionello and Scarascia, 2018). In recent years, severe streamflow droughts have been increasingly affecting the region. For example, in 2022 there was an unprecedented situation in which the Po river in Italy was estimated to have a water level two meters lower than normal (Figure 1.3a). Similarly, just last February (2024), when the water levels in reservoirs across Catalonia, Spain had fallen below the emergency threshold after three years of drought (Raphaëlle, 2023) (Figure 1.3b) and a state of emergency was declared leading to limited water consumption for industry, agriculture and private use such as filling swimming pools (Gonzalez-Cebrian, 2024; Wilks, 2024).



(a) Streamflow drought in Po river 2022, Italy (Hughes, 2022)

(b) Rialp reservoir in Catalonia, June 2023 (Gonzalez-Cebrian, 2024)

Figure 1.3: Streamflow droughts in Mediterranean river basins

Overall, these observations about the changing climate in the Mediterranean region, with decreasing precipitation and increasing temperature patterns, and their impact on streamflow droughts highlights the importance of further research into this topic. It is therefore important to analyse how streamflow droughts have changed in recent decades. If a deeper understanding is obtained about the evolution of streamflow droughts, it can be used for future water management strategies to mitigate their negative effects.

1.3. Problem Statement

In the previous section, the negative effects of streamflow droughts on society, economy and the environment were described, and the importance of research into streamflow droughts in the Mediterranean was highlighted. Drought events are a slow developing event and often develop unnoticed, until the drought has developed to such extent that the consequences can be felt. Therefore, droughts are often called the creeping disaster and there is a growing concern regarding droughts across the world and in Europe especially the Mediterranean is worried about its progress (Van Loon, 2015).

Despite extensive research done on droughts in the Mediterranean, there are still aspects unknown about streamflow droughts in the Mediterranean and gaps in knowledge still exist. Multiple studies have analysed the change in either meteorological and/or streamflow drought on catchment scale in the Mediterranean but not on a large regional scale. Lorenzo-Lacruz et al. (2013) for example, assessed the impact of meteorological droughts on streamflow droughts in the Iberian Peninsula. Or Altin and Altin (2021) who performed similar research for the eastern Mediterranean basin in Turkey analysing the response of hydrological drought to meteorological drought. However, Seneviratne et al. (2012) described that in general the development in space and time of streamflow droughts as a response to meteorological droughts needs to be studied more, and they include as well that such research needs to be extended on larger spatial scales. A similar challenge for future research was described by Merheb et al. (2016), who specifically mentioned that large-scale studies about streamflow droughts under Mediterranean conditions must be conducted more. Other studies focused on the whole Mediterranean but focused mostly on the change in meteorological droughts or set their sight on future climatic scenarios of precipitation and temperature distributions (Tramblay et al., 2020; Russo et al., 2019). However, the changes in streamflow droughts and how characteristics of these drought events are evolving, especially on larger scales for the Mediterranean, are still unknown.

As there is still a lot unknown about streamflow drought trends in the Mediterranean, further research is still required in the analysis of changes in streamflow droughts based on their drought characteristics. Changes in streamflow droughts can occur in different ways and can vary widely in spatial extent and temporal scales. A well-known method to determine these changes is by determining the drought characteristics corresponding to the drought events. Drought characteristics, such as the duration, severity and intensity, are used to systemically quantify drought events. Trend analyses can be performed on these drought characteristics to determine the change in drought events over time. However, despite the importance of such an analysis, large-scale studies focusing on the Mediterranean have not been done yet.

For that reason, this study determines how streamflow droughts have changed in space and time across the Mediterranean. To achieve this goal, changes in streamflow droughts are analysed by performing a trend analysis and a multi-temporal analysis based on streamflow drought characteristics to understand how they have evolved both spatially and temporally. In a time of increasing interest and urgency for climate change it is of utmost important to analyse these changes, resulting in a better understanding of streamflow drought projections and contributing to an improvement in the identification of droughts.

1.4. Research Question

As introduced previously, there is still a lot unknown about the changes in streamflow droughts in the Mediterranean. Therefore, the following main research question was devised:

How have streamflow droughts changed across Mediterranean river basins from 1970-2019?

To achieve an answer to this question, sub-goals have been formulated. These sub-goals align with the main set research question, and their combined results will enhance the ability to address the main research question comprehensively.

1. Quantify streamflow drought events in Mediterranean river basins.
2. Create a set of streamflow drought characteristics and quantify these characteristics.
3. Analyse trends and patterns in drought characteristics on temporal and spatial scale based on four fixed time periods.
4. Analyse trends and patterns in drought characteristics on temporal and spatial scale based on a multi-temporal analysis.

The results of the research question and its sub-goals will determine the way streamflow droughts have changed in the Mediterranean based on their drought characteristics, and this will be done by analysing these changes both on temporal and spatial scales.

2

Methodology

2.1. Data

The start of all data analysis research starts off with the data collection. The first sub-chapter outlines what the requirements were for the data during this research and defines the study area based on the data availability.

The most important type of data for this research was the streamflow/discharge data. This streamflow data was obtained from the newly created EStreams dataset (do Nascimento et al., 2024). The EStreams dataset provides, among other things, streamflow data for 17,130 catchments/gauging stations across 38 countries in the pan-European region, aggregated from over 50 different data providers. The dataset covers the time-period of 1900-2022 but the length of the time series varies for each catchment.

Based on this dataset, river basins were selected based on their location and the availability of data. The selected river basins were required to have a minimum of 30 years of daily mean streamflow data (m^3/s), which had to include data from 2019 to only include river basins with present data. Time series with more than 10% missing data in those 30 years were removed from the analysis in order to still maintain a representation of the streamflow in the river basin. For time series that fulfilled these conditions, the remaining missing data was replaced with the average daily streamflow for that specific date, calculated from all available data across the time series. Additionally, the river basins were required to be located in countries with a coastline on the Mediterranean Sea and to fall within the geographic boundaries defined by latitude 30° to $44^\circ N$ and longitude -10° to $40^\circ E$. For instance, only Southern France was included in the analysis. Intermittent streams (streams with flowing water in most times of the year, but during dry periods they may have no flowing water) were included in the selection, due to the fact that several river basins in the Mediterranean can be characterized as such and including them is therefore important to perform a comprehensive analysis (Galea et al., 2019). Of the selected basins based on these criteria, rivers with reservoirs located in their basins were still included in the research, as Mediterranean basins often have reservoirs along their course and removing them from the selected basins would leave very few basins. Only basins that were located directly downstream of a reservoir such that clear changes in streamflow patterns could be observed were excluded (around 3-4% loss). Additionally, shapefiles of river basin boundaries were provided by the EStreams dataset as well, which directly corresponded to river catchments upstream of each streamflow gauging station (do Nascimento et al., 2024).

Apart from the daily streamflow data, daily precipitation and temperature (air temperature near surface) datasets for the period between 1970-2019 were obtained from the E-OBS dataset provided by the European Climate Assessment & Dataset (Cornes et al., 2018). E-OBS is an ensemble dataset and

provides gridded data on both a 0.1 and 0.25 degree regular grid. For this research, the 0.1° grid (~11 km × 11 km) was used, and this data was aggregated to the corresponding selected river basins using the shapefiles from the EStreams dataset.

2.2. Study area

The selection criteria resulted in 386 catchments across five Mediterranean countries: Spain, France, Italy, Slovenia and Croatia (2.1). These countries provide a good spatial coverage of the western part of the Mediterranean. Unfortunately, streamflow data for countries more towards the eastern part of the Mediterranean and Northern Africa had very limited data and therefore did not fulfill the set requirements.

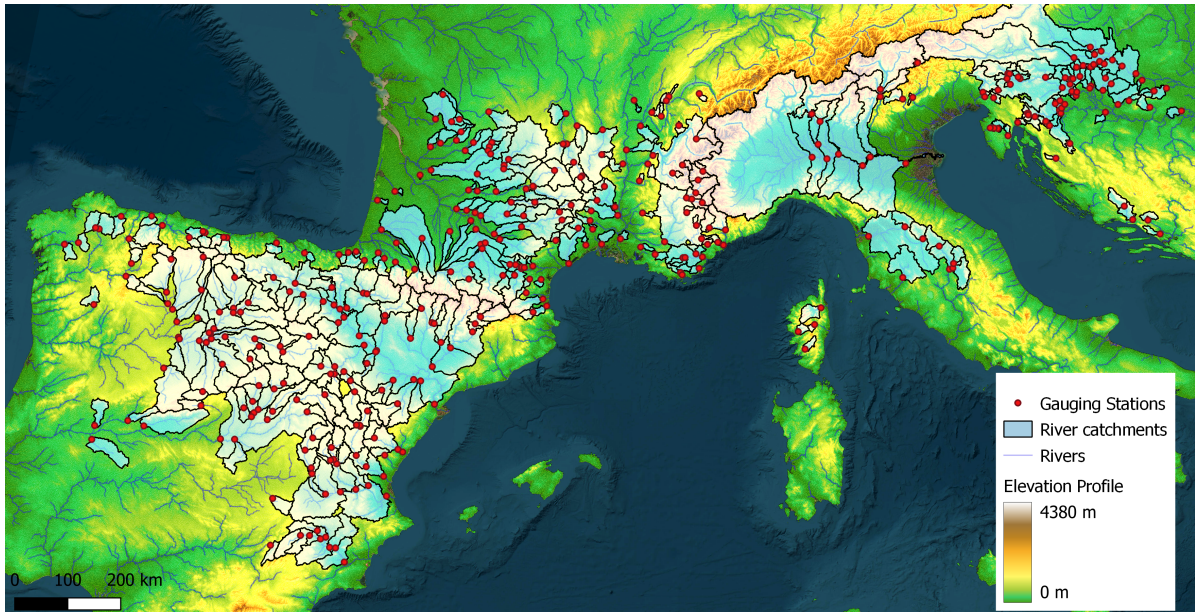


Figure 2.1: Study area including the elevation profile, the 386 selected river basins and their corresponding gauging stations.

The distribution of the 386 river basins is as follows: Spain (150), France (143), Croatia (56), Italy (22), and Slovenia (14). As most of these streamflow time series have different lengths the choice was made to create four different study areas depending on four time periods, which are used later in the trend analysis. On a decadal timescale four time periods were devised with a minimum temporal scale of 20 years. The time periods all end in 2019, as this is the most recent year with available data across the river basins, making it the most suitable to assess changes relative to the most recent year. This resulted in four time periods with different spatial coverage depending on the time period (Figure 2.2):

- Period 1 (1970-2019)
- Period 2 (1980-2019)
- Period 3 (1990-2019)
- Period 4 (2000-2019)

For an overview of the amount of basins in each country for each time period, see C.1.

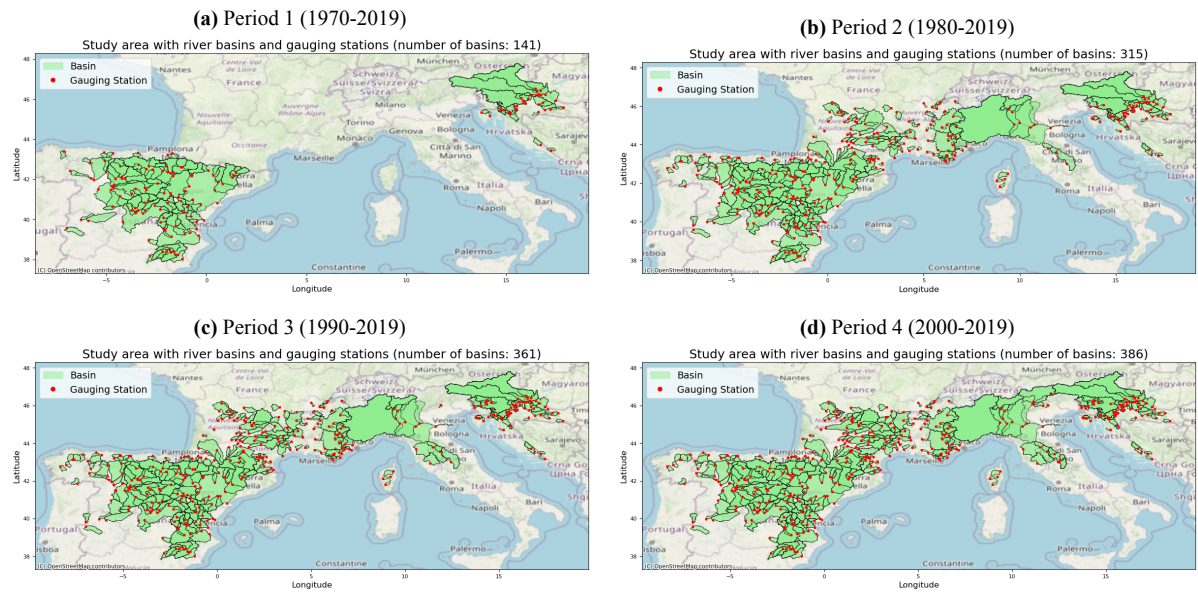


Figure 2.2: The river basins and gauging stations corresponding to the four different study periods, including the number of basins for each study period.

2.2.1. Climate classification

The selected river basins were classified based on their climatology. To do this the framework introduced by Berghuijs and Woods (2016) was used. This framework uses five indices to describe the monthly precipitation and temperature regimes in a simple way using a sinusoidal function (Figure 2.3).

These indices are:

- The mean annual precipitation rate (\bar{P})
- The mean annual temperature (\bar{T})
- The seasonal precipitation amplitude (δ_p): the difference in mean monthly precipitation between the months with the most and least precipitation
- The seasonal temperature amplitude (ΔT): the difference in mean monthly temperature between the hottest and coldest months
- The phase difference between the onset of the wet season and the hot season (s_d)

All these indices are derived from the precipitation and temperature data from the E-OBS dataset. An example of how the sinusoidal function describes climatic regimes using these indices is shown in Figure 2.3.

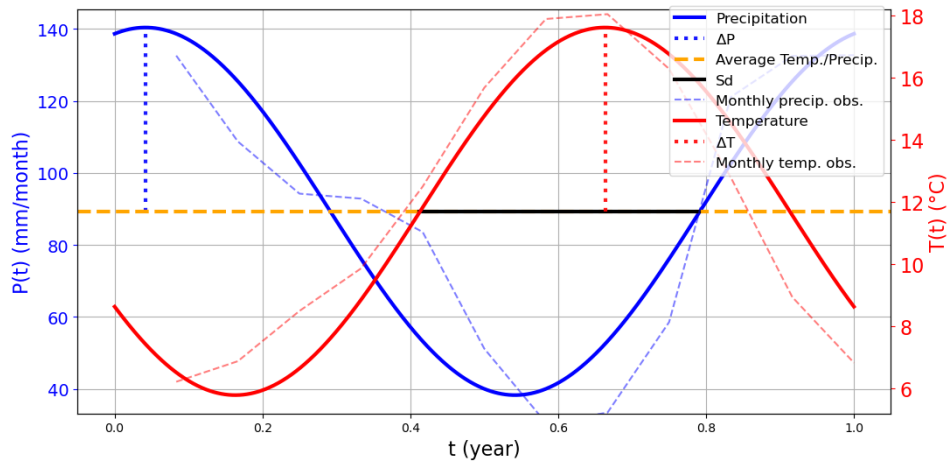
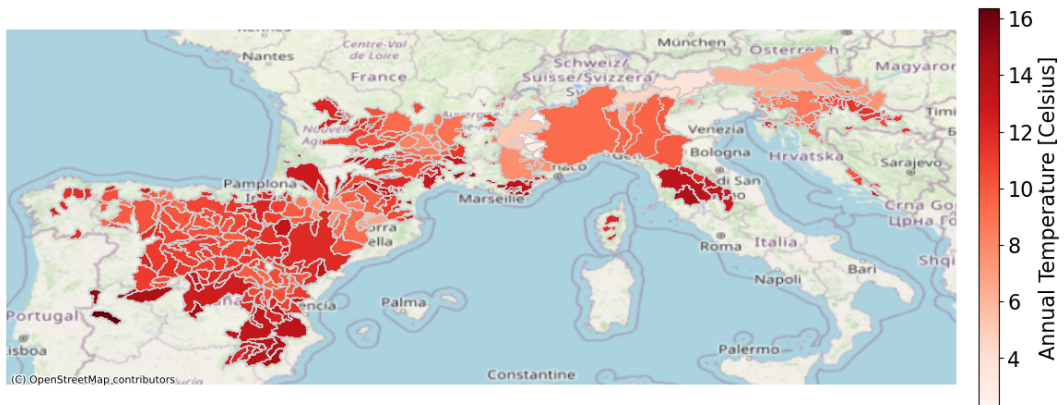


Figure 2.3: Conceptual description of the climate classification according to the framework devised by Berghuijs and Woods (2016)



(a) Annual precipitation

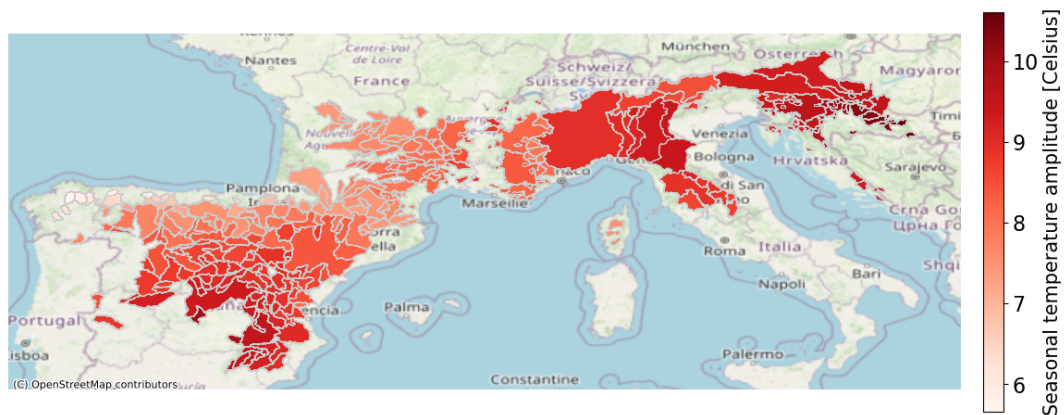


(b) Annual mean temperature (air temperature near surface)

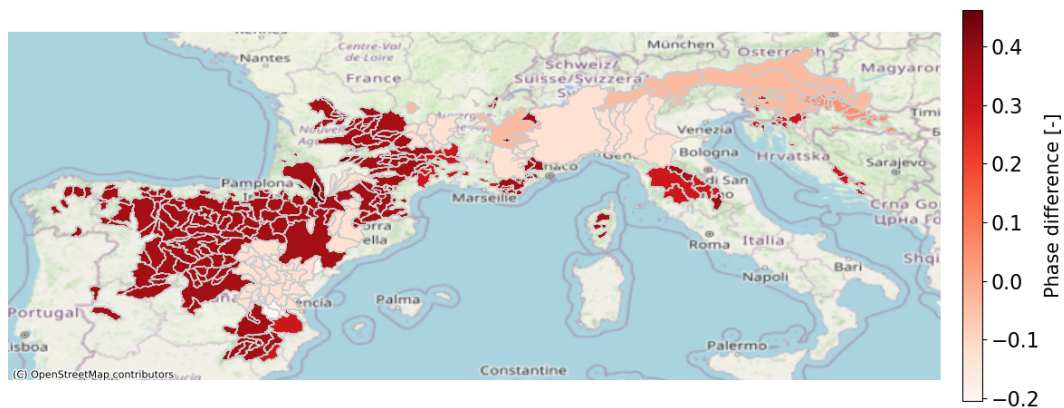
Figure 2.4: Climatic indices for each individual river basins (part 1).



(c) Seasonal difference in precipitation amplitudes



(d) Seasonal difference in temperature amplitudes



(e) Phase difference between precipitation and temperature regimes (the onset of the wet season and the hot season).

Figure 2.4: Climatic indices for each selected river basins (part 2).

Figure 2.4 shows the magnitude of the five indices for each river basin. Based on these magnitudes, the climatology of the river basins was assigned to a class based on class boundary conditions separating low (L), medium (M) and high (H) values, which were defined by Berghuijs and Woods (2016) (Appendix: Table C.2). Applying this framework to the selected river basins for this research resulted in seven different climate classes (Figure 2.5). An overview of the climatic classes with their climatic features, number of basins and their location can be seen in Table 2.1.

Class 1 (mainly Southern France and the Pyrenees) and class 2 (distributed across North-West Spain, Southern France and Tuscany in Italy) have similar climates consisting of high annual precipitation,

medium annual temperatures, a low seasonal difference in temperature and a high phase difference. The only difference is the difference in seasonal precipitation amplitude, which is higher for class 2.

Similarly, class 3, 5 and 7, spanning from the south of Spain to the Ebro basin below the Spanish Pyrenees, are classes that are classified by a medium annual precipitation, whereas the rest of the study area has a higher annual precipitation. The main difference between these three classes is that the seasonal precipitation and temperature amplitudes get higher towards the south.

The remaining two classes are mostly situated in Croatia and Slovenia. The main difference between these two climates and the rest of the study area is the higher seasonal temperature difference. Furthermore, class 4, which is more located in Slovenia and inland Croatia is the only climatic class that does not have a high phase difference between the onset of the wet and hot seasons.

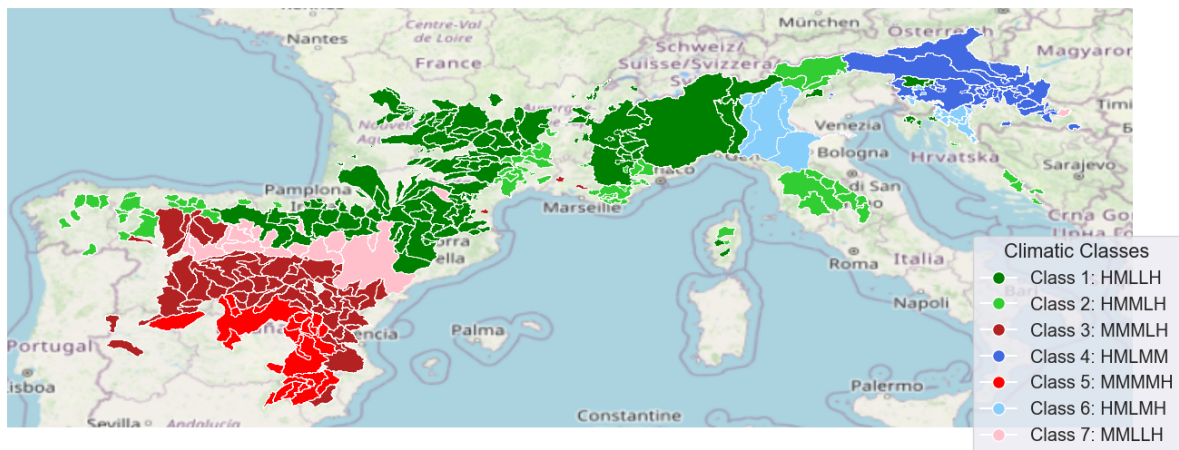


Figure 2.5: Climate classification applied to study area, classes are notated based on the values of the five indices using the notation: $(\bar{P}, \bar{T}, \delta_P, \Delta T, s_d)$

Class	Climatic Features	Amount of river basins	Region
1	High annual precipitation Medium annual temperature Low seasonal precipitation difference Low seasonal temperature difference High phase difference	139	Pyrenees Southern France
2	High annual precipitation Medium annual temperature Medium seasonal precipitation difference Low seasonal temperature difference High phase difference	72	North-West Spain Southern France Italy
3	Medium annual precipitation Medium annual temperature Medium seasonal precipitation difference Low seasonal temperature difference High phase difference	67	Central Spain: Tagus basin Jucar basin Duero basin
4	High annual precipitation Medium annual temperature Low seasonal precipitation difference Medium seasonal temperature difference Medium phase difference	44	Croatia Slovenia
5	Medium annual precipitation Medium annual temperature Medium seasonal precipitation difference Medium seasonal temperature difference High phase difference	26	Southern Spain: Segura basin Jucar basin Guadiana basin
6	High annual precipitation Medium annual temperature Low seasonal precipitation difference Medium seasonal temperature difference High phase difference	20	Croatia Italy: Po basin
7	Medium annual precipitation Medium annual temperature Low seasonal precipitation difference Low seasonal temperature difference High phase difference	18	Spain: Ebro basin

Table 2.1: The seven climatic classes with: their climatic features, the number of river basins per climatic class and their location.

2.3. Streamflow drought quantification

For each selected river basin, streamflow droughts were quantified using the threshold level method as outlined by Van Loon (2015). This method determines drought events when the variable of interest, which is streamflow in this case, falls below the predetermined threshold. A drought event starts when the streamflow is lower than the threshold level for the first time and the drought event ends once the streamflow exceeds the threshold again (Van Loon and Van Lanen, 2012; Brunner et al., 2022). This method was chosen as it provides a straightforward and intuitive way to identify when water levels drop below critical thresholds, triggering drought conditions. As drought characteristics are expressed in absolute values, direct changes in water deficit volume are presented, making it more useful for water

management practices. Furthermore, this method does not require the need to fit any distributions to the data (an approach often required by alternative drought quantification methods such as the Standardized Drought Indices). Fitting distributions could introduce new uncertainty and large discrepancies, whereas the threshold approach stays close to the original time series of the streamflow (Van Loon, 2013; Seneviratne et al., 2012; Vidal et al., 2010). Moreover, the clarity of this method simplifies the interpretation of results and comparison between other variables, making it a common choice in drought propagation research (Vidal et al., 2010; Tallaksen et al., 2009).

Selecting the threshold level which will be used is therefore a crucial part of the drought quantification. In this research a variable monthly threshold was used to account for seasonal patterns in the streamflow time series. This was chosen as it would represent drought events in each month equally, as for the management of droughts it is important to focus on all deviations compared to the normal streamflow patterns (Van Loon, 2013; Hannaford et al., 2011). The monthly threshold level is derived from the 80th percentile of the monthly streamflow duration curves, which were obtained by sorting the streamflow data from high to low for each month (Figure 2.6). This process resulted in a specific threshold level for each month and selected river basin. The chosen percentile used for determining the threshold does change the number of drought events and the magnitude of its drought characteristics. In most studies the percentiles used to determine the threshold range from the 70th - 95th percentile (Hisdal et al., 2001; Tallaksen et al., 2009). In this case for example, the 95th percentile would identify fewer but more extreme drought events, whereas on the contrary the 70th percentile would identify the opposite. However, according to Tate and Freeman (2000), the relationship between the drought characteristics is similar no matter the chosen percentile. Finally, by using a moving average of 30 days the determined monthly threshold values were smoothed in order to prevent a staircase pattern (Figure 2.6). This process helps in avoiding the sudden jumps in threshold values over time, which could lead to the calculation of inaccurate drought characteristics.

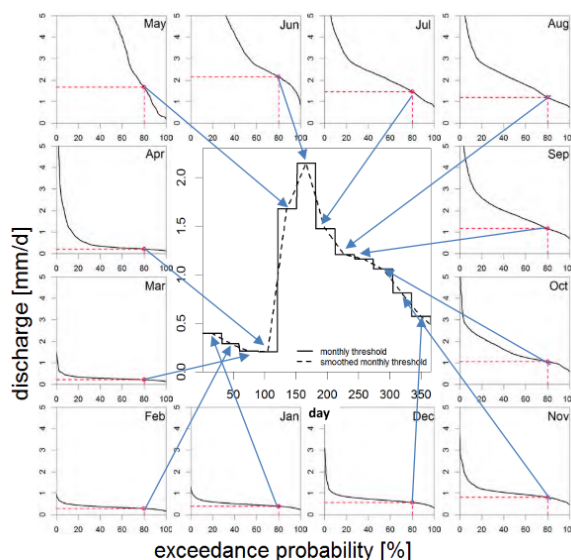


Figure 2.6: Derivation of monthly threshold from monthly flow duration curves (Van Loon, 2013)

After determining the smoothed monthly percentiles, still some actions are needed before determining the drought characteristics. This includes the pooling of dependent drought events and the removal of minor droughts. Mutual dependent drought events are identified drought events which occur in close succession after each other, but can be seen as the same drought event. For that reason it was chosen to use the inter-event time method, and grouping all drought events which occurred within a certain time period with each other. There has been a lot of research about what the order of the inter-event time

in streamflow should be (e.g. (Tallaksen et al., 1997; Fleig et al., 2006; Pandey et al., 2008)), however even now the inter-event time is still a very subjective parameter. Here, an inter-event time of 7 days was chosen, this way the amount of mutual dependent drought events was minimized, but also does not group too many drought events. Additionally, to exclude minor droughts, it was chosen to remove all drought events spanning less than 7 days and were therefore not included in the analysis. Figure 2.7 shows an example of two mutual dependent streamflow droughts and the elimination of some minor droughts.

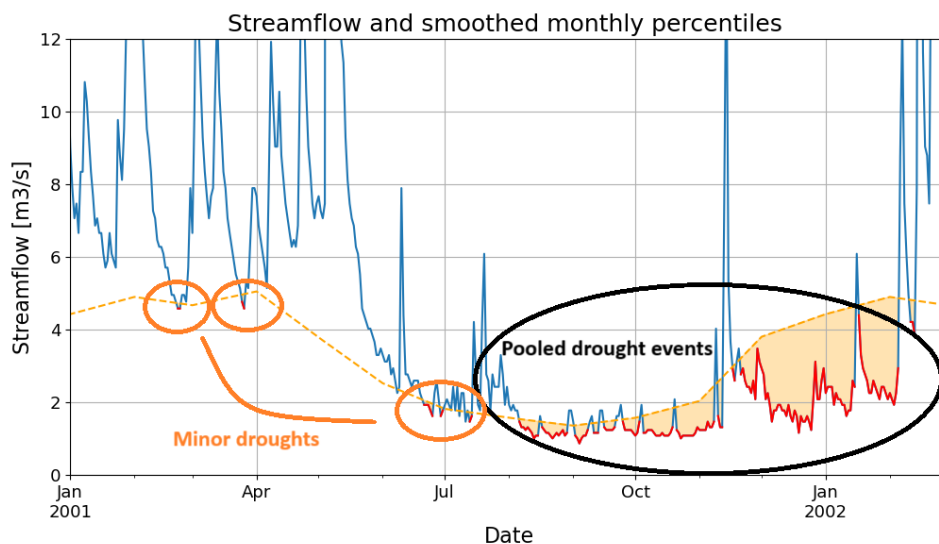


Figure 2.7: Example: streamflow drought quantification based on smoothed monthly threshold, including the pooling of drought events and the exclusion of minor droughts

2.3.1. Drought characteristics

To assess how streamflow droughts have changed across the Mediterranean, several drought characteristics were analysed. These characteristics include duration, severity, intensity, maximum deficit, inter-arrival time, recovery rate, decline rate, and the seasonal timing of droughts with maximum severity. Values for these characteristics were determined for each quantified streamflow drought events for all river basins.

- **Duration:** The number of days from the onset (the first day when streamflow falls below the threshold) to the end (the last day when streamflow exceeds the threshold) of a drought event.
- **Severity:** The total water deficit (m^3) during a streamflow drought, calculated by summing the differences between streamflow data and the threshold level over the drought duration.
- **Intensity:** The average deficit (m^3/d) over the duration of the streamflow drought event, calculated by dividing severity by duration.
- **Maximum Deficit:** The maximum difference (m^3) between the streamflow and the threshold level during the drought event.
- **Inter-Arrival Time:** The time (days) between the onset of consecutive drought events.
- **Recovery Rate:** The rate ($m^3 \cdot d^{-1}$) at which streamflow returns to non-drought conditions, calculated from the highest deficit to the threshold at the end of the drought event.
- **Decline Rate:** The rate of decline ($m^3 \cdot d^{-1}$) from the start of the drought to the highest deficit, calculated from the highest deficit to the threshold at the start of the drought event.

- **Seasonal Timing:** The timing of droughts with maximum severity, analysed by dividing the year into four seasons.

Figure 2.8 shows an illustration of a drought event with each drought characteristics that will be determined.

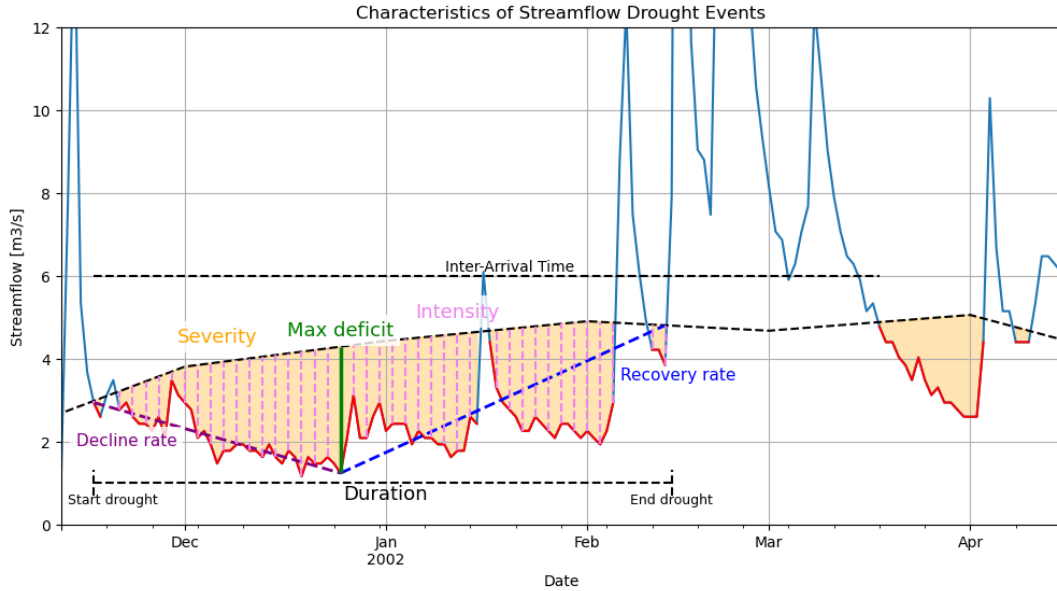


Figure 2.8: Overview of the determined streamflow drought characteristics.

2.4. Trend analysis

Based on the determined drought characteristics a trend analysis is performed for four different time periods, as mentioned before in Chapter 2.2. Basins were included in the time periods if the streamflow in both the starting and ending years of the period had data available. Trends are analysed for each individual river basin and climatic class.

For estimating the trend over time, the Theil-Sen average (TSA) was used. This non-parametric statistic is a robust way of fitting a line through a sample of data points by taking the median of all slopes between all pairs of points. As it takes the median of all slopes it is very robust against outliers in the data and is insensitive to missing data (Ohlson and Kim, 2015; Sen, 1968; Theil, 1992).

The Theil-Sen average is defined as:

Given a set of data points (x_i, y_i) for $i = 1, 2, \dots, n$

The Theil-Sen average for the slope β is the median of all the m_{ij} :

$$\beta = \text{median} \left(\left\{ \frac{y_j - y_i}{x_j - x_i} : 1 \leq i < j \leq n \right\} \right)$$

The result of the TSA is given in $[unit]/year$, where the unit corresponds to the unit of the respective drought characteristic. However, due to the fact that the river basins vary in size, the computed absolute trend magnitude can not be used to make a comparison between basins. To make a relative comparison between river basins possible, the trend magnitude of the TSA was transformed to the relative trend magnitude TSA_{rel} (%). This was done by multiplying the TSA slope (β) over the period of recorded

years n and expressed as a percentage of the long-term median drought characteristic μ (Stahl et al., 2012; Harrigan et al., 2018).

The formula for the Relative Theil-Sen Average (rTSA) is:

$$\text{rTSA} = \frac{\beta \times n}{\mu} \times 100\%$$

- β is the Theil-Sen Average (TSA).
- n is the number of years (period of recorded years).
- μ is the long-term median of the drought characteristic.

An example of a result of this trend analysis based on the four defined time periods can be seen in Figure 2.9, illustrating the transition between different trends. The time periods with the corresponding drought event data are highlighted and the trends are given in both TSA and relative TSA. This trend analysis is performed for each drought characteristic and for each river basin in order to get a full representation of the changes in the whole study area.

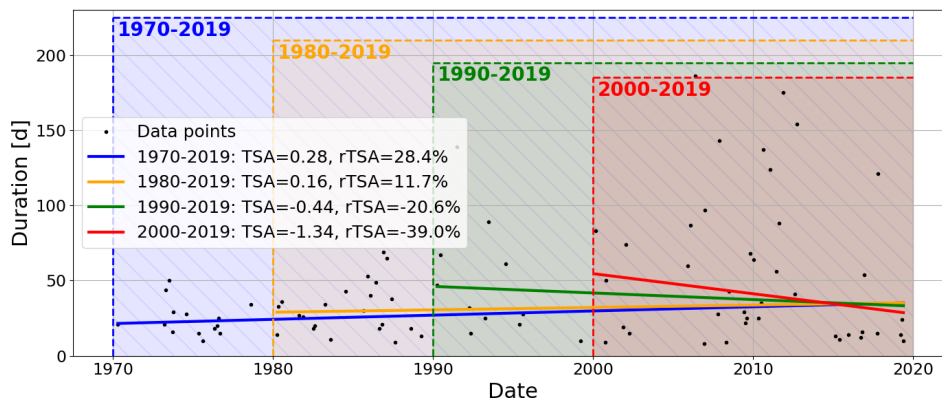


Figure 2.9: Example of the change in TSA trends in streamflow drought duration over four time periods: 1970-2019 (blue), 1980-2019 (orange), 1990-2019 (green), 2000-2019 (red).

One of the drought characteristics is the seasonal drought timing. The timing data was divided into four seasons: winter (Jan-Mar), spring (Apr-Jun), summer (Jul-Sep) and fall (Oct-Dec) (Figure 2.10). For each season the trend was calculated in the same way as before. As this characteristic is expressed in date format, the interpretation of the trend results is slightly different than the other characteristics. A decreasing trend in this case would represent a change of drought timing towards earlier in its respective season, whereas an increasing trend would mean later in the season.

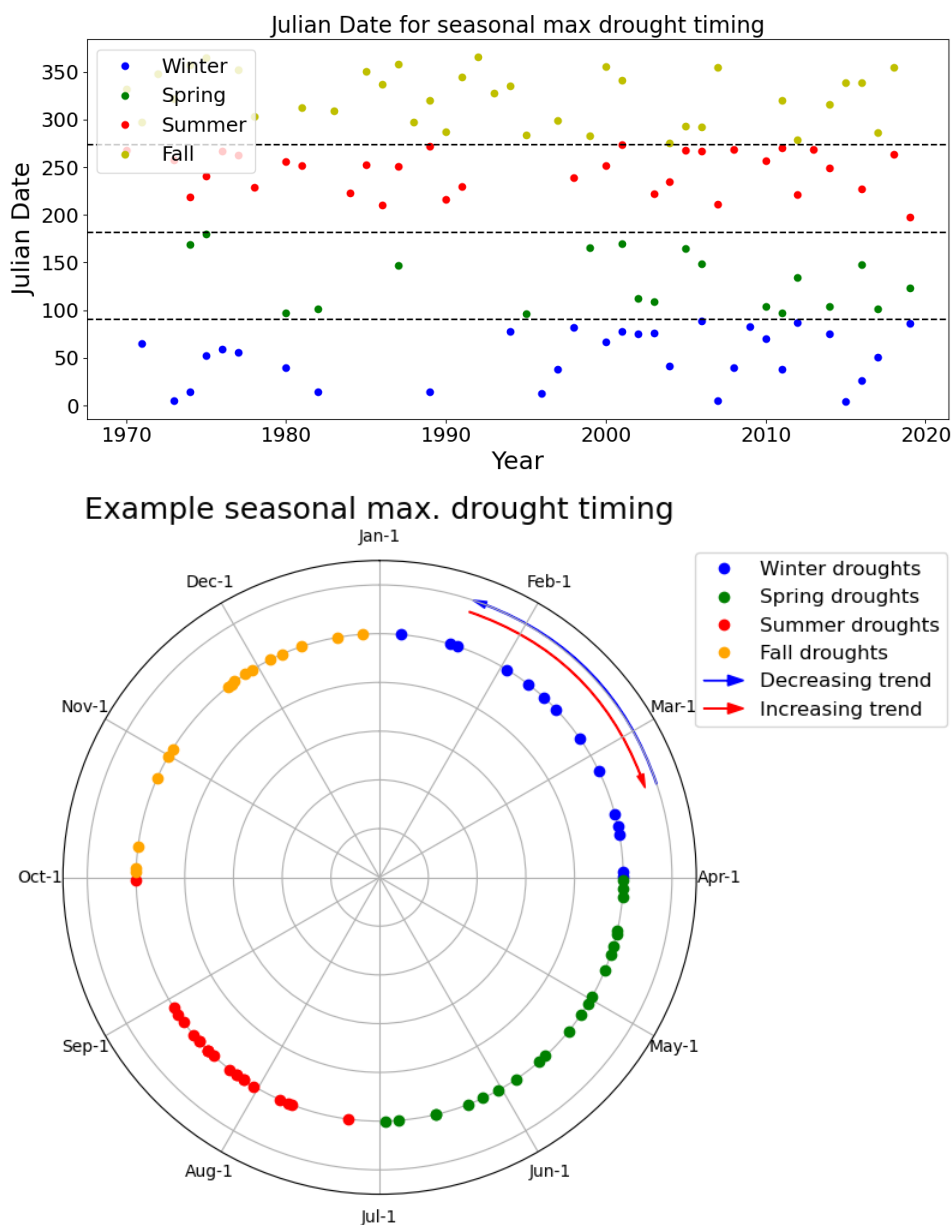


Figure 2.10: (a) Julian Dates for starting time of most severe droughts, divided into four seasons; (b) Polar plot of starting time of most severe droughts, divided into four seasons, and indicating the meaning of positive and negative trends.

2.5. Multi-temporal analysis

To determine the sensitivity of the chosen time periods and robustness of the results of the trend analysis, a multi-temporal analysis is performed. In a multi-temporal analysis all possible combinations of time periods within a longer time period are analysed. This way temporal patterns in drought characteristics can be determined more precisely compared to the previously used fixed time periods. Between 1970 and 2019, time periods for all possible start and end years with a minimum length of 20 years were selected. Instead of analysing only four time periods, the multi-temporal analysis resulted in an ensemble of 465 time periods in total. Similar to the previous trend analysis the trends over time were calculated using the TSA and rTSA. Multi-temporal analyses are performed for the entire study area and each climatic class, considering both annual and seasonal variations.

The results are shown as heatmaps, in which the x-axis corresponds to the start year and the y-axis to the end year of the study period (Figure 2.11a). Each individual grid cell coincides with a median trend for that specific time period, color-coded according to its trend magnitude. Figure 2.11b and 2.11c are examples of trend results for four different periods, which correspond to the highlighted grid cells in Figure 2.11a. The four highlighted grid cells in the green ellipse correspond to the trend lines shown in Figure 2.11b, while the four highlighted grid cells in the violet ellipse correspond to the trend lines shown in Figure 2.11c. The color used to highlight the grid cells in Figure 2.11a matches the color of the trend lines and associated time periods in the corresponding subplots.

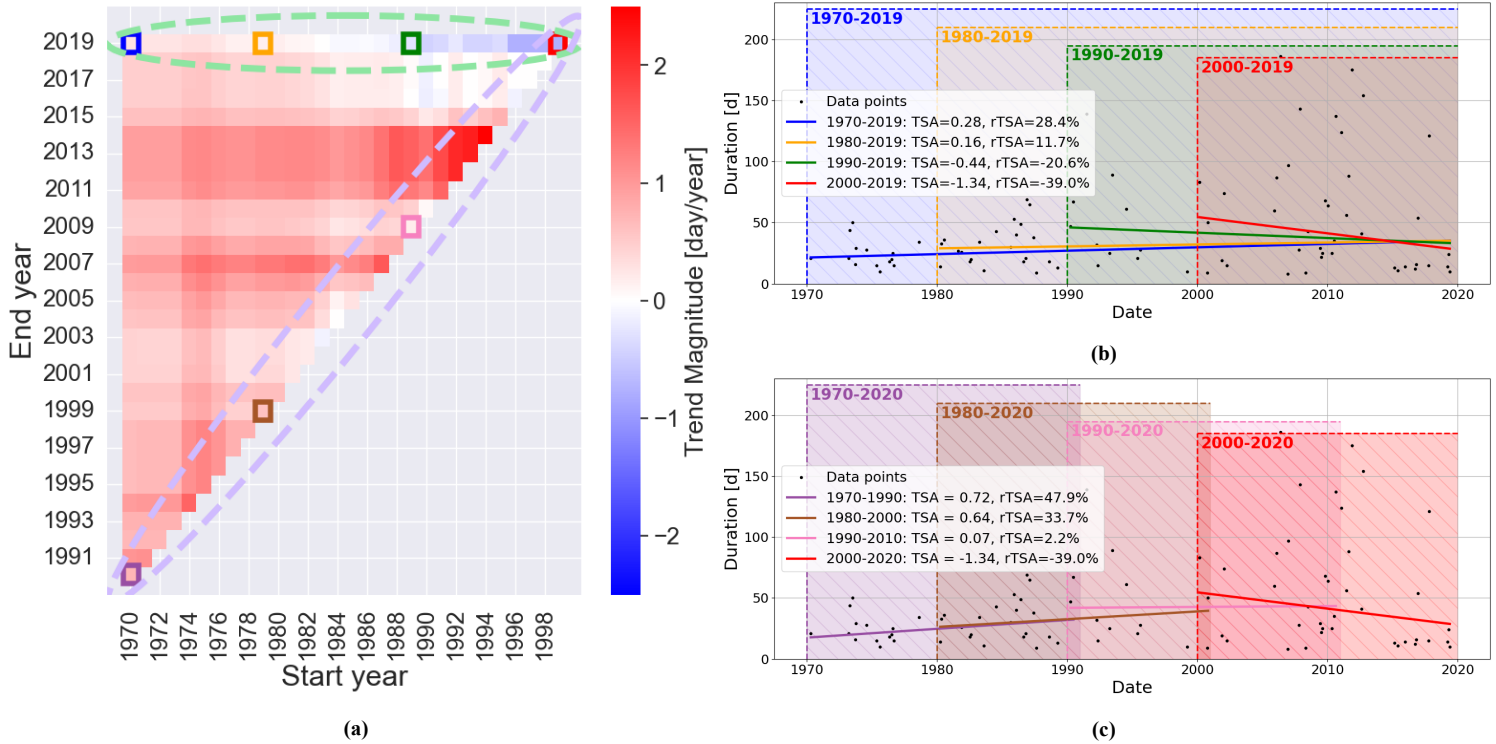


Figure 2.11: (a) Example of Multi-temporal analysis illustrated in a heatmap showing the median trend magnitude across all combinations of time periods; the x-axis represents the starting year and the y-axis represents the end year of the time period, (b) trends corresponding to the four highlighted grid cells in the green ellipse in the upper row of the heatmap, (c) trends corresponding to the four highlighted grid cells in the violet ellipse on the diagonal of the heatmap.

3

Results

3.1. Trend analysis: Fixed time periods

The trend analysis is performed for each of the nine distinct drought characteristics across four different fixed time periods. The selected river basins for each time period are illustrated in Figure 2.2. For each drought characteristic, the results of the trend analysis are illustrated using heatmaps. The objective of these heatmaps is to identify potential hotspots in drought characteristics across the study area. In these heatmaps all the river basins corresponding to the time period are included, with the colors given to the river basin representing the trend magnitude. In most cases the trend magnitude is expressed as a percentage (rTSA), only the seasonal timing is expressed in an absolute value for the rate (TSA). Trends indicating increasing drought characteristics are shown in red, whereas trends that indicate a decrease in drought characteristics are shown in blue.

Apart from the heatmaps, boxplots are provided to illustrate the distribution of trends across the entire study area as well as for each climate class. The range of each boxplot is defined by the maximum and minimum trend values excluding the outliers (defined by the whiskers of the boxplot).

To ensure that the observed changes in trends are not merely a result of the increased number of selected river basins, the same trend analysis was conducted only for basins that had data in the earliest time period for each country. This analysis was extended to all time periods and compared to the original boxplots. The results for this can be found in B.

Drought duration

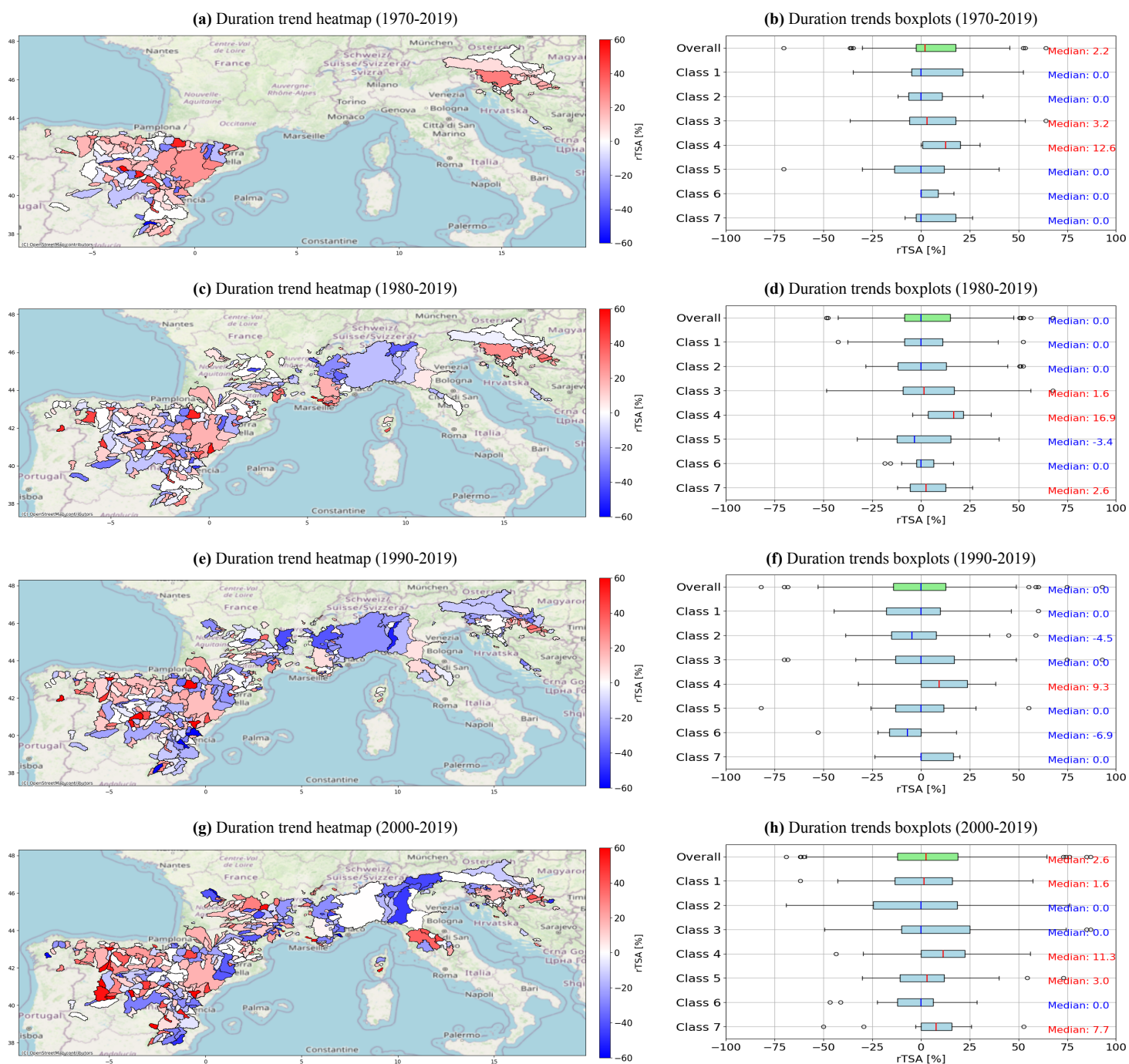


Figure 3.1: Trend results for four fixed time periods for drought duration. The heatmaps on the left side show the spatial distribution of the trends across the study area. Red shapes indicate an increasing trend and blue shapes indicate a decreasing trend. The boxplots on the right side display the distribution of trends for each specific region.

Figure 3.1 shows the results of the trend analysis for the drought duration, expressed in percentage. Here, red increasing trends indicate an increasing trend in drought duration (longer droughts), whereas blue decreasing trends represent a decreasing drought duration values (shorter droughts).

The first study period (1970-2019) shows a slight increase in drought duration. Of the 141 basins, 71

basins experience a positive trend, 37 basins experience a negative trend and 33 basins experience no clear change. The median trend for the entire ensemble of basins is 2.18%, with values ranging from -30.3% to 45.42%. The 25th percentile is equal to -2.6% and the 75th percentile is equal to 17.86%, indicating that overall the increasing trends are more extreme than the decreasing trends. Looking at the median trends of the climatic classes, classes 3 and 4 (Central Spain; Slovenia/Croatia) experience an increasing trend whereas all the other classes do not experience any change.

The second study period (1980-2019) shows a similar overall distribution of positive and negative trends across the entire study area, with 46.7% of the river basins experiencing an increase and 35% showing a decrease. The overall median resulted in being 0%, meaning the drought duration remained stable. Looking at the heatmap, it can be observed that river basins depending on water from the Alps (Po river basins in Italy, and the Rhone basins in Southern France), show a clear hotspot of decreasing trends. Main differences compared to the first study period is the decreasing trend of -3.4% observed in class 5 (Southern Spain) and the increasing trend of 2.6% in class 7 (Ebro basin).

The trends of the third study period (1990-2019) have an equal distribution between increasing (148) and decreasing trends (147), additionally it shows similar results to the second period for river basins in Spain, France and Italy. The main difference is the decreasing trend of -6.9% for class 6, which can be observed in heatmap by the decreasing hotspot in Slovenia and Croatia.

The last period (2000-2019) illustrates differences compared to the previous two study periods. Whereas in the third period the distribution between negative and positive trends was equal, here the distribution is positively favored with 51% basins showing an increase and 37.5% showing a decrease. This resulted in a median trend across the entire area of 2.63%, indicating a slight increase in drought duration. Additionally, the trends in the northern part of Spain have become positive which resulted in an increasing median trend of 7.7% for class 7.

Overall, the entire study area does not experience a clear trend across all time periods, with two periods showing an small increase and two periods showing no change. Based on these results no significant pattern can be observed in whether the duration of streamflow droughts duration is getting longer or remains mostly stable. The only hotspot showing clear changes are the river basins of class 4, situated in Croatia, which are experiencing a clear increase over all time periods. The other climatic classes do not show a clear trend towards either a decrease or increase.

Drought severity

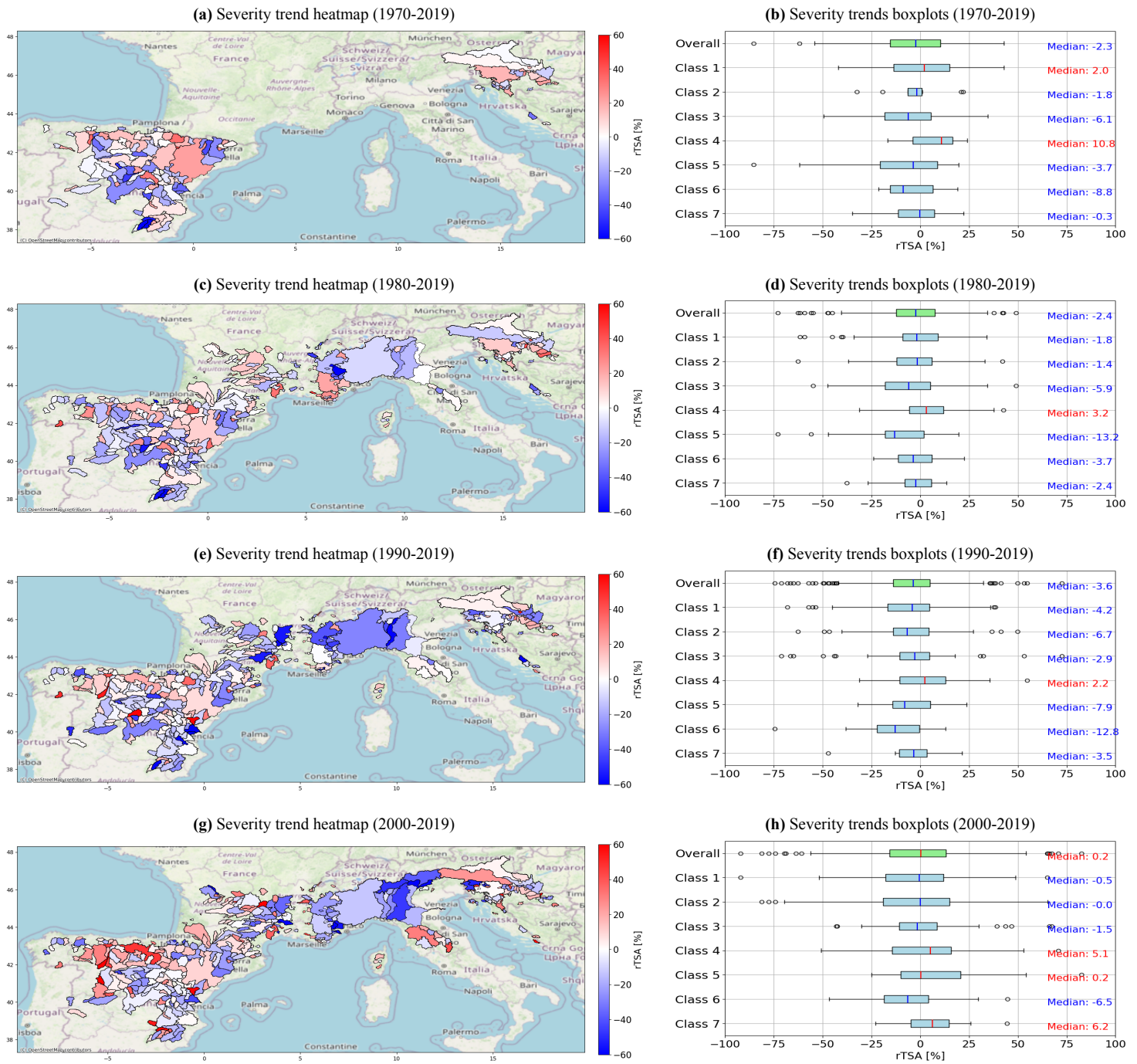


Figure 3.2: Trend results for four fixed time periods for drought severity. The heatmaps on the left side show the spatial distribution of the trends across the study area. Red shapes indicate an increasing trend and blue shapes indicate a decreasing trend. The boxplots on the right side display the distribution of trends for each specific region.

Figure 3.2 shows the heatmaps and boxplots with results of the trend analysis for the drought severity. In the heatmaps, decreasing trends, in blue, represent a trend towards less severe droughts (higher total water availability). Increasing trends, in red, represent a trend towards more severe droughts (lower total water availability).

The first study period (1970-2019) shows that 60 out of the 141 basins are experiencing an increase whereas 81 are experiencing a decrease in drought severity. Basins with increasing drought severity are mostly situated in Croatia leading to an increase of 10.8% for class 4 (Slovenia/Croatia). The more southern inland Spanish basins form a negative hotspot in trends, resulting in negative trends for the remaining classes. Overall, the entire study area shows a range of values between -54.30% and 42.74%, with a median trend of -2.30%, meaning that the water deficit during a streamflow drought is becoming smaller.

For the second study period (1980-2019) the overall distribution between positive and negative trends is similar to the first study period. Of the 341 river basins, 139 show an increasing trend and 176 show a decreasing trend. The statistical values from the boxplots for the entire study area are similar to that of the first period as well, with only less extreme minimum and maximum values. The hotspots identified in the first period stay the same across the different classes with only class 4 (Slovenia/Croatia) experiencing an increase. Furthermore, the decreasing hotspot in Central Spain has become more extreme, with a median trend of -13.2% for class 5.

The third study period (1990-2019) shows a similar pattern as the previous time period. The majority of river basins are now experiencing a decrease in drought severity, with values ranging from -41.9% to 32.3% resulting in an overall median trend of -3.62%. For all classes, except class 4 (Slovenia/Croatia), the median trends show negative trends similar to the second study period. Looking at the heatmap, negative hotspots dominate the study area, especially in inland Spain, Italy and Southern France.

The final study period (2000-2019) has experienced a shift in the trend values. For each of the first three study periods negative trends were in the majority, however in the final period there are more basins with positive trends resulting in a median trend of 0.16%. The main difference can be observed in the northern part of Spain. The classes in this area, classes 5 and 7, now experience an increase in drought severity for the first time.

Overall, the first three periods showed a small decrease in drought severity, insinuating droughts are become less severe and more water is available. In the last 20 years a slight shift can be observed as the overall trend shows a positive trend as do three climatic classes. But at the same time, basins originating from the Pyrenees and the Alps and the more southern Spanish river basins form decreasing hotspots. However, as most trends show such small relative changes a significant pattern in the total water deficit is not observed.

Drought intensity

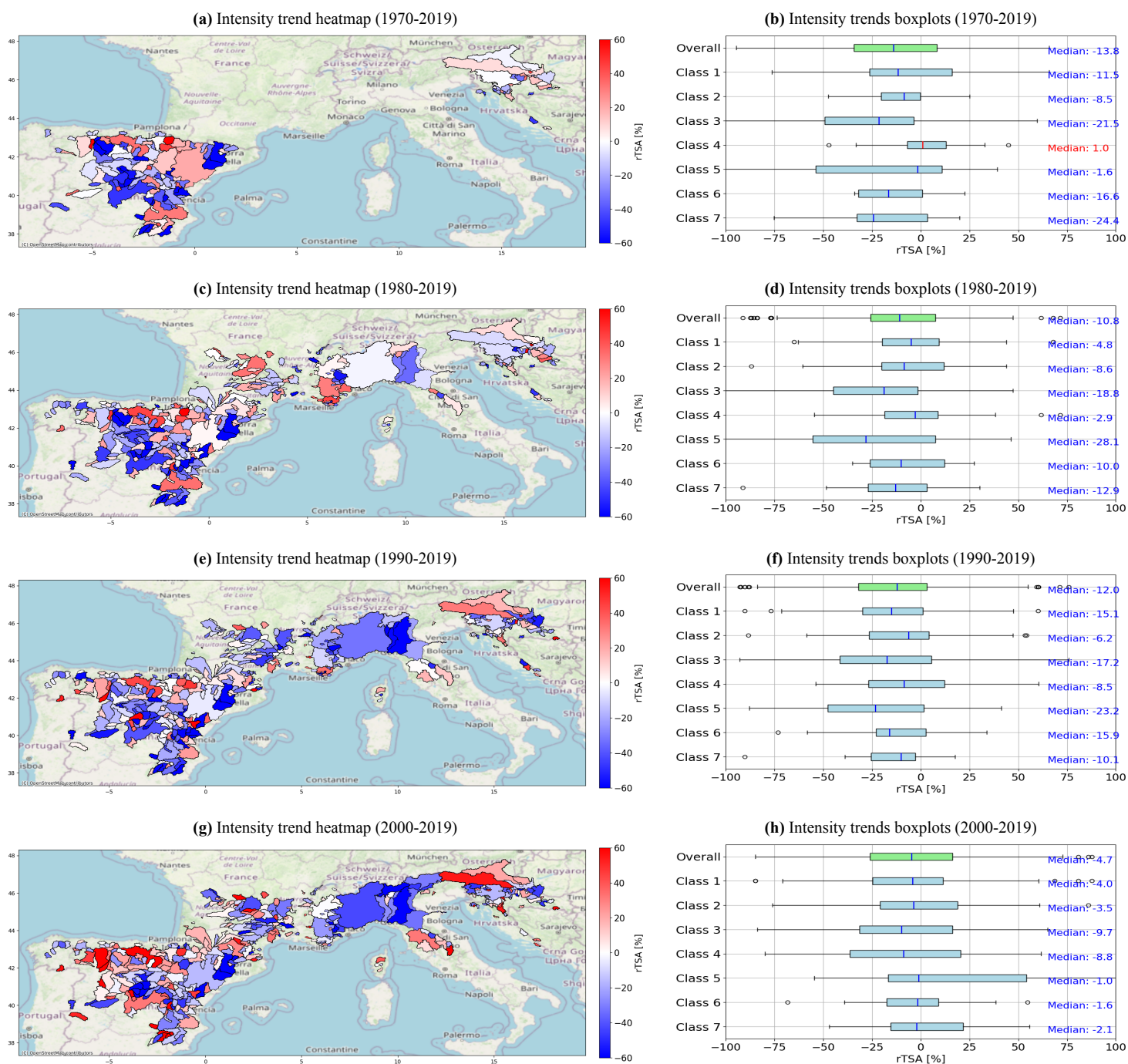


Figure 3.3: Trend results for four fixed time periods for drought intensity. The heatmaps on the left side show the spatial distribution of the trends across the study area. Red shapes indicate an increasing trend and blue shapes indicate a decreasing trend. The boxplots on the right side display the distribution of trends for each specific region.

Figure 3.3 illustrates the trends of the drought intensity for the different time periods. Positive trends indicate an increasing drought intensity (higher average water deficit), negative trends indicate a decreasing drought intensity (lower average water deficit).

The results of the first time period (1970-2019) show an overall decreasing trend, 90 out of the 141

basins are experiencing a decrease in drought intensity. For the entire study area this resulted in a median trend of -13.83%. Looking at the heatmap, Spain clearly shows a decreasing hotspot in the more inland river basins. This shows in the boxplot as well, as six of the classes experience a clear decrease, especially classes 3, 5 and 7.

The second study period (1980-2019) shows a similar distribution between positive and negative trends. Of the 315 river basins, 206 basins show a decrease and 109 show an increase in drought intensity. This resulted in a median trend for the entire area of -10.80%. Zooming into each class, all classes experience more decreasing trends than increasing trends, resulting in clear negative median trends across the study area. Spain shows a similar spatial distribution of trends compared to the first period, with the more inland basins showing a clear decrease.

The third study period (1990-2019) shows overwhelmingly negative trends. 68% of the river basins shows a decrease in drought intensity, resulting in an overall median trend of -12%. Just like the second study period the median trends of each class are negative, but the value of class 1 has decreased significantly to -15.1%. Across the whole spatial extent the trends are mostly decreasing, especially in inland Spain, Southern France and Italy.

In the last period (2000-2019) a slight shift can be observed in drought intensity trends. The majority of trends is still negative (56% of the basins), but the median trend is much less negative with -4.72%. An increase in median, Q75 and maximum values compared to the first three periods can be observed for each class. For each class the median trend is still negative but have become less extreme ranging between -1% of class 5 and -9.7% of class 3.

Overall, the median trends in drought intensity show a clear pattern towards towards less intense stream-flow drought events across the entire study area, except for class 4. This behaviour indicates that during a drought event the average daily water deficit is becoming smaller, resulting in relatively more water availability on daily basis and leading to improved conditions.

Maximum drought deficit

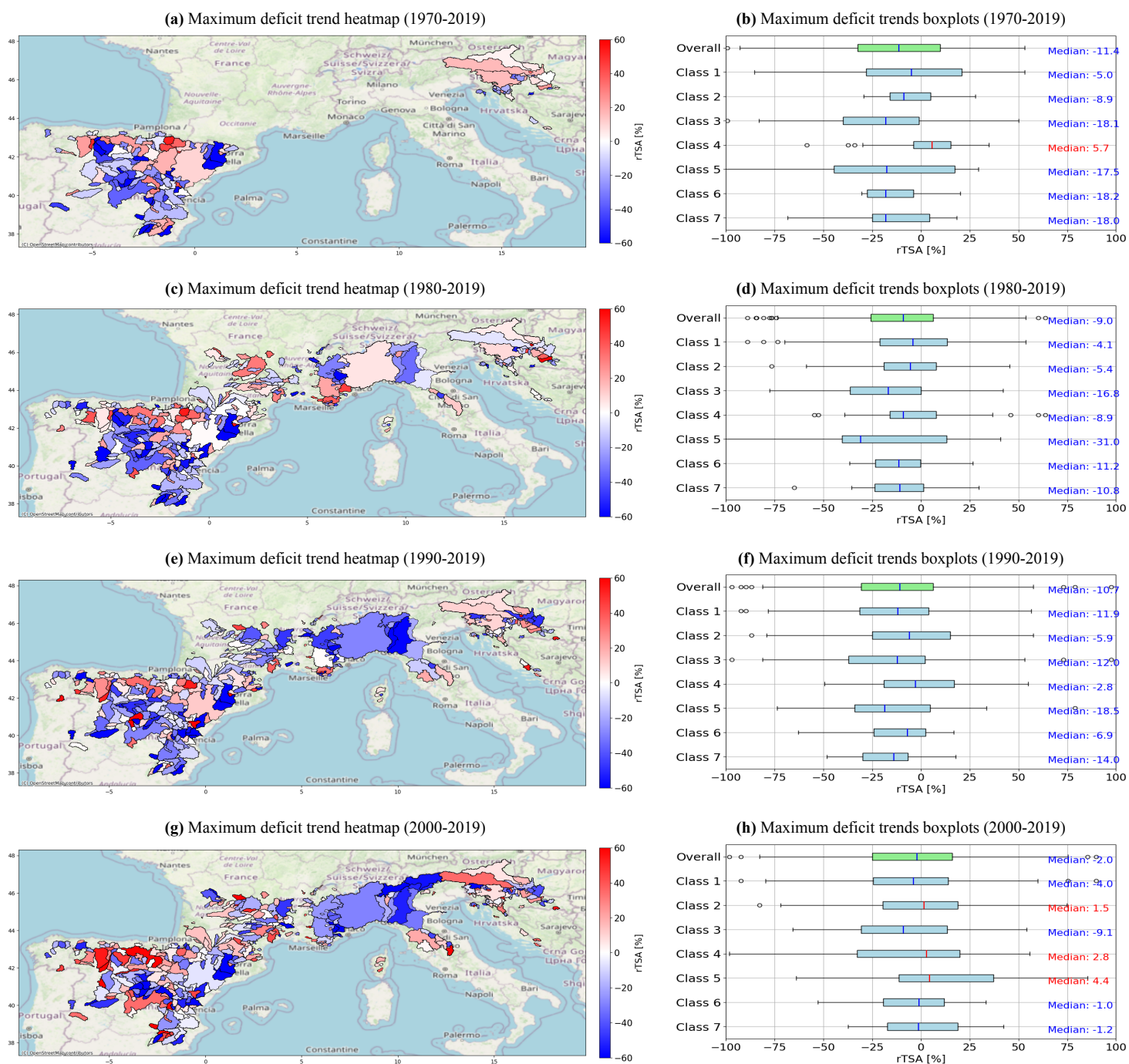


Figure 3.4: Trend results for four fixed time periods for maximum drought deficit. The heatmaps on the left side show the spatial distribution of the trends across the study area. Red shapes indicate an increasing trend and blue shapes indicate a decreasing trend. The boxplots on the right side display the distribution of trends for each specific region.

Figure 3.4 shows the results of the trend analysis for the maximum drought deficit. Positive trends indicate an increasing maximum drought deficit, negative trends indicate a decreasing maximum drought deficit.

As the maximum drought deficit is defined as the maximum daily drought intensity during a drought

event, the maximum drought deficit shows almost identical patterns to the trend analysis of the drought intensity. Over the first three study periods (1970-2019, 1980-2019, 1990-2019) the entire study area as well as each individual class experience a negative median trend. The main difference compared to the drought intensity is observed in the last study period. Similar to the changes in intensity, during this period all median trends have become higher, but in this case the median trends of classes 2, 4 and 5 are positive.

Inter-Arrival Time

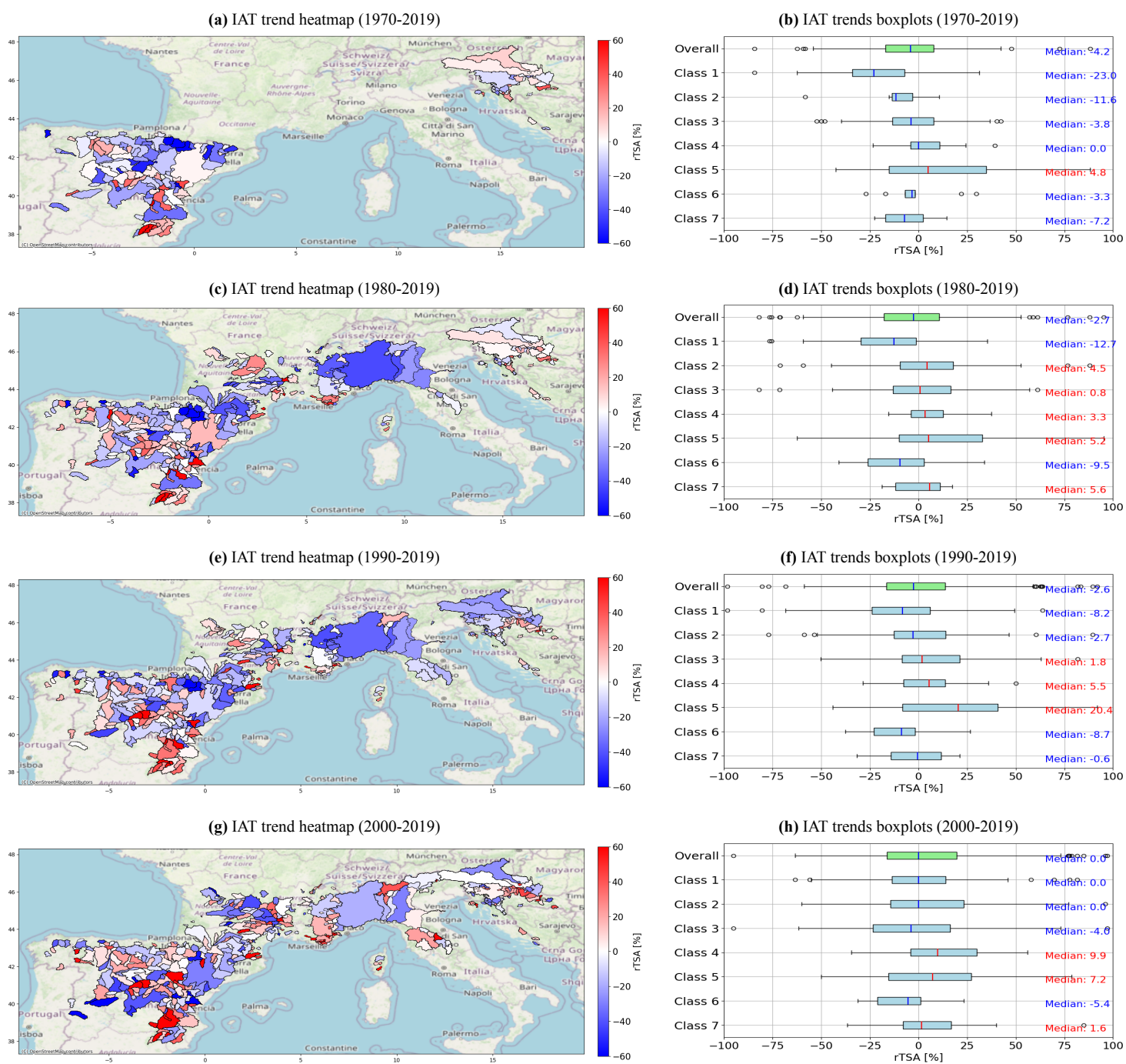


Figure 3.5: Trend results for four fixed time periods for drought inter-arrival time. The heatmaps on the left side show the spatial distribution of the trends across the study area. Red shapes indicate an increasing trend and blue shapes indicate a decreasing trend. The boxplots on the right side display the distribution of trends for each specific region.

Figure 3.5 shows the trends in the inter-arrival time between drought events. Positive trends, in red, indicate an increase in the inter-arrival time, as in the time between the starting times of drought events is become larger, whereas the blue trends indicate a decrease in inter-arrival time, it takes less time for a new drought to start.

The results of the first study period (1970-2019) show a mostly decreasing trend across the study area. Across the 141 river basins, a majority of 60.3% basins experience a decrease trend. For the entire study area this resulted in values ranging from -54.2% to 42.36%, with a median trend of -4.19%. Especially Spain experiences a decrease, resulting in negative median trends for the classes 1, 2, 3 that are located in this area.

The second study period (1980-2019) shows slight increase in the amount of positive trends, with 55.2% of the trends being negative. The entire study area has a median trend of -2.70%. The heatmap of this study period shows that especially in Northern Spain, the Pyrenees and the Alps decreasing hotspots can be identified. This is also observed from the median trend of -12.7% for class 1, which these areas are a part of.

The results of the third study period (1990-2019) show a similar distribution in trends as the previous study period. Of the 361 basins, 53% is negative which resulted in a median trend of -2.57%. The main difference is the positive trend of 20.4% belonging to class 5, located in most southern Spanish river basins.

The results of the last period (2000-2019) show a slight shift in trends, changing from negative to a constant trend. Of the 387 trends, 47% is negative, 49% is positive and the remaining experience no change. For the entire study area this resulted in a median of 0%. The spatial pattern is similar to the third time period.

Overall, most median trends show only a slight decrease in inter-arrival time or remain stable over time. For the cases with a slight decrease, this means that there is less time between consecutive streamflow droughts and indicates a potential increased drought frequency. However, a clear significant pattern towards cannot be observed across the different time periods.

Recovery Rate

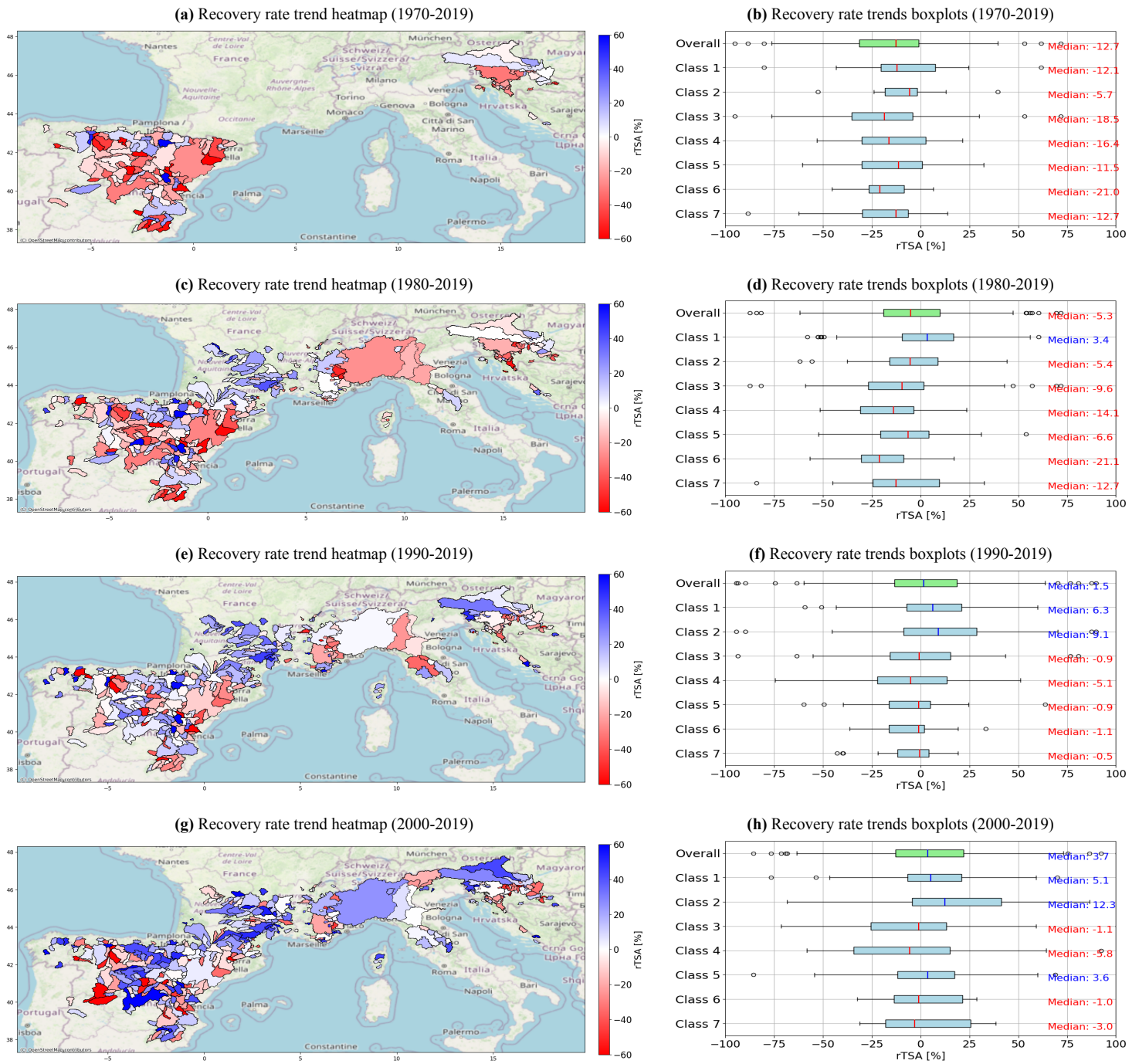


Figure 3.6: Trend results for drought recovery rate. The heatmaps on the left side show the spatial distribution of the trends across the study area. Red shapes indicate an increasing trend and blue shapes indicate a decreasing trend. The boxplots on the right side display the distribution of trends for each specific region.

Figure 3.6 shows the heatmaps and boxplots corresponding to the trend analysis results for the drought recovery rate. It must be noticed that in this figure increasing trends are given in blue and decreasing trends are given in red. This is done as an increasing recovery rate is often associated with being a positive effect as the river system recovers faster to its normal state. Oppositely, a decreasing trend in

recovery rate insinuates that the rate at which a river recovers from drought is getting slower.

During the first study period (1970-2019) the results show overwhelmingly negative distribution of trends, with 77% of trends being negative resulting in a median trend of -12.67%. Similar negative trends are observed for all classes as well.

The results of the second study period (1980-2019) show an increase in positive trends, with 37.6% being positive and 62% being negative. For the entire area this resulted in a median trend of -5.26%. The majority of climatic classes experience this decrease in recovery rates as well, except for class 1 which has a median trend of 3.4% as the south of France is a positive hotspot.

The last two study periods (1990-2019 and 2000-2019) show a transition in trend distributions. The majority of the trends has become positive, resulting in positive trends of 1.5% and 3.7% for the third and fourth period respectively. All classes either observe less negative trends or positive trends. Especially classes 1 and 2 form a positive hotspot in France and Northern Spain.

All in all, a shift is observed from decreasing to increasing recovery rates. River basins recover faster from a streamflow drought event in the last two periods compared to before. However, this increase is very small and not consistent across climatic regions.

Decline Rate

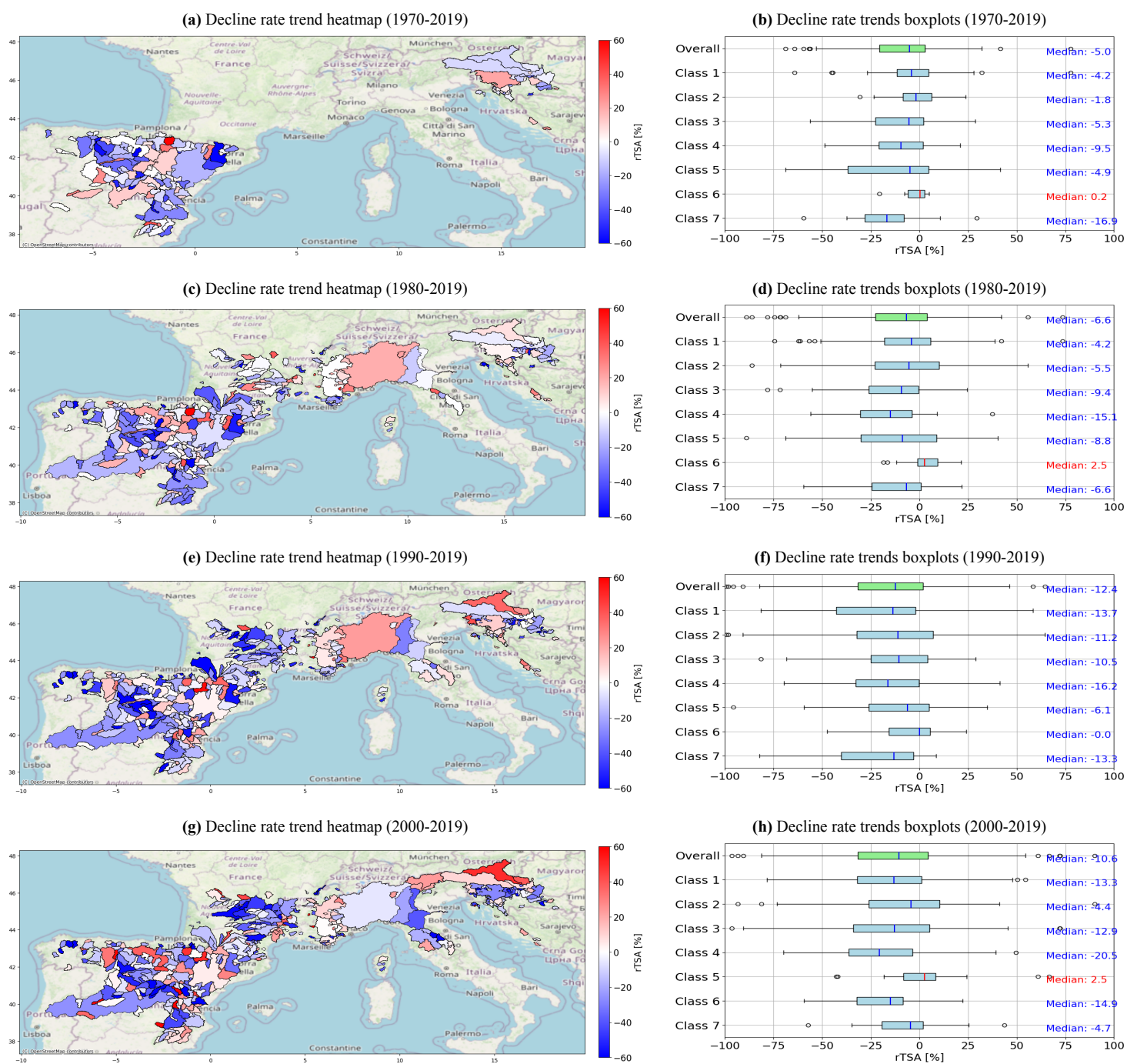


Figure 3.7: Trend results for drought decline rate. The heatmaps on the left side show the spatial distribution of the trends across the study area. Red shapes indicate an increasing trend and blue shapes indicate a decreasing trend. The boxplots on the right side display the distribution of trends for each specific region.

Figure 3.7 shows the results of trend analysis for the drought decline rate. The decline rate is a negative rate by default, therefore a decreasing trend indicates a less negative decline rate (water availability is reduced slower), whereas an increasing trend indicates faster decline rate (faster reduction of available water).

The results across all four time periods are overwhelmingly negative. The median trend for the entire study area shows an overall decreasing trend ranging between -5% and -12.4%. Similar results are obtained for the majority of climatic classes, all experiencing a decrease in decline rate. These results indicate that between the onset of drought event and the timing of its peak the water deficit worsens at a slower rate, alleviating water availability issues and giving more time to prepare for the peak of the drought.

3.1.1. Main observations

The main findings of the trend analysis with four fixed time periods reveal predominantly negative trends for all drought characteristics, except for the drought duration. The median trend values for the drought duration fluctuate between zero and slightly positive values, and do not show a clear trend towards streamflow droughts becoming longer or shorter over time. The only region demonstrating a clear hotspot are the river basins of climatic class 4, located in Croatia and Slovenia. Here, the drought duration is increasing significantly across all four time periods, meaning that in this area river basins are experiencing longer periods of low water availability.

On the other hand, the drought severity shows a consistent small negative trend over the first three periods for most of the study area, shifting slightly in the last period towards a positive trend. This indicates that the total water deficit during a streamflow drought event is getting smaller and that more water is available during more recent streamflow droughts than in the past, alleviating drought conditions. However, the changes are small and significant patterns cannot be observed. The drought intensity, directly depended on the duration and severity, exhibits an overwhelmingly negative trend and so does the maximum drought deficit as well. These trends indicate that during streamflow droughts the average and maximum daily water deficit have become smaller, and that on daily basis more water is available.

Overall, the results of the key drought characteristics (drought duration and severity) do not exhibit clear or significant patterns and remain relatively stable. In fact, the drought severity even tends to be slightly decreasing. These results, however, are the exact opposite of the expected trends. The main consensus, both in public as in scientific literature, is that streamflow droughts are becoming more extreme in the Mediterranean area, with longer duration and higher total water deficits. The obtained results here do not align with that pattern, indicating the need for extra research.

3.2. Multi-Temporal Analysis

The unexpected results from the trend analysis stand in contrast to the common idea that streamflow droughts in the Mediterranean region are becoming more extreme. Both scientific literature and public consensus suggest increasing streamflow drought extremes in the region, which raises questions about the validity or scope of the initial analysis. To analyse the changes in streamflow droughts in-depth, a more detailed multi-temporal analysis was conducted.

This multi-temporal analysis provides a more comprehensive view by calculating median trends in streamflow drought characteristics across all possible time period combinations within the study period. For that reason this method accounts for the sensitivity of the selected time period and allows for a better understanding about the temporal changes in drought characteristics compared to only the four fixed time periods used in the initial analysis.

In this section, both annual and seasonal trends across the study area are computed using this multi-temporal analysis to precisely determine the spatial and temporal changes in streamflow droughts. The median trends for the entire study area and the individual climatic classes are analysed in order to determine clusters in temporal and spatial trends in drought characteristics. Only the multi-temporal analyses of drought characteristics for climatic classes are shown which deviate from the general annual and seasonal trends. Similar to the trend analysis with four fixed time periods, the multi-temporal

analysis was first performed for basins with data starting in 1970 to validate the observed patterns by comparing it to the overall annual trends. These multi-temporal analyses and the entire ensemble of heatmaps showing the results of each multi-temporal analysis can be found in Appendix B.

3.2.1. Annual Trends

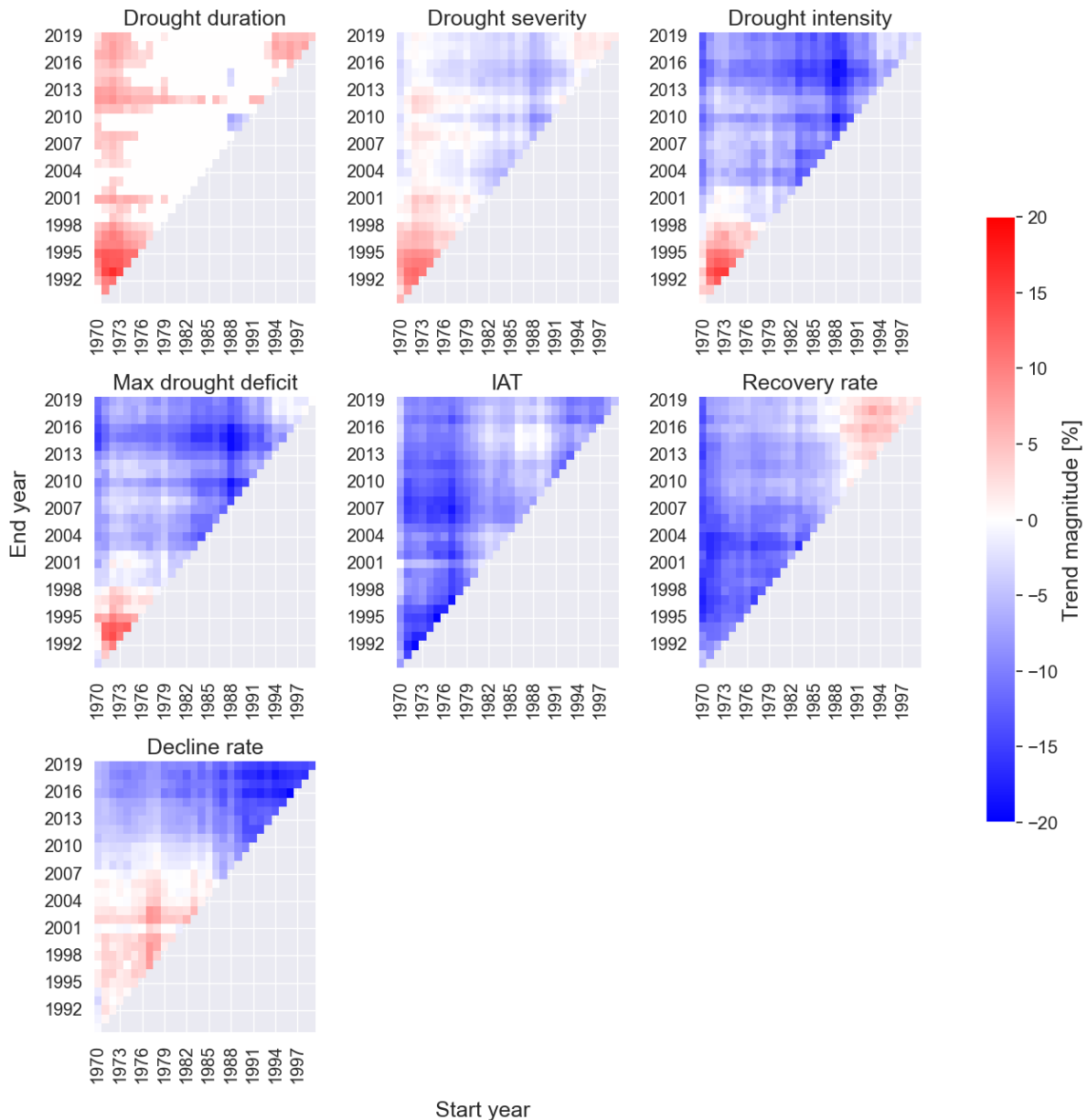


Figure 3.8: Multi-temporal analysis of annual median trends for each drought characteristic, expressed as a percentage, across all river basins. The heatmap illustrates the magnitude of trends for all combinations of time periods between 1970-2019, with the x-axis representing the start year and the y-axis representing the end year of each time period. Red indicates increasing trends, while blue represents decreasing trends.

Figure 3.8 shows heatmaps of the multi-temporal analysis performed for annual streamflow droughts (occurring throughout the entire year) across the entire study area. These heatmaps contain the median trend for each of the drought characteristics over every possible combination of start and end years. Every individual grid cell represents the value of the median trend for its corresponding period. The

color-scheme of the heatmaps for the median trends is the same as in the trend analysis; the color red indicates an increase whereas the color blue indicates a decrease in the specified drought characteristic.

The heatmap for the drought duration shows a bimodal pattern. For time periods starting between 1970 and 1978 the majority of trends is positive. Time periods starting between 1978 and 1992 mostly have a median trend equal to zero and do not experience a change. In the later periods starting from 1994 an overall increase up till 8% can again be observed. This suggests that, although most time periods show no change, in the most recent time periods streamflow droughts have been getting longer.

The drought severity heatmap does not show a clear pattern over time. Time periods starting between 1970 and 1980 show a significant cluster of increasing trends up until 2001, measuring values up to 15%. However, for the periods ending after 2001 there is no clear pattern and there is a lot of variability in positive, zero and negative trends. Trends calculated for start years between 1982 and 1992 do form a clear cluster of negative trends, with values between -1 to -5%, no matter what the end year is. Similarly to the drought duration, a slight cluster of increasing trends can be observed after starting year 1994. Based on these results, the total water deficit of streamflow droughts has been increasing from 1970 till 1994, but after 1994 it has actually been decreasing resulting in more water availability during a drought event.

The drought intensity depends directly on the drought duration and severity. This relationship can be seen in the heatmap as well, as with a stable duration and decreasing severity, resulting in overwhelming decreasing trends for the intensity. For end years of 1999 and before all periods show a positive median trend, whereas for end years after 2000 show a negative trend, with trend magnitudes mostly ranging between -10 to -20%. The heatmap for the maximum drought deficit shows almost the exact same patterns as the drought intensity. Only difference is that after start years 1995 have become much less negative and close to zero. These trends suggest that, especially since 1980, the average and maximum daily water deficit has become smaller. This means that during a drought event more water is available on a daily basis and that the point of lowest water availability is getting higher as well.

The heatmap for the inter-arrival time shows a clear pattern. Regardless of the start or end year the multi-temporal analysis consists entirely of negative trends with values between -8 to -18%. These decreasing trends indicate that consecutive streamflow drought events are occurring more rapidly, there is less time between drought events. This suggests an increase in drought frequency, and therefore more streamflow droughts which could create issues regarding the sustainability of water resources.

The recovery rate shows a clear shift in trends after start year 1992. For start years before this year all trends are negative (-10 to -20%), but for all years starting after 1990 all trends have become positive showing an increase around 5%. The heatmap for the decline rate shows an overall increasing trend up until end year 2006. For end years later than 2006 and all periods starting from around 1988 the trends are negative, with more extreme values as the start year increases. The changes in both of these drought characteristics indicate that since 1990 streamflow droughts decline at slower rates, the daily water deficit is increasing slower leading up to the peak of the drought event. This trend makes it easier for people to adapt to and prepare for the drought event. Furthermore, an increase in the recovery rate indicates that river systems are returning to non-drought conditions quicker after the peak of the drought event. This can enhance the resilience of aquatic ecosystems and water supplies, potentially alleviating some of the pressures that droughts impose on water resources.

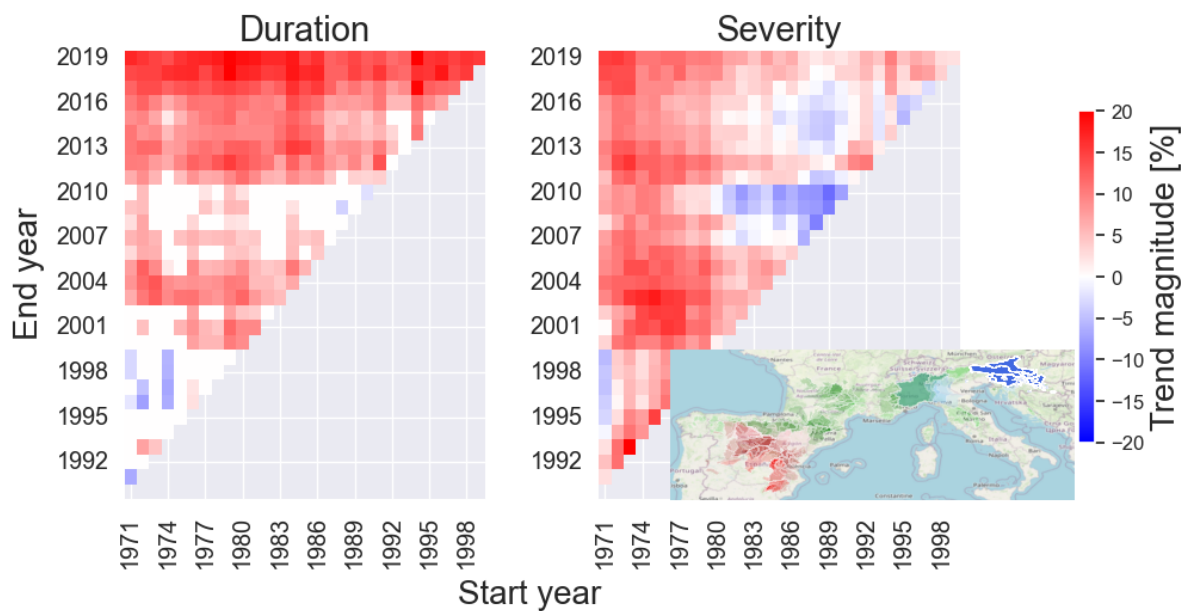


Figure 3.9: Multi-temporal analysis of annual median trends for drought duration and severity, expressed as a percentage, across river basins of class 4. The heatmap illustrates the magnitude of trends for all combinations of time periods between 1970-2019, with the x-axis representing the start year and the y-axis representing the end year of each time period. Red indicates increasing trends, while blue represents decreasing trends.

In the same fashion the annual trends of each drought characteristic were determined for the individual climatic classes, revealing similar temporal patterns in their multi-temporal analyses to those observed across the entire study area (Appendix B). The only outliers were the drought duration and severity trends of river basins of class 4 which exhibited clear deviations (see Figures 3.9). The multi-temporal analysis of the drought duration within this climatic class indicates an almost overall pattern of increased drought duration across all time periods. Studied time periods starting after 1976 have been predominantly positive, with values reaching 15-20% in the last 5 years, regardless of the starting year. Similarly, these river basins experienced a clear increase in drought severity, with only some negative trends in periods ending in 2008-2010. The periods experiencing the most severe change are those starting between 1970 and 1980, as droughts have become on average 15% more severe over these periods. All in all, this means that in this region during periods of streamflow drought the total water availability is getting smaller and that these periods tend to last longer.

In summary, the analysis of annual trends in streamflow drought characteristics reveals a complex relationship between drought duration, severity, intensity across the study area. Overall, the findings indicate that while drought duration has been increasing, drought severity and intensity have been decreasing, especially since the mid 1980s. Even though the duration of annual streamflow droughts is increasing, the total water availability is getting bigger leading to less challenges for water management. However, it is important to note that these changes are small and not always clear, and significant patterns in duration and severity are not observed.

3.2.2. Winter Trends

The seasonal winter trends in drought characteristics show a clear distinction compared to the temporal patterns in annual trends. The annual trends were almost entirely negative for most drought characteristics, except for the drought duration. However, the trends computed for winter streamflow droughts experience a clear change in the drought duration, severity, intensity and maximum deficit, changing from initially positive to negative trends later on.

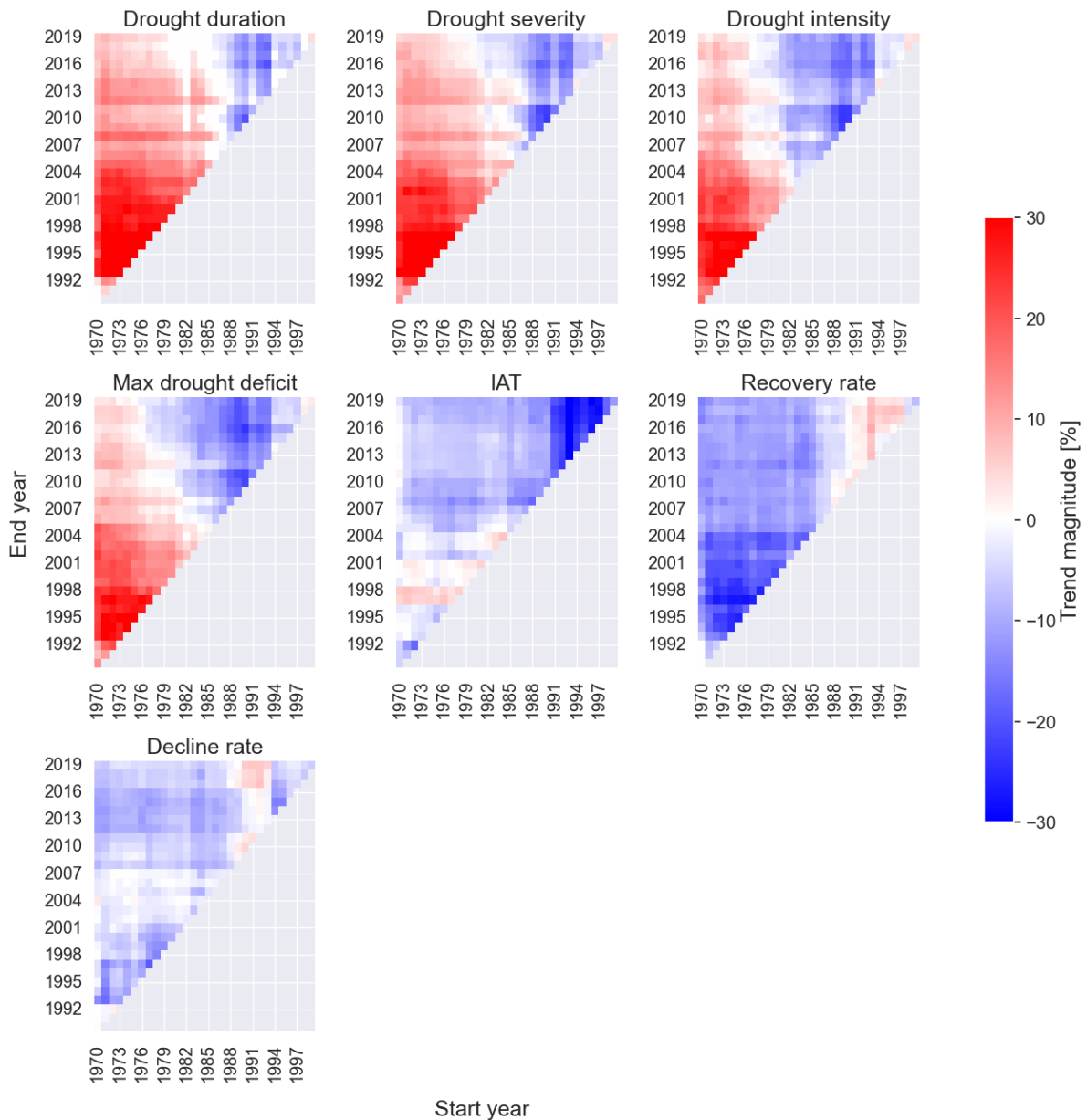


Figure 3.10: Multi-temporal analysis of winter median trends for each drought characteristic, expressed as a percentage, across all river basins. The heatmap illustrates the magnitude of trends for all combinations of time periods between 1970-2019, with the x-axis representing the start year and the y-axis representing the end year of each time period. Red indicates increasing trends, while blue represents decreasing trends.

Figure 3.10 shows the multi-temporal analyses in seasonal winter drought characteristics for the entire study area. The multi-temporal analysis of the drought duration resulted in positive trends for starting years from 1970 till 1985, with trend magnitude reaching 30% for periods ending before 2002. After

this period of increasingly longer streamflow droughts a shift can be observed, as for starting years from 1985-1988 have become zero and after 1988 the trends are mostly negative reaching a decrease in drought duration of 22% for time periods starting between 1988-1993. This pattern shows that winter streamflow droughts in the last 30 years have been significantly getting shorter, leading shorter periods of low water availability.

The temporal trends in drought severity have also experienced changes during winter compared to the annual trends. Similar to the drought duration, the trends in drought severity show a bifurcation with first a period of increasing severity in streamflow droughts changing to a period of less severe streamflow droughts. For time periods starting between 1970 and 1983 the multi-temporal analysis shows overwhelmingly positive trends reaching trend magnitudes of 30% for periods ending before 2004. After 1988 this pattern of increasing severity shifts towards a period of entirely negative trends, leading to streamflow droughts with a lower total water deficit and therefore a higher water availability.

The drought intensity and maximum deficit both follow the same pattern. Time periods starting between 1970 and 1978 are mostly positive with trend magnitudes ranging between 5-30%. Starting from around 1982 these characteristics underwent a change with entirely negative trends fluctuating between -5 to -20%. This overall pattern is very similar to those observed in the multi-temporal analyses of the drought duration and severity, but the onset of decreasing trends occurs five years earlier. Similar to the implications of the severity trends, it means that the average and maximum daily water deficits are getting smaller, increasing the water availability during winter streamflow droughts.

The inter-arrival time, the recovery rate and the decline rate all experienced mostly similar patterns for winter streamflow droughts as annual streamflow droughts. The inter-arrival time experiences a downward trend no matter the selected time period. The main change is the extremely negative tail of the multi-temporal analysis, with trend magnitudes reaching -34% in for the periods between 1992-2019. The recovery rate experiences the exact same trend patterns during winter as annually. The decline rate, which initially still showed a slight increase for the earlier time periods, is entirely negative during winter.

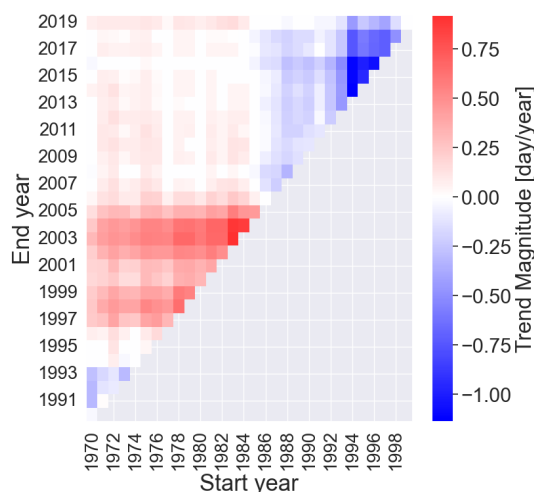


Figure 3.11: Multi-temporal analysis of median trends in winter drought timing, expressed in day/year, across all river basins. The heatmap illustrates the magnitude of trends for all combinations of time periods between 1970-2019, with the x-axis representing the start year and the y-axis representing the end year of each time period. Red indicates droughts occurring later in the season, while blue represents droughts occurring earlier in the season.

Figure 3.11 demonstrates the multi-temporal analysis of the timing in winter streamflow droughts. The computed results have to be interpreted differently those of the other drought characteristics. The trend magnitude is given the amount of days per year that the timing of drought has shifted over the selected

time period. A decreasing trend indicates that streamflow droughts are occurring earlier in the season, where an increasing trend means streamflow droughts occur later in the season.

The multi-temporal analysis of the winter drought timing shows three clear temporal hotspots. Over time periods ending before 2005 winter droughts have been occurring later in the season, with trend magnitudes between 0.15-0.8 day/year. However, starting from 1988 the temporal trends transition to negative trends and eventually reaching even -1 day/year in the last 20 years. This transition in trends is similar to the patterns observed for the drought duration and severity, meaning that in the last thirty years the peaks of streamflow droughts occur earlier in winter but are less extreme.

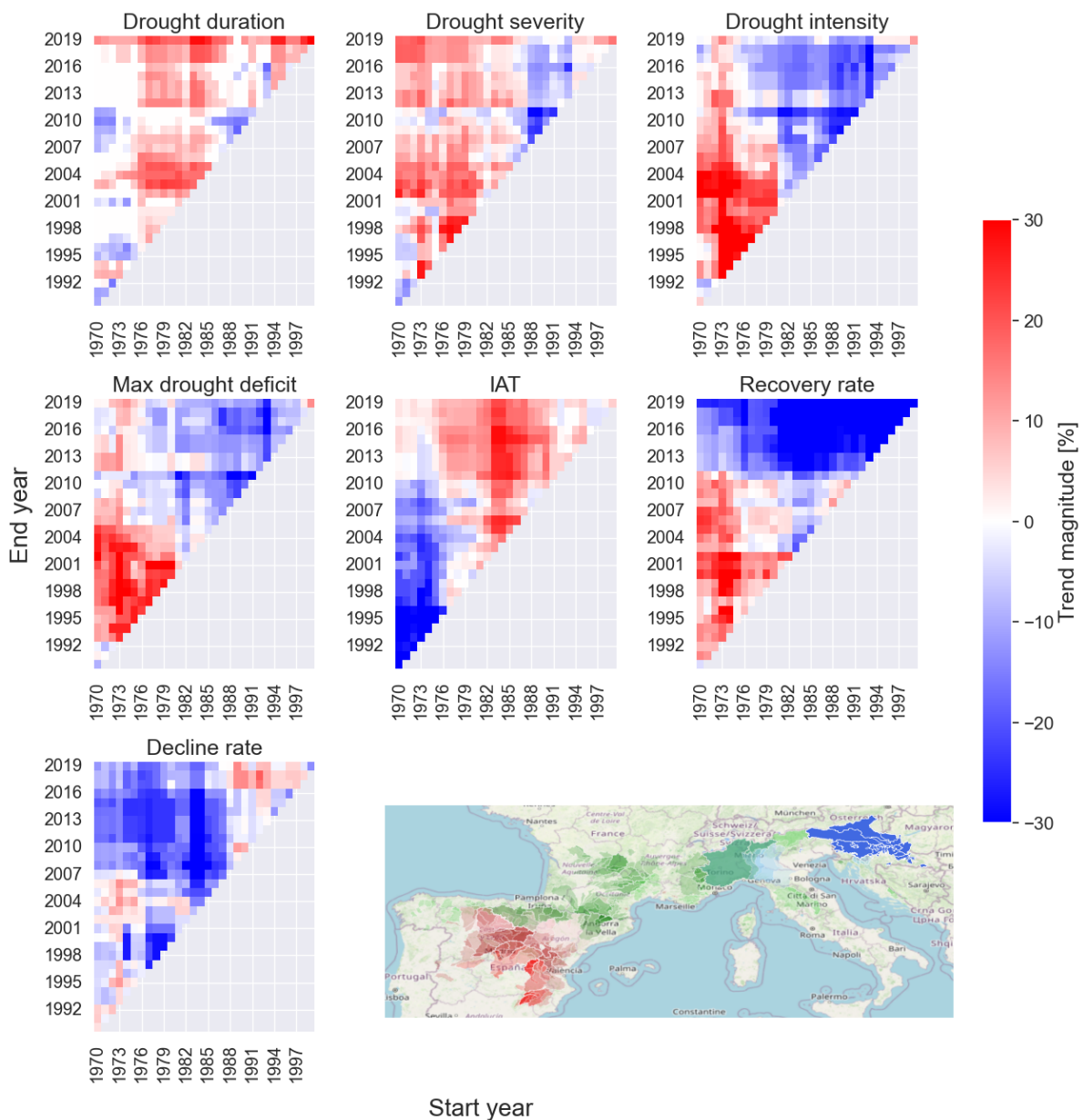


Figure 3.12: Multi-temporal analysis of median trends, expressed as percentage, in winter drought characteristics for river basins of class 4 (location shown in bottom right corner). The heatmap illustrates the magnitude of trends for all combinations of time periods between 1970-2019, with the x-axis representing the start year and the y-axis representing the end year of each time period. Red indicates increasing trends, while blue represents decreasing trends.

Zooming in on the climatic classes, most classes experience similar changes as the entire study area,

with winter streamflow droughts becoming shorter, less severe and less intense over the last 30-35 years. Classes 4 and 6, situated around Croatia and Slovenia, showed deviations from these patterns. Class 4 showed similar patterns as the overall winter trends for the drought intensity and the maximum deficit (Figure 3.12). However, the drought duration and severity do not experience any clear patterns. Whereas the overall winter trend showed a clear shift towards shorter and less severe droughts, the trends for class 4 fluctuate between being positive, negative and zero following no clear hotspots or patterns. This inconsistency makes it difficult to determine whether winter streamflow droughts have become less extreme or if they now have more or less water available.

Additionally, the inter-arrival time undergoes a clear shift from negative to positive trends around starting year 1982, leading to more time between consecutive streamflow droughts. The recovery rate displays the exact opposite as the trends in inter-arrival time. After the year 1982 all time periods show a negative trend with values reaching -30%.

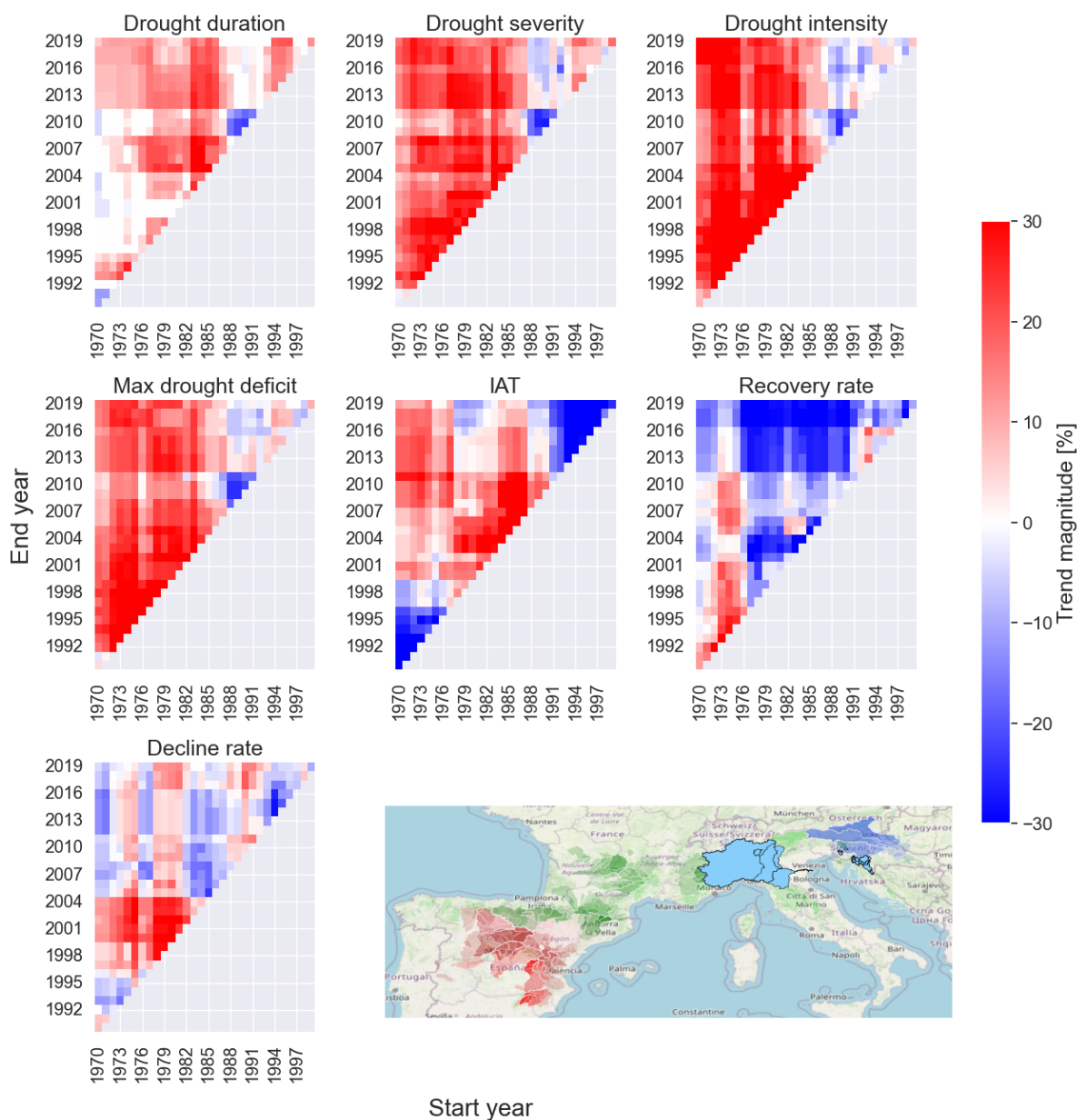


Figure 3.13: Multi-temporal analysis of median trends, expressed as percentage, in winter drought characteristics for river basins of class 6 (location shown in bottom right corner). The heatmap illustrates the magnitude of trends for all combinations of time periods between 1970-2019, with the x-axis representing the start year and the y-axis representing the end year of each time period. Red indicates increasing trends, while blue represents decreasing trends.

In contrast, class 6, which differs from the other classes as it is characterized by both a high phase difference between wet and hot seasons and moderate seasonal temperature variation, shows significant deviations in duration, severity, intensity and maximum deficit trends (Figure 3.13). Multi-temporal analyses computed for these four characteristics show almost entirely positive trends, mostly ranging from 10-25% but reaching even up till 35% for some time periods. These patterns show that in class 6 winter streamflow droughts are becoming more extreme, with significantly longer duration and lower water availability. Although more recent periods display some variability, with trends fluctuating between positive and negative, this difference is less pronounced than the winter drought patterns in the overall study area. Just like for class 4, the inter-arrival time displays differences from the overall winter trends. For time periods with starting years between 1979-1988 the majority of trends are positive.

After 1988-1990 however a shift can be observed towards negative trends, averaging around -30%.

In summary, these multi-temporal analyses for winter drought characteristics show that streamflow droughts during winter have been getting less extreme. Especially, the drought duration, severity and intensity have all been decreasing significantly since 1990. Practically, this means that drought events are getting shorter and that more water is available, which will alleviate water management problems stemming from streamflow droughts.

3.2.3. Summer Trends

Figure 3.14 shows the multi-temporal analyses of the summer streamflow drought characteristics, which reveals clear deviations from the observed annual trends in all drought characteristics, except for the decline rate. Deviations are observed for the entire study area as well as between many of the climate classes. This highlights the significance of analysing trends during summer.

The drought duration trends for time periods starting between 1970-1985 show similar patterns to the annual trend in drought duration. During these period no clear pattern can be distinguished and trend values are fluctuating between being positive, negative or zero. Whereas the annual trend remained mostly zero, the drought duration in summer sees a sharp increase in trend magnitude starting after 1988. Trend magnitudes gradually increased over the last 30 years and reached up to 25% for the time period of the last 20 years, indicating longer summer streamflow droughts.

This same shift from negative trend values to positive trend values around the years 1988-1990 is also seen in the multi-temporal analyses of all other key drought characteristics. The drought severity experiences an overall negative trend for time periods with starting years between 1970-1986, similar to the annual trend, but time periods after 1990 showed an overall pattern of increased drought severity of 5-15%. The drought intensity and maximum deficit demonstrate this exact same pattern, but with values ranging up to 20-25%. For water management practices this implies that during summer severely less water is available during a drought event, amplifying the already existing limited water availability in the Mediterranean.

The drought inter-arrival time, which experienced entirely negative trends for annual and winter trends, mostly experiences negative trends during summer as well. However, similar to the other characteristics, a shift is seen after 1988 towards trends close to zero. This pattern shows that the time between consecutive summer streamflow droughts has been stable and suggests that the frequency has remained the same. The recovery rate, which already showed an increasing annual trend after 1993, now experiences this same shift five years earlier. The decline rates during summer are almost identical to the observed annual trends. Just like the practical implications for the annual trends, these trends imply that the daily water availability is decreasing slower leading up to the peak of the drought event and increases faster after the peak to non-drought conditions.

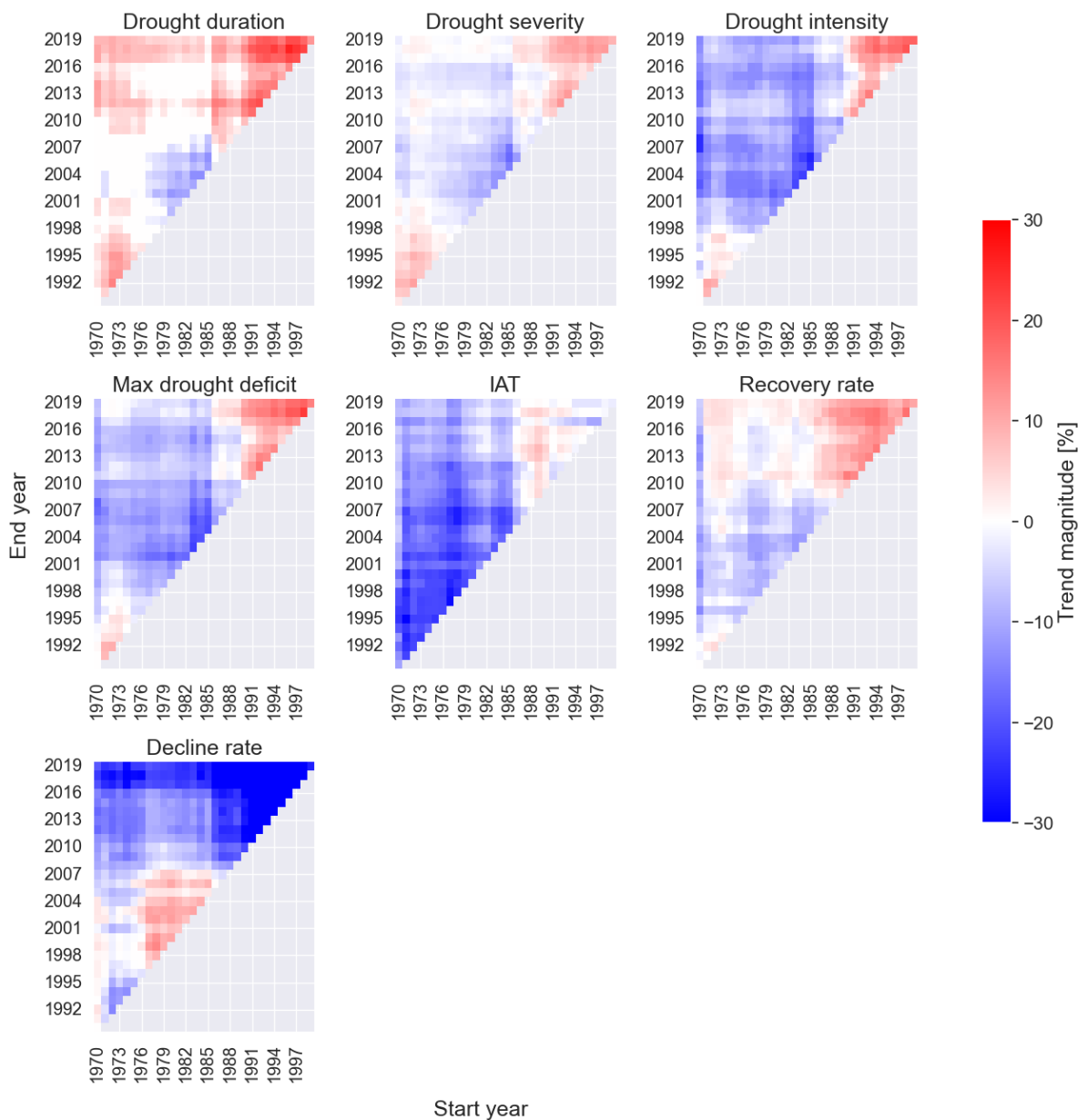


Figure 3.14: Multi-temporal analysis of summer median trends for each drought characteristic, expressed as a percentage, across all river basins. The heatmap illustrates the magnitude of trends for all combinations of time periods between 1970-2019, with the x-axis representing the start year and the y-axis representing the end year of each time period. Red indicates increasing trends, while blue represents decreasing trends.

The multi-temporal analysis of the maximum summer drought timing demonstrates a clear change in the maximum summer drought timing around the year 1989 (Figure 3.15). Time periods with starting years before this tipping point are mostly negative up to 2007 and start transitioning to zero trends after. After 1989 only positive trends are seen indicating that the timing of peak of summer droughts is occurring later in summer.

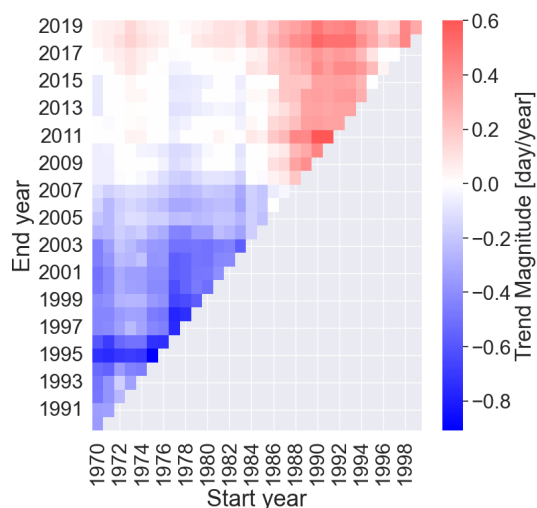


Figure 3.15: Multi-temporal analysis of median trends in summer drought timing, expressed in day/year, across all river basins. The heatmap illustrates the magnitude of trends for all combinations of time periods between 1970-2019, with the x-axis representing the start year and the y-axis representing the end year of each time period. Red indicates droughts occurring later in the season, while blue represents droughts occurring earlier in the season.

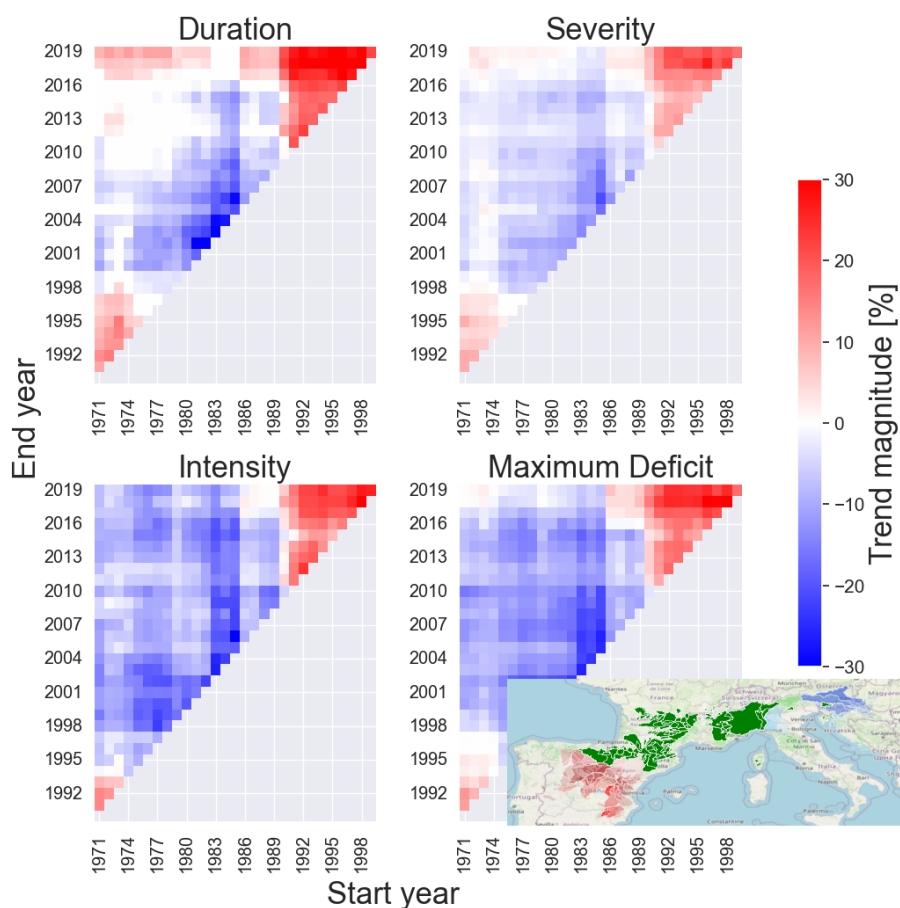


Figure 3.16: Multi-temporal analysis of median trends, expressed as percentage, in summer drought characteristics (duration, severity, intensity, and maximum deficit) for river basins of class 1 (location shown in bottom right corner). The heatmap illustrates the magnitude of trends for all combinations of time periods between 1970-2019, with the x-axis representing the start year and the y-axis representing the end year of each time period. Red indicates increasing trends, while blue represents decreasing trends.

While the climate classes during winter mostly followed the similar patterns as the overall winter trend, they experience significant variations during the summer season. For summer, the inter-arrival time, recovery rate and decline rate trends remained relatively stable across climate classes, but the drought duration, severity, intensity and maximum deficit exhibit a lot of deviations between each climate class and the observed overall summer trends.

The river basins corresponding to class 1, located around the Pyrenees and southern France, displayed similar patterns to the summer trends of the entire study area. However, the trend magnitudes for class 1 reach far more extreme values for the more recent periods with increasing trend values (Figure 3.16). The trends for drought duration, severity, intensity and maximum drought deficit all undergo the same shift in patterns around 1988-1990, changing from mostly negative trends towards a positive pattern. All these patterns point towards more extreme summer droughts in the last 30 years, both lasting longer and with significantly lower water availability.

For time periods starting between 1970 and 1988, the majority of the trends for class 1 were negative and their trend magnitude values comparable and in the same order of magnitude as the overall summer trends. After 1990 the trend values become positive, but the order of magnitude is much higher compared to the entire study area, reaching increasing trend magnitudes of 30-40%.

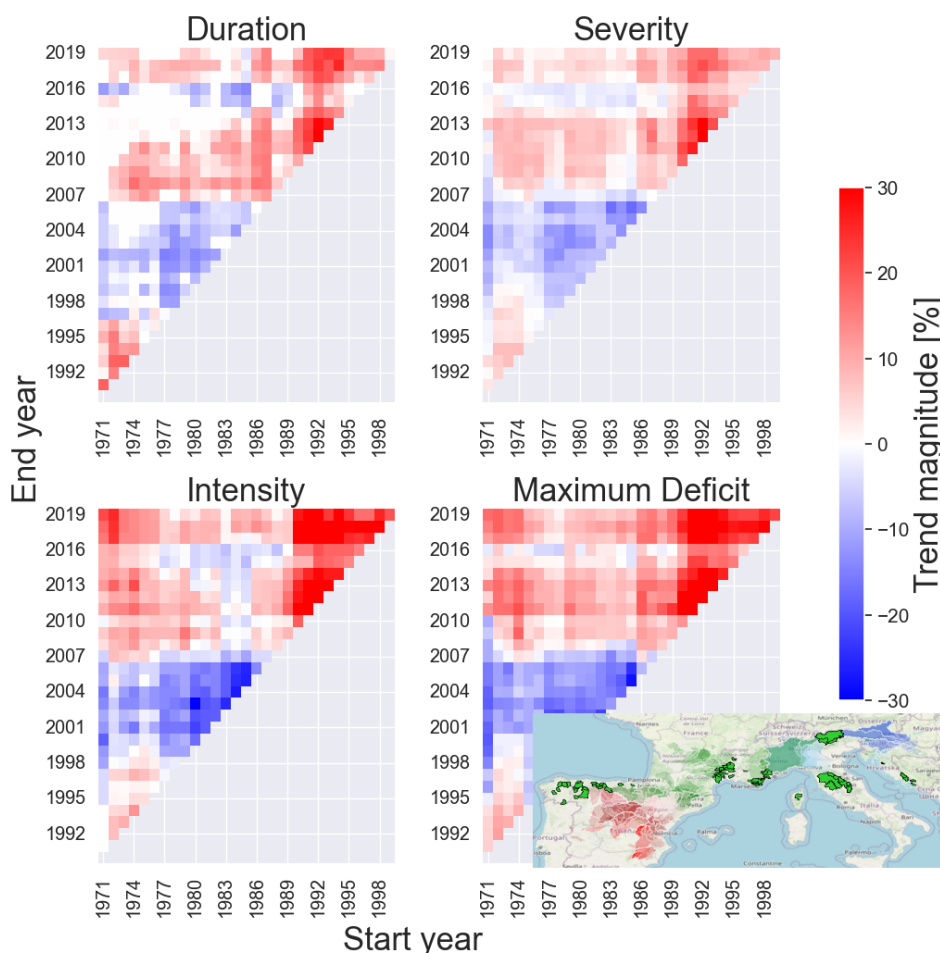


Figure 3.17: Multi-temporal analysis of median trends, expressed as percentage, in summer drought characteristics (duration, severity, intensity, and maximum deficit) for river basins of class 2 (location shown in bottom right corner). The heatmap illustrates the magnitude of trends for all combinations of time periods between 1970-2019, with the x-axis representing the start year and the y-axis representing the end year of each time period. Red indicates increasing trends, while blue represents decreasing trends.

More clear differences could be observed for class 2, which is characterized with a higher seasonal precipitation difference than class 1. The multi-temporal analyses for the drought duration, severity, intensity and maximum drought deficit all follow the same pattern (Figure 3.17). For time periods with ending years before 2007 the majority of trends are negative, with values ranging between -2 to -15%. All time periods with ending years after 2007 and periods starting after 1988, however, show a clear pattern of increasing trend values. The most extreme trend values can be observed for the periods between 1990-2019, during these periods the trend magnitude reach up to 30%. Here, summer streamflow droughts will have less water available, creating issues for water management.

Class 4, located around Slovenia and Croatia, differentiates itself from class 1 and 2 as it is characterized with a medium instead of low seasonal temperature difference. This class displays the most clear increasing patterns among the climatic classes during summer (Figure 3.18). The multi-temporal analyses for the drought duration and severity both consists of almost entirely positive trends, with most trend magnitudes ranging between 7-25% but with extreme values reaching over 40%.

The multi-temporal analyses of both the drought intensity and maximum deficit for class 4 follow similar patterns to each other. They differentiate themselves from the drought duration and severity with time periods starting between 1982-1986 and ending before 2008 showing a hotspot of decreasing trend magnitudes.

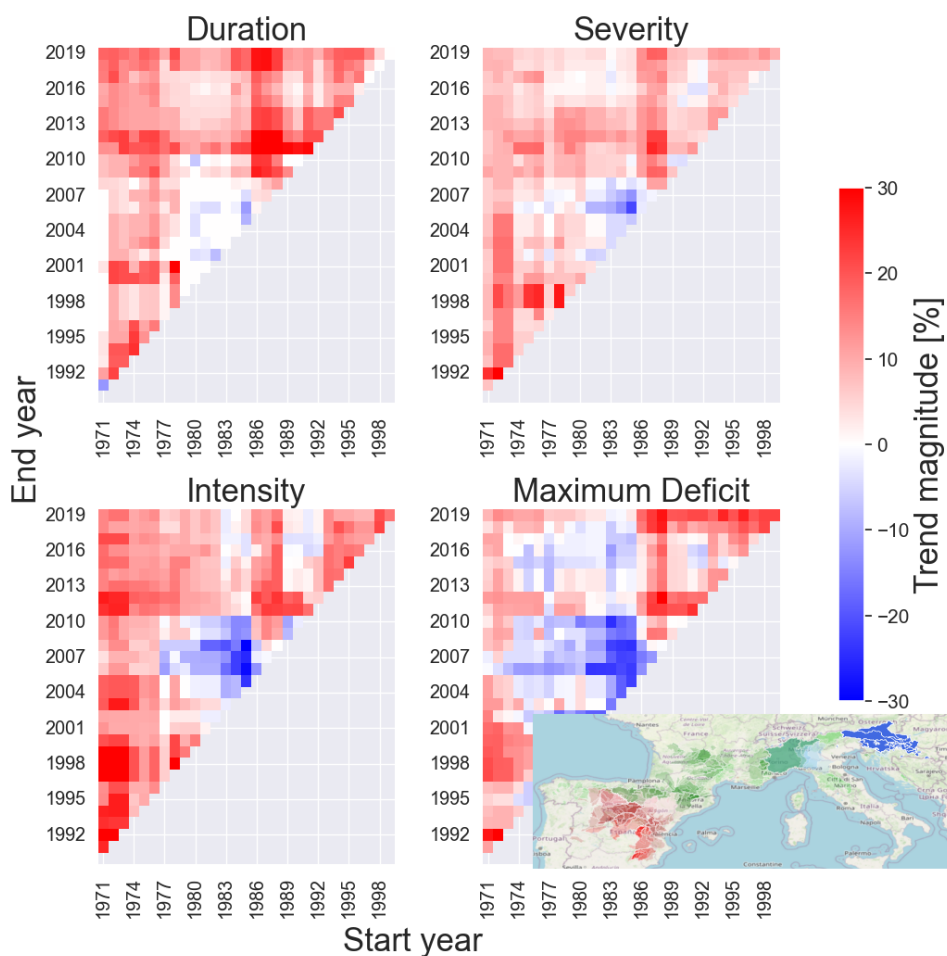


Figure 3.18: Multi-temporal analysis of median trends, expressed as percentage, in summer drought characteristics (duration, severity, intensity, and maximum deficit) for river basins of class 4 (location shown in bottom right corner). The heatmap illustrates the magnitude of trends for all combinations of time periods between 1970-2019, with the x-axis representing the start year and the y-axis representing the end year of each time period. Red indicates increasing trends, while blue represents decreasing trends.

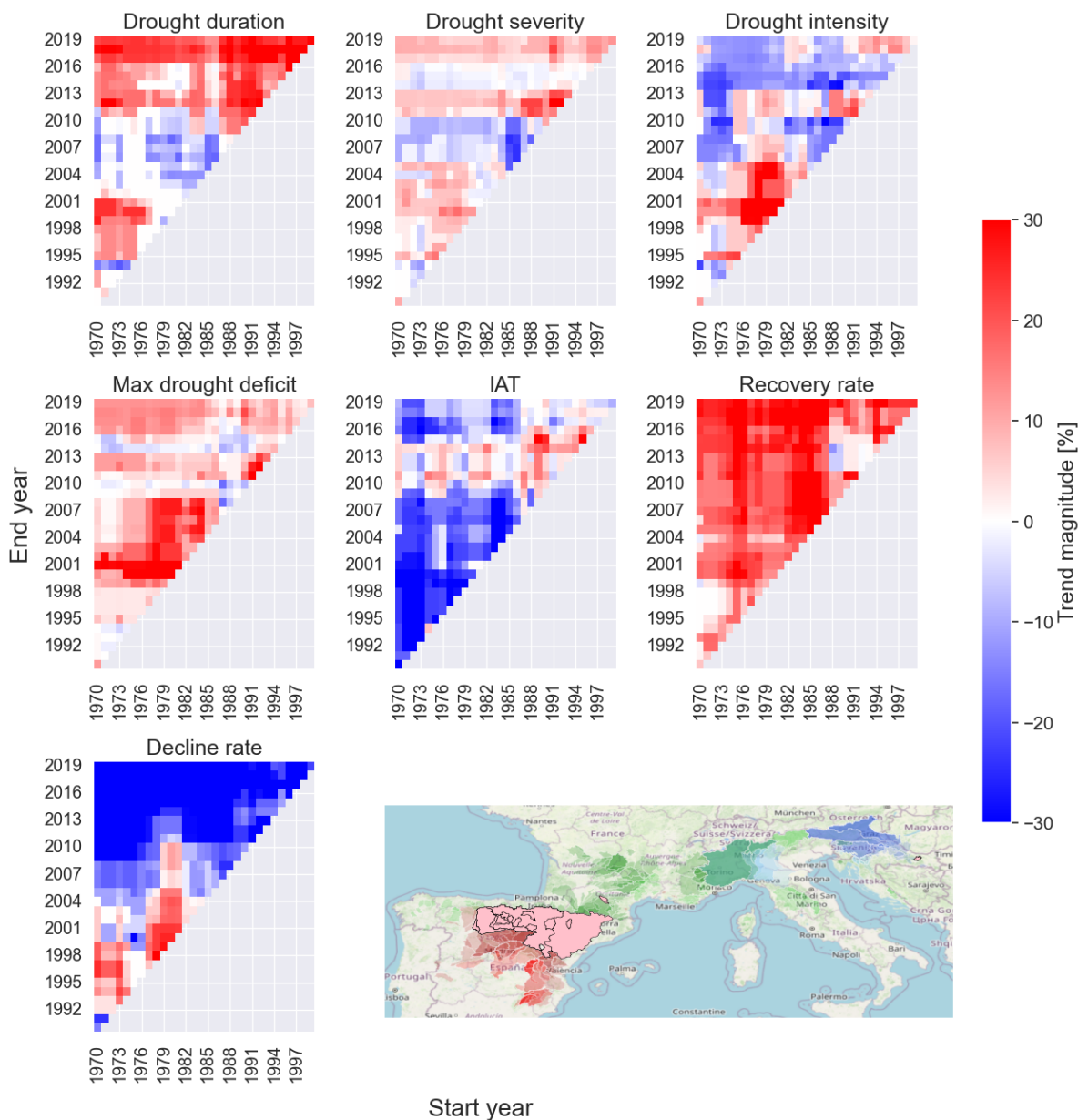


Figure 3.19: Multi-temporal analysis of median trends, expressed as percentage, in summer drought characteristics for river basins of class 7 (location shown in bottom right corner). The heatmap illustrates the magnitude of trends for all combinations of time periods between 1970-2019, with the x-axis representing the start year and the y-axis representing the end year of each time period. Red indicates increasing trends, while blue represents decreasing trends.

The river basins located from the southern part of the Ebro basin to the most southern Spanish basins were divided into three different climatic classes: class 7 (the southern Ebro basin), class 3 (central Spain: Tagus and Jucar basins) and class 5 (southern Spain: Jucar, Segura and Guadiana basins). Going from North to South a clear pattern and change in drought characteristic trends can be observed.

The river basins corresponding to class 7, which are basins mostly located in southern part of the Ebro basin, shows a less clear pattern across the multi-temporal analyses (Figure 3.19). The patterns in drought duration are almost identical to the overall summer trend, with no clear pattern before end years 2010 and a increasing pattern after. The drought severity and intensity trends do not show a clear pattern. Both characteristics experience highly fluctuating trend magnitudes, alternating between

negative and positive trend values. In contrast, the maximum drought deficit shows different results from the other characteristics. Whereas the intensity did not show a clear pattern in trends, the maximum drought deficit shows an almost entirely increasing trend across all time periods. Especially in the periods starting between 1976-1984 till 2008 have extremely high trend magnitudes reaching an 50% increase in maximum drought deficit. Additionally, the recovery rate undergoes an overall positive pattern regardless of the selected time period. Overall, based on these observations it can only be concluded that streamflow droughts are becoming longer but the changes in water availability are unclear and not significant.

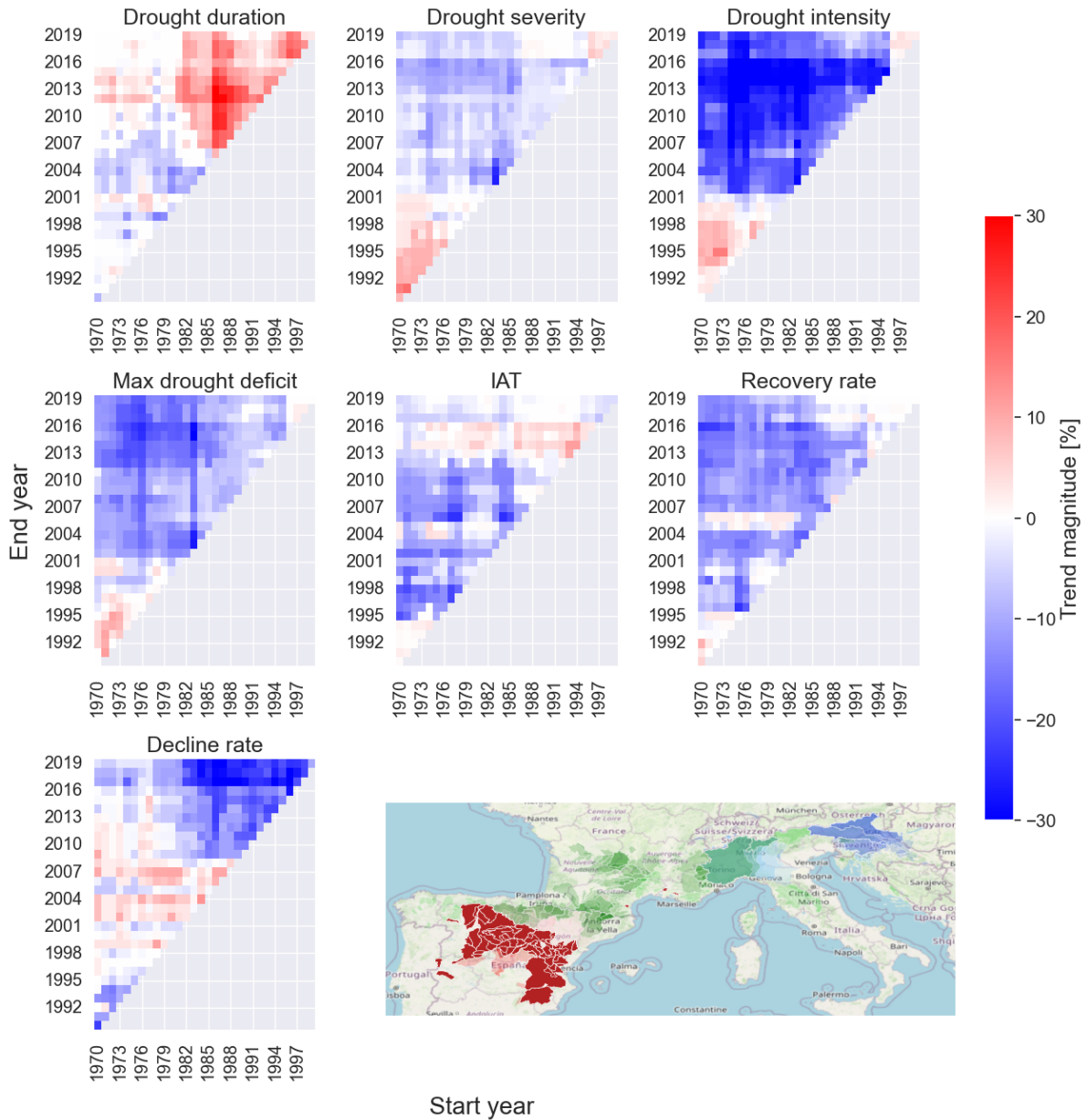


Figure 3.20: Multi-temporal analysis of median trends, expressed as percentage, in summer drought characteristics for river basins of class 3 (location shown in bottom right corner). The heatmap illustrates the magnitude of trends for all combinations of time periods between 1970-2019, with the x-axis representing the start year and the y-axis representing the end year of each time period. Red indicates increasing trends, while blue represents decreasing trends.

The multi-temporal analysis of drought duration for class 3 reveals a consistent pattern as the overall

summer trend, with increasing drought duration after 1988 (Figure 3.20). The trends of the drought severity, intensity and maximum deficit diverge from the overall summer trend and the other climatic classes. While for the previously analysed classes exhibited increasing trend magnitudes after 1988, these drought characteristics in class 3 do not undergo this shift. Instead, in the time periods with end years before 1998 they all experience an increase in trend magnitudes between 3-10%. However, the time periods starting from 1980 all experience overall negative trends, with some periods showing no trend. Notably, the drought intensity is decreasing significantly with values reaching -20%. The inter-arrival time and the decline rate follow the same trends as the overall summer trends. The recovery rate however shows an overall decrease.

Class 5 shows almost identical results to the multi-temporal analyses of class 3 (Figure 3.21). The main exceptions being that for class 5 the drought duration experiences an almost entire increasing pattern across all time periods, and the drought intensity and maximum deficit trends are entirely negative and more extreme, as values exceed -30%. Additionally, the inter-arrival time increases severely for time periods ending after 2004 and, similar to class 5, the recovery rate trends are almost entirely negative.

Similar to the results of other classes, streamflow droughts in river basins of classes 3 and 5 are getting longer. However, the severity and intensity have decreased significantly, leading to a higher water availability and reducing the negative consequences of streamflow droughts.

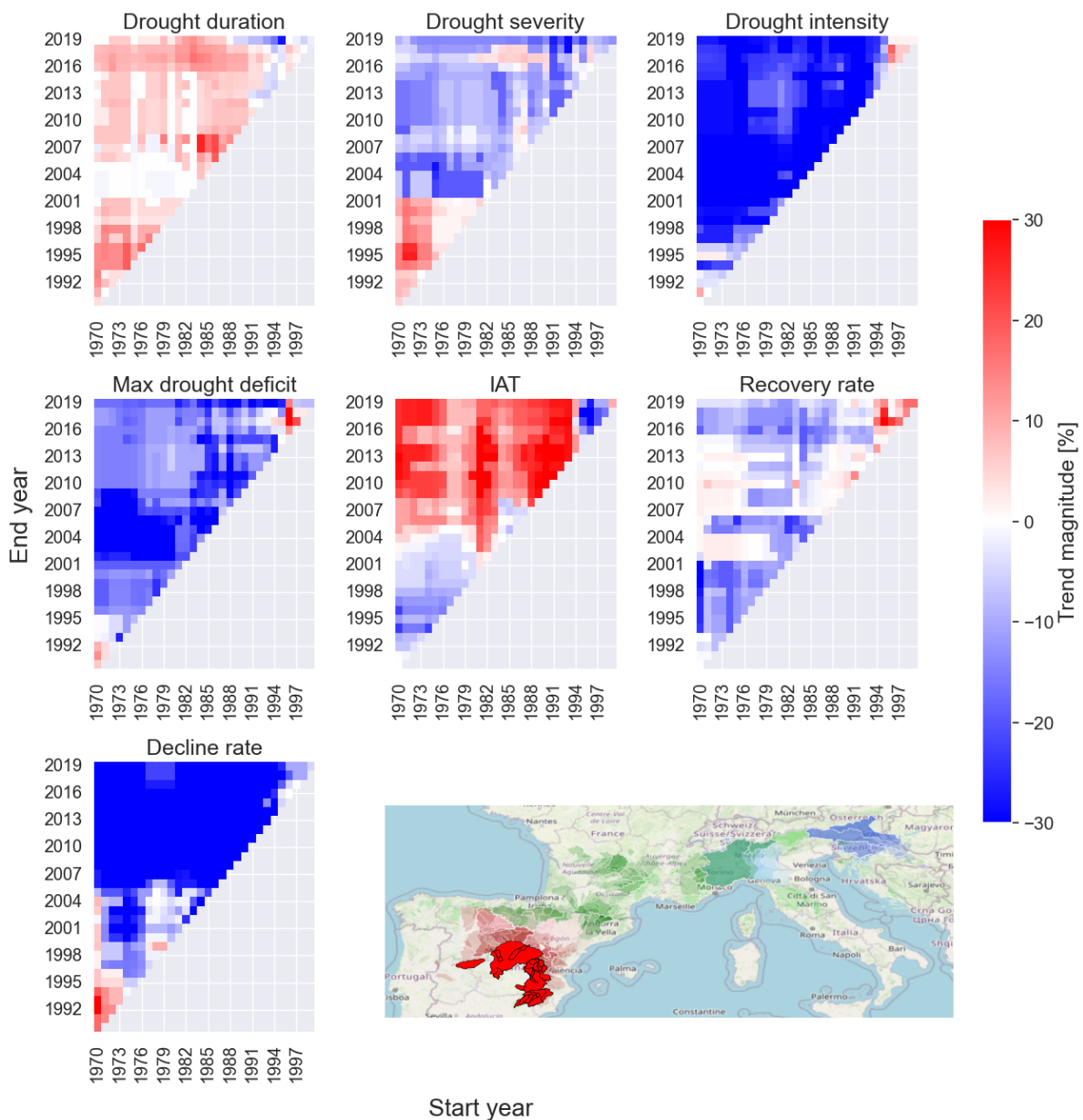


Figure 3.21: Multi-temporal analysis of median trends, expressed as percentage, in summer drought characteristics for river basins of class 5 (location shown in bottom right corner). The heatmap illustrates the magnitude of trends for all combinations of time periods between 1970-2019, with the x-axis representing the start year and the y-axis representing the end year of each time period. Red indicates increasing trends, while blue represents decreasing trends.

Overall, the summer streamflow droughts in the Mediterranean have become longer and more severe in the last 30 years. These patterns can be observed for the majority of the study area, including the classes 1, 2, 4 and 6, which encompass northern Spain, the Pyrenees, Southern France, Italy, Croatia and Slovenia. This will create more extreme summer drought events with a higher water deficit and less available water, leading to an amplification of the already limited water availability. On the other hand, Central and Southern Spain experience the opposite trends with a higher water availability during streamflow drought.

3.2.4. Spring & Fall Trends

The remaining two seasons, spring and fall, demonstrated similar patterns to winter and summer respectively and their results are therefore not included in this section but can be found in Appendix A.

Similar to the situation in winter, the drought characteristics for spring streamflow droughts exhibit mostly decreasing trends, though the negative trend magnitudes were less extreme. In fall, the temporal and spatial patterns in streamflow drought characteristics were a less pronounced version of the observed changes in summer streamflow droughts.

3.2.5. Summary

In general, the multi-temporal analyses resulted in changes for each streamflow drought characteristic across the entire study area and for each climatic class, both annually and seasonally. The annual trends showed only small changes towards slightly longer but less severe streamflow droughts.

However, the seasonal drought characteristics showed completely different results from the annual trends, with the most pronounced changes being observed in winter and summer. Since 1985, streamflow droughts in winter have become extremely less extreme. The water availability during drought events is higher and the drought events are shorter. Totally different are the results for summer streamflow droughts, which show that for the majority of the study area droughts have become more extreme and less water is available. The only exceptions being river basins in Central and Southern Spain, which experience an increase in water availability during periods of streamflow drought.

4

Discussion

4.1. Fixed vs. Multi-temporal trend analysis

In this research two distinct methods were performed to analyse trends in drought characteristics. The first used the traditional fixed time periods and the second applied the multi-temporal analysis, in which each possible combination of time periods was used. While initially the drought characteristics were analysed by the fixed time periods, it quickly became apparent that this method was insufficient for precisely capturing detailed temporal changes as it used only four time periods.

This issue became clear when comparing the results of the annual trend analysis for both methods. For example, the multi-temporal analysis resulted in increasing drought severity, intensity and maximum deficit between 1970 and 1995, but the fixed four time periods did not capture this pattern and showed negative values for each time period. Similarly, the seasonal multi-temporal analysis revealed patterns that would not have been noticed when using only four fixed periods.

These findings prove that trend analyses in general are very sensitive to the selected time periods, a conclusion that was also reached by Hannaford et al. (2021), who demonstrated the limitations of fixed-period trend analyses. But using a multi-temporal analysis mitigates this problem as it does not require the predefinition of time periods and instead analyses trends across all intervals. This method allows for a more precise and comprehensive understanding of drought trends over time. After it was determined that multi-temporal analyses would provide better results, this research continued with only this method to determine all seasonal changes and the changes across each climatic class.

4.2. Spatiotemporal changes in streamflow drought characteristics

In general, the multi-temporal analyses resulted in changes for each streamflow drought characteristic across the entire study area and for each climatic class, both annually and seasonally. The annual trends showed that, across the entire study area, streamflow droughts in the Mediterranean area remain mostly stable in drought duration and showed decreasing trends for the drought severity, intensity and maximum deficit.

Overall, these findings are surprising as the general consensus is that, due to annual precipitation decrease and temperature increase, droughts are getting more extreme and more frequent due to climate change (López-Moreno et al., 2009; Seneviratne et al., 2016). An explanation for this behaviour is that annual precipitation is not necessarily decreasing but mostly experiences a seasonal shift in precipitation. Therefore, it might not result in more extreme drought conditions annually. The only drought characteristic trend that agrees with that is the inter-arrival time which shows an overall decrease, meaning that there is less time between consecutive streamflow drought events, potentially resulting in a higher

drought frequency. The only regions for which more severe streamflow droughts are observed annually are river basins in Slovenia and Croatia classified as class 4. The streamflow droughts in these river basins are getting both longer and more severe.

The situation changes completely once looking at changes in seasonal drought characteristics. The most pronounced changes can be observed during the winter and summer months. Streamflow droughts occurring in winter have been showing a decrease in all major drought characteristics. The drought duration, severity, intensity and maximum deficit all experience a clear decrease in magnitude since 1985-1988. At the same point in time, the timing of winter streamflow droughts is moving towards earlier in the season. The majority of climatic classes follow these overall patterns for winter streamflow droughts, only the river basins in Slovenia and Croatia experience slight differences. For these basins a similar change towards negative trends is observed, however this change is less noticeable and is initiated later than for the overall winter trends. Overall, these changes in winter streamflow droughts align with the observed and predicted changes in winter precipitation and temperature. The seasonal precipitation during winter is increasing in large parts of the Mediterranean and expected to increase even further in the future (Giorgi and Lionello, 2008; MedECC, 2020). This increase in seasonal precipitation, either snowfall or rainfall, would lead to an increase in measured streamflow and could alleviate drought conditions and reduce streamflow drought severity. Additionally, temperatures are observed to be increasing during winter. This temperature shift could result in more precipitation in the form of rainfall instead of snow and the earlier melt of the snowpack, leading to more immediate runoff and less severe streamflow droughts. The multi-temporal analysis for the maximum winter drought timing also showed that winter droughts have been occurring earlier in winter. This pattern could support the statement that earlier snowmelt is a potential cause of the less severe winter droughts.

The analysis of streamflow drought conditions reveals contrasting trends between winter and summer seasons. While winter streamflow drought showed overall decreasing trends in streamflow drought conditions, summer presents a more concerning situation. Since 1988-1990, a clear change in summer streamflow drought characteristics is seen across the study area. The drought duration, severity, intensity and maximum deficit all increased. These trends coincide with the rapidly increasing summer temperatures across all of Europe including the Mediterranean (Brogli et al., 2019) and decreasing summer precipitation (MedECC, 2020). Time periods before this shifting point showed predominantly negative trends, which can be explained by the significant droughts afflicting the western Mediterranean in the 1980s and early 1990s (as noted by Cook et al. (2016)). Due to this period of severe droughts, all time periods that start during this period result in negative trends for the drought severity, intensity and maximum deficit. This does bring into question whether the observed increasing trends in drought characteristics in recent years represents the real long-term trend or whether this trend is only a temporary fluctuation influenced by earlier extreme drought periods. However, evaluating whether these are truly long-term trends requires a lot more data and additional work, and was therefore outside the scope of this thesis.

Spatially, the summer trends experience quite a few fluctuations between the different climatic classes. River basins belonging to classes 1 and 2, located in northern Spain, the Pyrenees, southern France and Italy, experience similar patterns to the overall summer trends but with more extreme trend magnitudes. These climatic regions are connected spatially spanning all river basins from the north of Spain to Croatia, and have in common that they are all characterized by a high annual precipitation.

The river basins located from the southern part of the Ebro basin to the most southern Spanish basins all experienced less extreme drought conditions, with decreasing severity, intensity and maximum deficit. The main difference between these classes and the rest of the study area is the fact that they are characterized by a lower annual precipitation. This pattern contrasts with the rest of the study area, where summer streamflow drought severity has generally increased since 1988-1990. This finding is sur-

prising as, similar to the rest of the study area, temperatures have been increasing and precipitation has been decreasing in these regions. Therefore similar responses in streamflow drought characteristics was expected. However, it can be partially explained by the fact that the central and southern sectors of the Iberian peninsula recorded one of the worst period of meteorological droughts during 2004-2005 (García-Herrera et al., 2007), which led to a reduction in streamflow in these regions. In the multi-temporal analysis this skewed the trend towards negative trends for drought severity for the more recent periods. While the rest of the study area experienced a shift towards increasing streamflow drought severity around 1988-1990, this same pattern could therefore not be observed here and continued its negative trend.

Another potential factor that could have reduced the severity of streamflow droughts in these regions is the impact of human activities or changes in water management practices. Spain has always had issues with sufficient water availability and therefore it has the highest density in reservoirs and dams in Europe in order to mitigate problems such as droughts. This could have led to more manageable and less impactful streamflow droughts events. An example of such a water management project is the Tagus-Segura Water Transfer that was completed in 1979. This transfer system transports water from the Tagus river basin to the more southern Segura basin in order to provide extra water availability for the drier regions. Lorenzo-Lacruz et al. (2013), who analysed the response of hydrological drought to meteorological drought in Spain, observed a decrease in streamflow drought duration and magnitude in the Segura basin following the implementation of this transfer system, which might partially explain the negative trends in drought severity for class 5.

4.3. Relationship between streamflow drought characteristics

The multi-temporal analyses for the drought characteristics showed clearly the relationship between the different drought characteristics. The drought severity is the accumulated deficit during a drought event and is therefore depended on the drought duration. Therefore, the drought duration and severity were assumed to have a positive relationship with each other. Meaning that with an increase in drought duration the severity increases as well, and vice versa. This positive correlation, partially due to auto-correlation as they are dependent variables, can be observed for most seasons when looking at the entire study area or the climatic regions. However, there are cases in which this pattern deviates. The multi-temporal analysis for spring streamflow droughts across the entire study area (Appendix A) showed trends towards longer but slightly less severe droughts. Similarly, this can be seen for classes 3 and 5, central and southern Spain, where summer streamflow droughts are becoming longer but less severe as well.

The drought intensity is depended on both the drought duration and severity, as it is defined as the average daily deficit during a drought event. In other words, it is computed by dividing the drought severity over the drought duration. As mentioned before, the drought duration and severity have a positive correlation with each other, but this does not necessarily indicate that drought intensity increases as well. Drought intensity increases when the severity rises more sharply than the duration, or when a reduction in duration is higher than the decrease in severity. In most cases the changes drought intensity showed a similar behaviour as the changes in drought severity. The only exception in this pattern is during spring, as even though the drought severity showed an increase over several time periods the drought duration increased relatively more, resulting in overall decreasing trends for intensity (Appendix A). Interesting to mention is the extreme reduction in drought intensity for summer streamflow droughts in classes 3 and 5. As mentioned before, these classes experienced longer but less severe droughts. The combination of the changes in these two drought characteristics led to the extreme decrease in intensity across all analysed time periods (Figure 3.20, 3.21).

While the drought intensity mostly follows the same changes as the drought severity, the maximum drought deficit has shown almost identical patterns as the drought intensity for each season. This was

to be expected to some extent as the maximum deficit is defined as the maximum daily deficit during a drought event, and is therefore closely related to the drought intensity.

The inter-arrival time is the only drought characteristic in this research that does not show a clear dependency on one of the other drought characteristics. As it is defined as the time between the timing of the onsets of two consecutive drought events, inter-arrival time trends indicate changes in the duration it takes for a new streamflow drought to start. Therefore, it gives an indication of the change in drought frequency. Both annually and seasonally, the inter-arrival time experienced a clear decrease across all selected time periods, suggesting that the frequency of streamflow droughts is increasing.

Finally, there is a relationship between the drought duration, maximum deficit, recovery rate and the decline rate. The recovery rate and the decline rate are the respective rates at which a streamflow 'recovers' after the peak of the drought and 'declines' before the peak of the drought is reached. These rates are mainly impacted by the maximum drought deficit and the drought duration. In general, an increase in the maximum drought deficit would lead to more extreme rates, as would a decrease in drought duration. For winter and spring this resulted in the expected outcome of less extreme rates, as the maximum deficit decreased and the duration either increased or decreased slower. However, summer and fall streamflow droughts, which are becoming longer with higher peaks, see a contradicting pattern in which the recovery rates are getting higher but the decline rates are getting less negative. This indicates that for these seasons the timing of the maximum deficit is shifting towards later in the drought event, which corresponds to their shift of seasonal drought timing (Figure 3.15).

4.4. Implications & Significance

All in all, the spatiotemporal changes in streamflow drought characteristics indicate that streamflow droughts certainly have changed over time. Consequently, the water availability during streamflow drought events has changed, affecting stakeholders relying on the water in the river system.

Between 1988 and 2019, the entirety of the study area (except for Slovenia/Croatia) experienced that streamflow droughts occurring in winter have become shorter, less severe, less intense and with lower peak deficits. During periods of streamflow drought, the total water deficit has decreased, the duration of streamflow droughts has become shorter, and both the average and maximum daily water deficits have reduced. Similar patterns are seen for spring streamflow droughts for the entire study area, observing reductions in severity, intensity and maximum deficits, only the duration of these droughts does not experience a decrease.

Practically, this implies that during periods of both winter and spring streamflow droughts more water is available compared to previous years. In winter, these periods of low water availability end sooner and therefore rivers return quicker to their normal flow. Additionally, for both seasons more water is available during the days with the most extreme water shortages than before. Overall, the shift in winter and spring streamflow drought characteristics results in a higher water availability during more recent drought events, which in turn will alleviate problems stemming from insufficient water resources.

Summer and fall streamflow droughts experienced the exact opposite pattern to the changes in winter and spring droughts. In the same period, from 1988-2019, summer and fall streamflow droughts have become longer, more severe, more frequent, more intense and with higher peak deficits. This pattern is observed for Northern Spain, the Pyrenees, Southern France, Croatia and Slovenia. Only Central and Southern Spain show deviations from this pattern, showing decreasing trends in these characteristics.

This means that for most of the Mediterranean less water is available compared to earlier years during summer and fall streamflow droughts. These drought events have become longer, extending periods of severely lower water availability. On top of that, as the intensity and maximum deficit are increasing, the average and maximum daily water shortage have become larger resulting in even lower river flow

levels, reducing the water availability and increasing the stress on water resources. As summer already is the season with the highest water demand, which is expected to increase further in the future, the even lower water availability during summer streamflow droughts will intensify problems related to the management of water resources. The increased pressure on available water resources during the critical summer months can lead to higher water shortages and increased competition for water. This will lead to problems in ensuring a sufficient water supply for both ecosystems and human water demand.

Overall, the different trends in winter/spring and summer/fall drought characteristics highlight the complexity of streamflow droughts and their changing impact on available water resources. While the increased water availability in winter and spring streamflow droughts offer some relief, the worsening summer and fall droughts present growing challenges for future water management to ensure sufficient water availability. However, while summer conditions are becoming more extreme with increasing water deficits, it is important to note that more water is becoming available during winter and spring. This presents an opportunity to store additional water during these wetter seasons, which could help mitigate the growing severity of summer droughts.

4.5. Limitations & Uncertainties

The EStreams dataset offers a dynamic collection of streamflow data from 17,130 gauges across Europe from over 50 different providers. While this does result in the most up-to-date and dense data, it is less accurately tested for quality checks. As it is from different data providers, the measuring techniques can differ significantly, leading to potential inconsistencies. This can in turn lead to uncertainty when deriving streamflow droughts from the data. Additionally, providers vary in their data collection frequency, some might monitor continuously, while others conduct manual measurements. Calibration standards also differ, which can introduce bias over time. Moreover, many providers do not include quality flags with their data, making it difficult to identify errors. Despite EStreams conducting quality checks on each data record to assess reliability, uncertainties remain due to these factors.

National providers also rarely made available catchment boundary shapefiles and typically only provide information on the catchment area. To address this gap, EStreams determined the catchment boundaries and included the corresponding shapefiles in the dataset. However, discrepancies have been noted between the areas reported by the providers and the areas represented in the EStreams shapefiles. This inconsistency introduces uncertainty regarding the precise catchment area, which is particularly important for aggregating the meteorological E-OBS data.

E-OBS is an observational dataset derived from the interpolation of in-situ measurements supplied by national providers. Similar to streamflow data, uncertainties arise from potential differences in measuring methods among providers. However, the most significant source of uncertainty in the E-OBS dataset is station density. Since the data relies on interpolation between measurement stations, higher station density typically leads to more accurate and reliable results. Unfortunately, this density varies considerably across regions, with notably lower station density observed in countries like Spain (218) and Croatia (14) compared to France (1100+) and Italy (1400+)

The study area for this research was originally the entire Mediterranean area. However, streamflow data availability was quite limited in many parts of the area. Northern Africa and the eastern Mediterranean region did not have any available streamflow data spanning over 30 years before 2019, which was set as the minimum data requirement for the trend analysis. Meaning that the research area was centred around the western Mediterranean area and does not give a representation of changes in streamflow droughts across the entire Mediterranean, which potentially could have resulted in different spatial patterns.

Another aspect that creates uncertainty in the analysis is the limited number of streamflow drought events per season. This issue is not caused due to limited streamflow data availability, but relates to how streamflow droughts are not an often occurring event and therefore streamflow drought events are

limited in number. By dividing the annual streamflow droughts into separate seasons, the number of drought events per basin for each season can be quite low. This results in identified trends becoming more sensitive to the selected time periods, which can in turn affect the robustness of the observed trends.

Additionally, the method of streamflow drought quantification could have introduced uncertainty. During the drought quantification several assumptions were made, such as defining ‘below-normal’ streamflow as all daily streamflow data below the monthly 80th percentile, or setting the required minimum drought duration to one week to avoid minor droughts. Although these choices are commonly used in literature, it does introduce uncertainty to the results. Even though scientific literature suggested that the overall trends in drought characteristics would not be affected significantly by these choices, it does impact it to some extent. For example, a different threshold (e.g. 90th or 95th percentile) would determine less frequent but more extreme streamflow droughts, which could experience different trends in their drought characteristics. Similarly, another parameter for the minimum drought duration could result in different quantified drought characteristics and their change over time.

Given these assumptions, determining the sensitivity to these chosen parameters was not in the scope of this research, but could be important for future studies. For that reason, it is suggested to perform an uncertainty analysis to test different thresholds or minimum drought duration to analyse whether the same trends in streamflow drought characteristics can be observed as in this research.

Another topic of discussion is the way trends in streamflow droughts are determined. In the current situation, trends are analysed assuming that there is a streamflow drought, disregarding periods without streamflow drought. As a result, the intervals between consecutive drought events vary, periods without drought are not considered, and multiple droughts can occur in the same year. This introduces uncertainty into the results of the multi-temporal analyses.

To address this issue and validate the results, the multi-temporal analyses were repeated using three different methods to analyse the changes in streamflow drought:

- **Mean annual streamflow drought:** This method calculates the trend over the average annual streamflow drought, focusing only on years with drought events.
- **Mean annual streamflow drought (including years with no drought):** This method calculates the trend over the average annual streamflow drought, focusing on all years, even those without drought, to provide a more comprehensive analysis.
- **Mean seasonal streamflow drought:** This method calculates the trend over the mean seasonal streamflow drought, focusing only on years with drought events.

Overall, the multi-temporal analyses for these different ways result in very similar patterns in drought characteristics to the original results. Figure B.10 and B.11 show the mean annual streamflow drought trends with and without including years with no drought events (as zero value). In both cases, the overall patterns closely match the original annual trends, although the mean annual streamflow drought trends show slightly more extreme values. For instance, the drought duration does not show the same period of stable trends for starting years between 1983-1990 but instead shows slightly negative trends. Additionally, the positive and negative trends reach up to 30% and -30% respectively, which are slightly more extreme than before.

When including the years with no drought events into the trend analysis, the overall patterns remain largely the same. However, due to inclusion of many years with no drought events, the multi-temporal analyses have more zero trends. The extreme case of this can be observed for class 3, where the number of years without drought was so high that this resulted in multi-temporal analyses almost completely filled with zero trends (Figure B.12).

Similar to the annual trends, the seasonal trends were compared to the trends in mean seasonal streamflow drought as well. As most seasons did not have more than one streamflow drought per year, the results are almost identical to the original results (see Figures B.14 and B.13). An additional analysis was performed to assess the impact of including years without seasonal drought as zero. However, as the number of seasonal droughts is small it resulted in many zero values and therefore completely ‘zero’ multi-temporal analyses for all regions.

Overall, these analyses show similar patterns as the original results, effectively validating those findings. This similarity was observed for both the annual and seasonal streamflow droughts. However, when years without drought were included in the analysis, the resulting patterns were often dominated by zero values, making this approach less useful for comparison with the original results.

5

Conclusion

This study determined how streamflow droughts have changed based on their characteristics across the Mediterranean in the time period of 1970-2019, as posed in the research question in Chapter 1.4.

The main findings of this research are:

- Considering droughts throughout the entire year, streamflow droughts across the Mediterranean have become less severe and intense since 1979, while their duration has become longer between 1995 and 2019. The main exception is in the river basins of class 4 (Slovenia/Croatia), which are experiencing a 15% increase in severity compared to the 1970s.
- Winter streamflow droughts are becoming less extreme across the Mediterranean. Since 1988, winter streamflow droughts show sharp decreases in drought duration, severity, intensity, and maximum deficit (up to -30%). This pattern is consistent across all river basins in the study area, with the only exception being basins of class 6 (Croatia/Po basin), which recorded longer and more severe winter streamflow droughts.
- Since 1990, summer streamflow droughts have exhibited contrasting patterns across the Mediterranean. Summer streamflow droughts have become more extreme in duration, severity, intensity, and maximum deficit for classes 1, 2, 4, and 6, which cover the majority of the study area including all river basins from Northern Spain, the Pyrenees, Southern France, Italy, Slovenia, and Croatia. The most extreme changes in these characteristics are observed for class 1 in the Pyrenees, Southern France, and Italy, with values ranging between 20-30% and reaching up to 35-40% for the drought duration. In contrast, summer streamflow droughts for river basins in classes 3 and 5 (Central and Southern Spain) have shown the opposite trend, becoming less severe, less intense, and with less extreme peaks. Severity values decreased by -5 to -15%, while intensity and maximum deficit decreased by -20 to -40%.
- Streamflow droughts in spring and fall follow the similar patterns as winter and summer respectively but with less pronounced changes, showing less extreme droughts in spring and more extreme droughts in fall.

Overall, it can be concluded that streamflow droughts in the Mediterranean certainly are changing, no matter the specific drought characteristic. However, the extend of these changes fluctuate a lot depending on the studied time period, the seasonality of the streamflow droughts and the specific region being analysed.

Bibliography

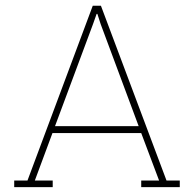
- Altin, T. B. and Altin, B. N. (2021). Response of hydrological drought to meteorological drought in the eastern mediterranean basin of turkey. *Journal of Arid Land*, 13:470–486. doi: 10.1007/s40333-021-0064-7.
- Behrangi, A., Fetzer, E. J., and Granger, S. L. (2016). Early detection of drought onset using near surface temperature and humidity observed from space. *International Journal of Remote Sensing*, 37. doi: 10.1080/01431161.2016.1204478.
- Berghuijs, W. R. and Woods, R. A. (2016). A simple framework to quantitatively describe monthly precipitation and temperature climatology. *International Journal of Climatology*, 36. doi: 10.1002/joc.4544.
- Brogli, R., Sørland, S. L., Kröner, N., and Schär, C. (2019). Causes of future mediterranean precipitation decline depend on the season. *Environmental Research Letters*, 14. doi: 10.1088/1748-9326/ab4438.
- Brunner, M. I., Loon, A. F. V., and Stahl, K. (2022). Moderate and severe hydrological droughts in europe differ in their hydrometeorological drivers. *Water Resources Research*, 58. doi: 10.1029/2022WR032871.
- Cook, B. I., Anchukaitis, K. J., Touchan, R., Meko, D. M., and Cook, E. R. (2016). Spatiotemporal drought variability in the mediterranean over the last 900 years. *Journal of Geophysical Research*, 121. doi: 10.1002/2015JD023929.
- Cornes, R. C., van der Schrier, G., van den Besselaar, E. J., and Jones, P. D. (2018). An ensemble version of the e-obs temperature and precipitation data sets. *Journal of Geophysical Research: Atmospheres*, 123. doi: 10.1029/2017JD028200.
- Cramer, W., Guiot, J., Fader, M., Garrabou, J., Gattuso, J. P., Iglesias, A., Lange, M. A., Lionello, P., Llasat, M. C., Paz, S., Peñuelas, J., Snoussi, M., Toreti, A., Tsimplis, M. N., and Xoplaki, E. (2018). Climate change and interconnected risks to sustainable development in the mediterranean. doi: 10.1038/s41558-018-0299-2.
- de Dios Gomez-Gomez, J., Pulido-Velazquez, D., Collados-Lara, A. J., and Fernandez-Chacon, F. (2022). The impact of climate change scenarios on droughts and their propagation in an arid mediterranean basin. a useful approach for planning adaptation strategies. *Science of the Total Environment*, 820. doi: 10.1016/j.scitotenv.2022.153128.
- do Nascimento, T. V. M., Rudlang, J., Höge, M., van der Ent, R., Chappon, M., Seibert, J., Hrachowitz, M., and Fenicia, F. (2024). Estreams: An integrated dataset and catalogue of streamflow, hydroclimatic variables and landscape descriptors for europe (v.0.1.0). *Zenodo*.
- Fleig, A. K., Tallaksen, L. M., Hisdal, H., and Demuth, S. (2006). A global evaluation of streamflow drought characteristics. *Hydrology and Earth System Sciences*, 10. doi: 10.5194/hess-10-535-2006.
- Galea, A. B., Sadler, J. P., Hannah, D. M., Datry, T., and Dugdale, S. J. (2019). Mediterranean intermit-

- tent rivers and ephemeral streams: Challenges in monitoring complexity. *Ecohydrology*, 12. doi: 10.1002/eco.2149.
- García-Herrera, R., Paredes, D., Trigo, R. M., Trigo, I. F., Hernández, E., Barriopedro, D., and Mendes, M. A. (2007). The outstanding 2004/05 drought in the iberian peninsula: Associated atmospheric circulation. *Journal of Hydrometeorology*, 8. doi: 10.1175/JHM578.1.
- Giorgi, F. (2006). Climate change hot-spots. *Geophysical Research Letters*, 33. doi: 10.1029/2006GL025734.
- Giorgi, F. and Lionello, P. (2008). Climate change projections for the mediterranean region. *Global and Planetary Change*, 63. doi: 10.1016/j.gloplacha.2007.09.005.
- Gonzalez-Cebrian, P. (2024). Catalonia declares drought emergency in 202 municipalities, including barcelona and girona. <https://smartwatermagazine.com/news/smart-water-magazine/catalonia-declares-drought-emergency-202-municipalities-including>.
- Hannaford, J., Lloyd-Hughes, B., Keef, C., Parry, S., and Prudhomme, C. (2011). Examining the large-scale spatial coherence of european drought using regional indicators of precipitation and streamflow deficit. *Hydrological Processes*, 25. doi: 10.1002/hyp.7725.
- Hannaford, J., Mastrantonas, N., Vesuviano, G., and Turner, S. (2021). An updated national-scale assessment of trends in uk peak river flow data: How robust are observed increases in flooding? *Hydrology Research*, 52. doi: 10.2166/nh.2021.156.
- Harrigan, S., Hannaford, J., Muchan, K., and Marsh, T. J. (2018). Designation and trend analysis of the updated uk benchmark network of river flow stations: The ukbn2 dataset. *Hydrology Research*, 49. doi: 10.2166/nh.2017.058.
- Herrero, J., Polo, M. J., Moñino, A., and Losada, M. A. (2009). An energy balance snowmelt model in a mediterranean site. *Journal of Hydrology*, 371. doi: 10.1016/j.jhydrol.2009.03.021.
- Hisdal, H., Stahl, K., Tallaksen, L. M., and Demuth, S. (2001). Have streamflow droughts in europe become more severe or frequent? *International Journal of Climatology*, 21. doi: 10.1002/joc.619.
- Hughes, R. A. (2022). Italy's water crisis sees archeological remains emerge from drought-stricken rivers. <https://www.forbes.com/sites/rebeccahughes/2022/07/16/italys-water-crisis-sees-archeological-remains-emerge-from-drought-stricken-rivers/>.
- IPCC (2014). *Climate Change 2014: Synthesis Report*. IPCC, Geneva, Switzerland.
- Lionello, P. and Scarascia, L. (2018). The relation between climate change in the mediterranean region and global warming. *Regional Environmental Change*, 18. doi: 10.1007/s10113-018-1290-1.
- Lorenzo-Lacruz, J., Vicente-Serrano, S. M., González-Hidalgo, J. C., López-Moreno, J. I., and Cortesi, N. (2013). Hydrological drought response to meteorological drought in the iberian peninsula. *Climate Research*, 58:117–131. doi: 10.3354/cr01177.
- López-Moreno, J. I., Vicente-Serrano, S. M., Gimeno, L., and Nieto, R. (2009). Stability of the seasonal distribution of precipitation in the mediterranean region: Observations since 1950 and projections for the 21st century. *Geophysical Research Letters*, 36. doi: 10.1029/2009GL037956.
- Masseroni, D., Camici, S., Cislighi, A., Vacchiano, G., Massari, C., and Brocca, L. (2021). The 63-year changes in annual streamflow volumes across europe with a focus on the mediterranean basin. *Hydrology and Earth System Sciences*, 25. doi: 10.5194/hess-25-5589-2021.

- MedECC (2020). Climate and environmental change in the mediterranean basin - current situation and risks for the future, first mediterranean assessmnet report.
- Merheb, M., Moussa, R., Abdallah, C., Colin, F., Perrin, C., and Baghdadi, N. (2016). Hydrological response characteristics of mediterranean catchments at different time scales: a meta-analysis. *Hydrological Sciences Journal*, 61:2520–2539. doi: 10.1080/02626667.2016.1140174.
- Milly, P. C., Dunne, K. A., and Vecchia, A. V. (2005). Global pattern of trends in streamflow and water availability in a changing climate. *Nature*, 438. doi: 10.1038/nature04312.
- Morán-Tejeda, E., Ceballos-Barbancho, A., and Llorente-Pinto, J. M. (2010). Hydrological response of mediterranean headwaters to climate oscillations and land-cover changes: The mountains of duero river basin (central spain). *Global and Planetary Change*, 72. doi: 10.1016/j.gloplacha.2010.03.003.
- Ohlson, J. A. and Kim, S. (2015). Linear valuation without ols: the theil-sen estimation approach. *Review of Accounting Studies*, 20. doi: 10.1007/s11142-014-9300-0.
- Orlowsky, B. and Seneviratne, S. I. (2012). Global changes in extreme events: Regional and seasonal dimension. *Climatic Change*, 110. doi: 10.1007/s10584-011-0122-9.
- Pandey, R. P., Mishra, S. K., Singh, R., and Ramasastri, K. S. (2008). Streamflow drought severity analysis of betwa river system (india). *Water Resources Management*, 22. doi: 10.1007/s11269-007-9216-6.
- Raphaëlle, M. C. (2023). A comparison analysis: the 2022 drought on the rhone and the po basins. *Politecnico di Torino, Corso di laurea magistrale in Ingegneria Per L'Ambiente E Il Territorio*. <https://webthesis.biblio.polito.it/29158/>.
- Russo, A., Gouveia, C. M., Dutra, E., Soares, P. M., and Trigo, R. M. (2019). The synergy between drought and extremely hot summers in the mediterranean. *Environmental Research Letters*, 14. doi: 10.1088/1748-9326/aaf09e.
- Sen, P. K. (1968). Estimates of the regression coefficient based on kendall's tau. *Journal of the American Statistical Association*, 63. doi: 10.1080/01621459.1968.10480934.
- Seneviratne, S. I., Donat, M. G., Pitman, A. J., Knutti, R., and Wilby, R. L. (2016). Allowable co2 emissions based on regional and impact-related climate targets. *Nature*, 529. doi: 10.1038/nature16542.
- Seneviratne, S. I., Nicholls, N., Easterling, D., Goodess, C. M., Kanae, S., Kossin, J., Luo, Y., Marengo, J., Innes, K. M., Rahimi, M., Reichstein, M., Sorteberg, A., Vera, C., Zhang, X., Rusticucci, M., Semenov, V., Alexander, L. V., Allen, S., Benito, G., Cavazos, T., Clague, J., Conway, D., Della-Marta, P. M., Gerber, M., Gong, S., Goswami, B. N., Hemer, M., Huggel, C., den Hurk, B. V., Kharin, V. V., Kitoh, A., Tank, A. M. K., Li, G., Mason, S., Guire, W. M., Oldenborgh, G. J. V., Orlowsky, B., Smith, S., Thiaw, W., Velegrakis, A., Yiou, P., Zhang, T., Zhou, T., and Zwiers, F. W. (2012). Changes in climate extremes and their impacts on the natural physical environment. *Managing the Risks of Extreme Events and Disasters to Advance Climate Change Adaptation: Special Report of the Intergovernmental Panel on Climate Change*, 9781107025066. doi: 10.1017/CBO9781139177245.006.
- Sheffield, J., Wood, E. F., and Roderick, M. L. (2012). Little change in global drought over the past 60 years. *Nature*, 491. doi: 10.1038/nature11575.
- Stahl, K., Hisdal, H., Hannaford, J., Tallaksen, L. M., Lanen, H. A. V., Sauquet, E., Demuth, S., Fend-

- ekova, M., and Jodar, J. (2010). Streamflow trends in europe: Evidence from a dataset of near-natural catchments. *Hydrology and Earth System Sciences*, 14. doi: 10.5194/hess-14-2367-2010.
- Stahl, K., Tallaksen, L. M., Hannaford, J., and Lanen, H. A. V. (2012). Filling the white space on maps of european runoff trends: Estimates from a multi-model ensemble. *Hydrology and Earth System Sciences*, 16. doi: 10.5194/hess-16-2035-2012.
- Tallaksen, L. M., Hisdal, H., and Lanen, H. A. (2009). Space-time modelling of catchment scale drought characteristics. *Journal of Hydrology*, 375. doi: 10.1016/j.jhydrol.2009.06.032.
- Tallaksen, L. M., Madsen, H., and Clausen, B. (1997). On the definition and modelling of streamflow drought duration and deficit volume. *Hydrological Sciences Journal*, 42. doi: 10.1080/02626669709492003.
- Tallaksen, L. M. and van Lanen, H. A. (2023). Hydrological drought: Processes and estimation methods for streamflow and groundwater, second edition. *Hydrological Drought: Processes and Estimation Methods for Streamflow and Groundwater, Second Edition*. doi: 10.1016/C2017-0-03464-X.
- Tate, E. L. and Freeman, S. N. (2000). Three modelling approaches for seasonal streamflow droughts in southern africa: the use of censored data. *Hydrological Sciences Journal*, 45. doi: 10.1080/02626660009492304.
- Theil, H. (1992). A rank-invariant method of linear and polynomial regression analysis. *Advanced Studies in Theoretical and Applied Econometrics*. doi: 10.1007/978-94-011-2546-8_20.
- Tramblay, Y., Koutroulis, A., Samaniego, L., Vicente-Serrano, S. M., Volaire, F., Boone, A., Page, M. L., Llasat, M. C., Albergel, C., Burak, S., Cailleret, M., Kalin, K. C., Davi, H., Dupuy, J. L., Greve, P., Grillakis, M., Hanich, L., Jarlan, L., Martin-StPaul, N., Martínez-Vilalta, J., Mouillot, F., Pulido-Velazquez, D., Quintana-Seguí, P., Renard, D., Turco, M., Türkeş, M., Trigo, R., Vidal, J. P., Vilagrosa, A., Zribi, M., and Polcher, J. (2020). Challenges for drought assessment in the mediterranean region under future climate scenarios. *Earth-Science Reviews*, 210. doi: 10.1016/j.earscirev.2020.103348.
- UN (2022). World urbanization prospects - population division. <https://population.un.org/wup/>.
- Van Loon, A. (2013). On the propagation of drought. how climate and catchment characteristics influence hydrological drought development and recovery. *Graduate School of WIMEK-SENSE*.
- Van Loon, A. F. (2015). Hydrological drought explained. *Wiley Interdisciplinary Reviews: Water*, 2:359–392. doi: 10.1002/WAT2.1085.
- Van Loon, A. F. and Van Lanen, H. A. (2012). A process-based typology of hydrological drought. *Hydrology and Earth System Sciences*, 16:1915–1946. doi: 10.5194/hess-16-1915-2012.
- Vidal, J. P., Martin, E., Franchistéguy, L., Habets, F., Soubeyroux, J. M., Blanchard, M., and Baillon, M. (2010). Multilevel and multiscale drought reanalysis over france with the safran-isba-modcou hydrometeorological suite. *Hydrology and Earth System Sciences*, 14. doi: 10.5194/hess-14-459-2010.
- Vogel, J., Paton, E., Aich, V., and Bronstert, A. (2021). Increasing compound warm spells and droughts in the mediterranean basin. *Weather and Climate Extremes*, 32. doi: 10.1016/j.wace.2021.100312.
- Wilks, J. (2024). Can catalonia learn to live with drought? <https://www.euronews.com/green/2024/03/18/can-catalonia-learn-to-live-with-drought>.
- Zhang, X., Hao, Z., Singh, V. P., Zhang, Y., Feng, S., Xu, Y., and Hao, F. (2022). Drought propagation

under global warming: Characteristics, approaches, processes, and controlling factors. *Science of the Total Environment*, 838. doi: 10.1016/j.scitotenv.2022.156021.



Spring & Fall trends

A.1. Spring

The multi-temporal analyses for the drought characteristics during the spring season show predominantly negative overall trends, as can be seen in the results for five out of the seven drought characteristics (Figure A.1). The drought intensity, maximum deficit, inter-arrival time, recovery rate and decline rate all show an almost entirely negative ensemble of decreasing trend magnitudes. The drought intensity and maximum deficit reach similar trend magnitudes mostly ranging from -2 to -8%. The inter-arrival time, recovery rate and decline rate experience more extreme negative trends compared to the intensity and maximum deficit, with trend magnitudes reaching around -20% for certain time periods.

The drought duration and drought severity show experience different temporal changes than the other characteristics. The drought duration undergoes no change for the time periods with ending years between 1996-2004, but for all time periods with ending years after 2004 the multi-temporal analysis shows an almost overall increasing trend, with the highest trend magnitudes, ranging 5-12%, for the time periods with ending years between 2004-2014. Whereas all other drought characteristics experience a clear pattern towards either decreasing or increasing trends, the drought severity does not show a similar pattern. For the drought severity, the multi-temporal analyses results in an unclear pattern with trend magnitudes fluctuating between negative and positive values. Time periods with ending years between 1990-1995 demonstrate an increase, followed by a decreasing pattern for time periods ending from 1998-2004, a mostly zero and slight positive pattern for time periods ending from 2005-2013 and decreasing again for all time periods ending after 2013. Overall, the trend magnitudes for the severity do not reach quite extreme values and fluctuate in the range of -5 to 5%.

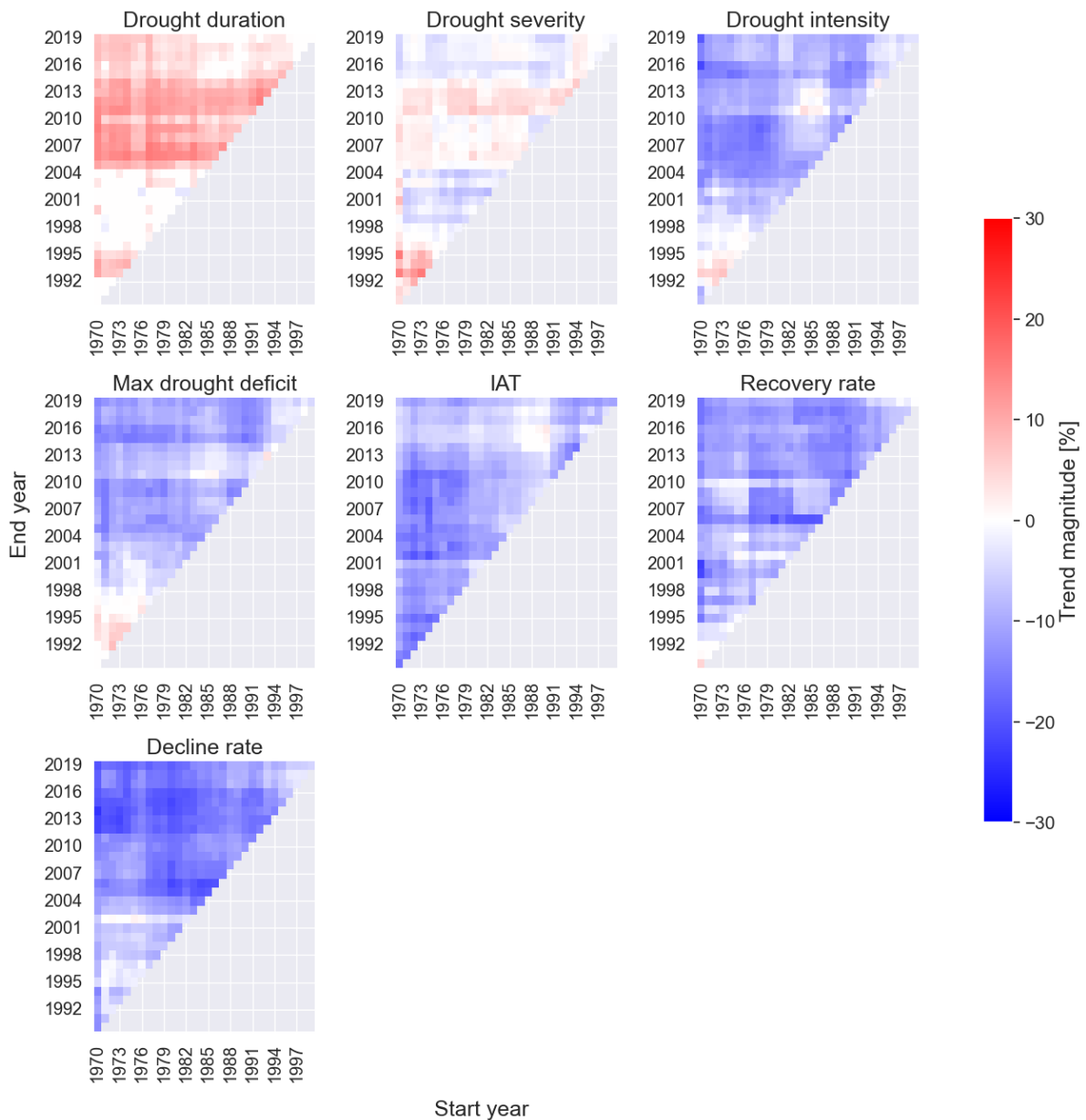


Figure A.1: Multi-temporal analysis of spring median trends for each drought characteristic, expressed as a percentage, across all river basins. The heatmap illustrates the magnitude of trends for all combinations of time periods between 1970-2019, with the x-axis representing the start year and the y-axis representing the end year of each time period. Red indicates increasing trends, while blue represents decreasing trends.

Figure A.2 demonstrates the changes in spring streamflow drought timing. Overall, most time periods have either a negative or zero trend magnitude. The time periods starting between 1982-1990 experience the most severe change as trend magnitudes go up to -0.4 days/year.

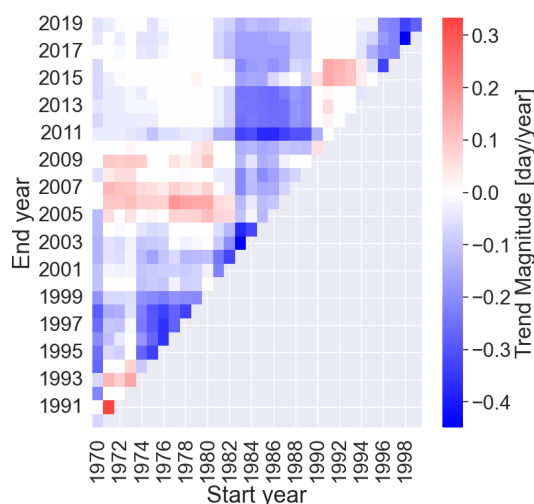


Figure A.2: Multi-temporal analysis of median trends in spring drought timing, expressed in day/year, across all river basins. The heatmap illustrates the magnitude of trends for all combinations of time periods between 1970-2019, with the x-axis representing the start year and the y-axis representing the end year of each time period. Red indicates increasing trends, while blue represents decreasing trends.

These patterns in drought characteristics during for the entire study area can be observed in the majority of climatic classes as well. The main differences are observed in the multi-temporal analyses for class 2 (Figure A.3). River basins of class 2 see an overall increase in drought severity during spring with values reaching up to 22%. This increase in drought severity and the unchanged increase in drought duration impacted the drought intensity as the majority of time periods now show positive increasing trend values. The maximum drought deficit changed in a similar way as the drought intensity, however as the changes were less severe the pattern does not show a clear pattern towards either positive or negative.

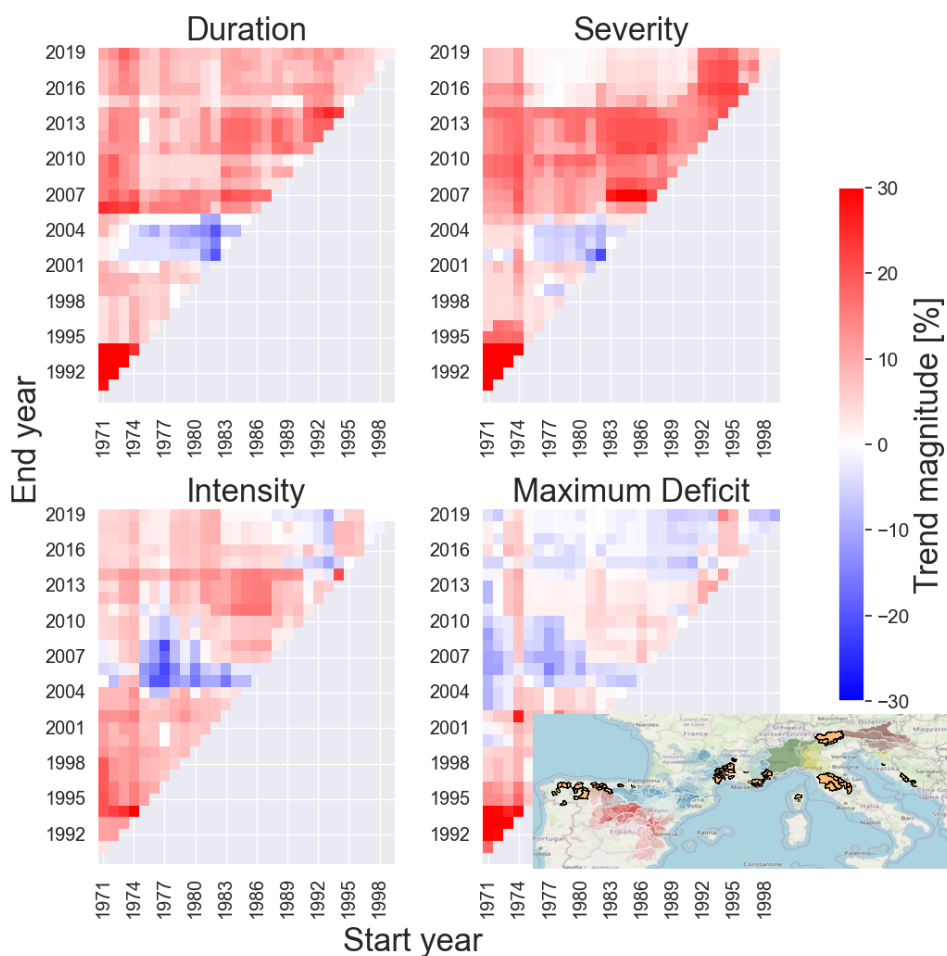


Figure A.3: Multi-temporal analysis of median trends, expressed as percentage, in spring drought characteristics for river basins of class 2. The heatmap illustrates the magnitude of trends for all combinations of time periods between 1970-2019, with the x-axis representing the start year and the y-axis representing the end year of each time period. Red indicates increasing trends, while blue represents decreasing trends.

A.2. Fall

The overall patterns for the entire study area during fall show almost identical patterns as the overall trend results from the summer season (Figure A.4). Similar to the summer patterns, the multi-temporal analyses for the drought duration, severity, intensity and maximum deficit experience a shift from negative to positive trends around 1988-1990. However, whereas the summer drought characteristics reached trend magnitudes up to 20-30%, the positive trend values for fall were less extreme ranging between 5-10%.

The temporal patterns for the inter-arrival time, recovery rate and decline rate were similar to those of summer as well, as the inter-arrival time and decline rate were predominantly negative and the recovery rate experiences a shift towards positive trends after 1988 as well.

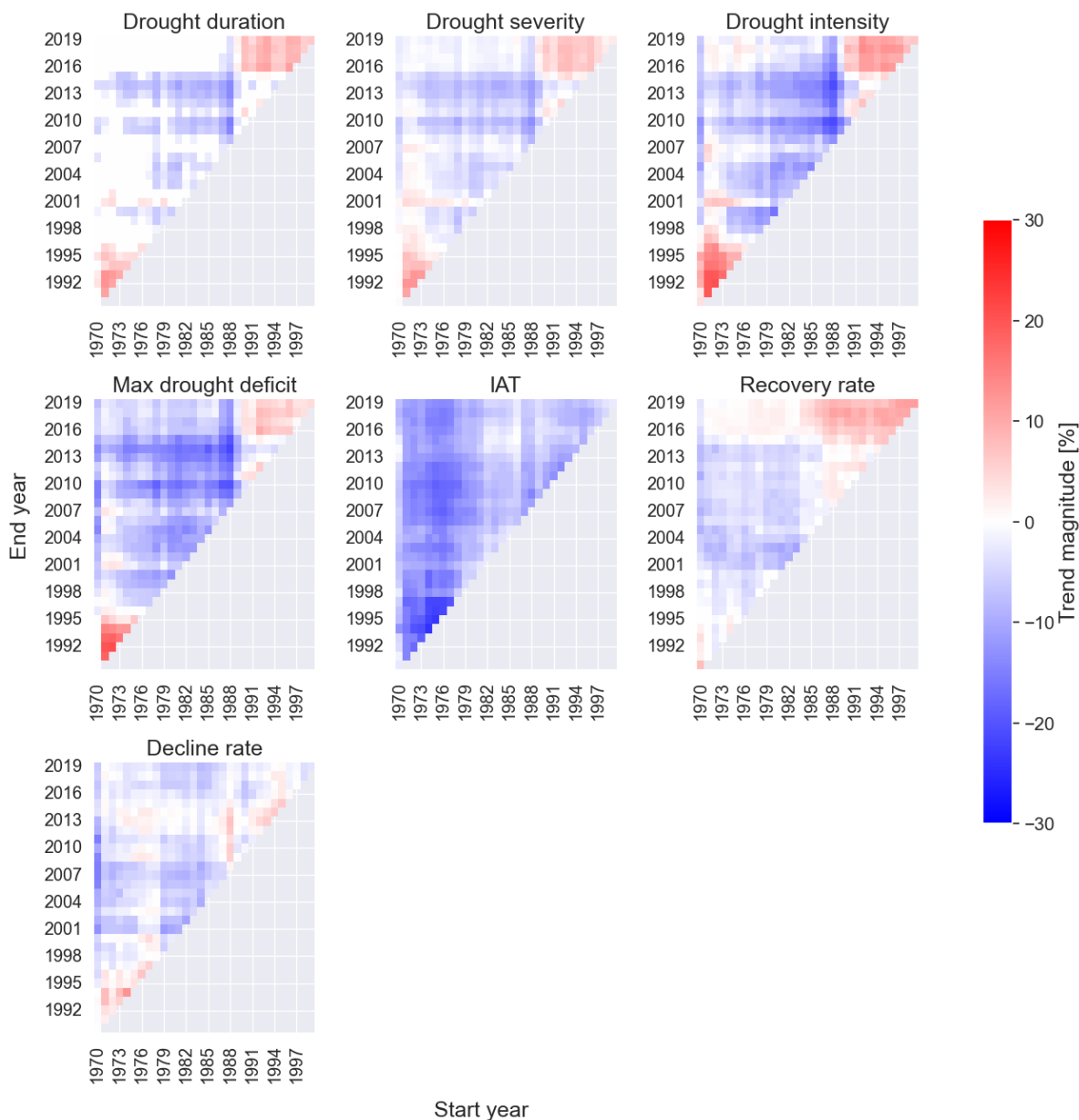


Figure A.4: Multi-temporal analysis of fall median trends for each drought characteristic, expressed as a percentage, across all river basins. The heatmap illustrates the magnitude of trends for all combinations of time periods between 1970-2019, with the x-axis representing the start year and the y-axis representing the end year of each time period. Red indicates increasing trends, while blue represents decreasing trends.

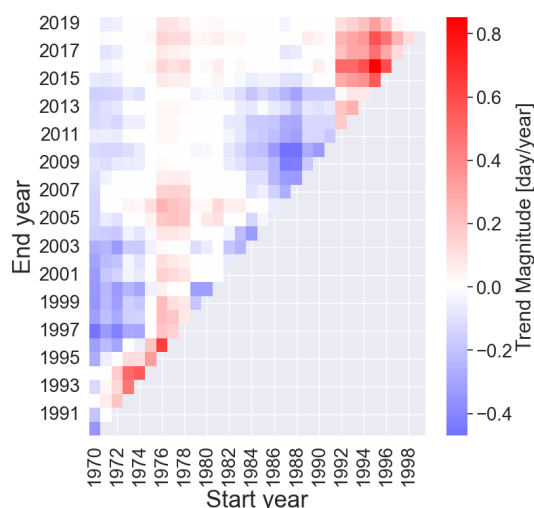


Figure A.5: Multi-temporal analysis of median trends in fall drought timing, expressed in day/year, across all river basins. The heatmap illustrates the magnitude of trends for all combinations of time periods between 1970-2019, with the x-axis representing the start year and the y-axis representing the end year of each time period. Red indicates droughts occurring later in the season, while blue represents droughts occurring earlier in the season.

All climatic classes except for classes 3 and 5 showed similar patterns as the overall fall trends. River basins of class 5, located in the south of Spain, experience overwhelmingly negative trend values for the drought severity, intensity and maximum deficit. The trends do not undergo the same shift from negative to positive trends around 1988, but are negative regardless of the selected time period with values reaching below -30%. The river basins corresponding to class 3, located in middle of Spain, experience the same patterns as class 5. Both the drought intensity and maximum deficit are overwhelmingly negative regardless of the time period. The drought severity also experiences an overall decreasing trend but undergoes less extreme changes with trend magnitudes ranging between 0-5%. The remaining drought characteristics do not deviate from the overall patterns for fall.

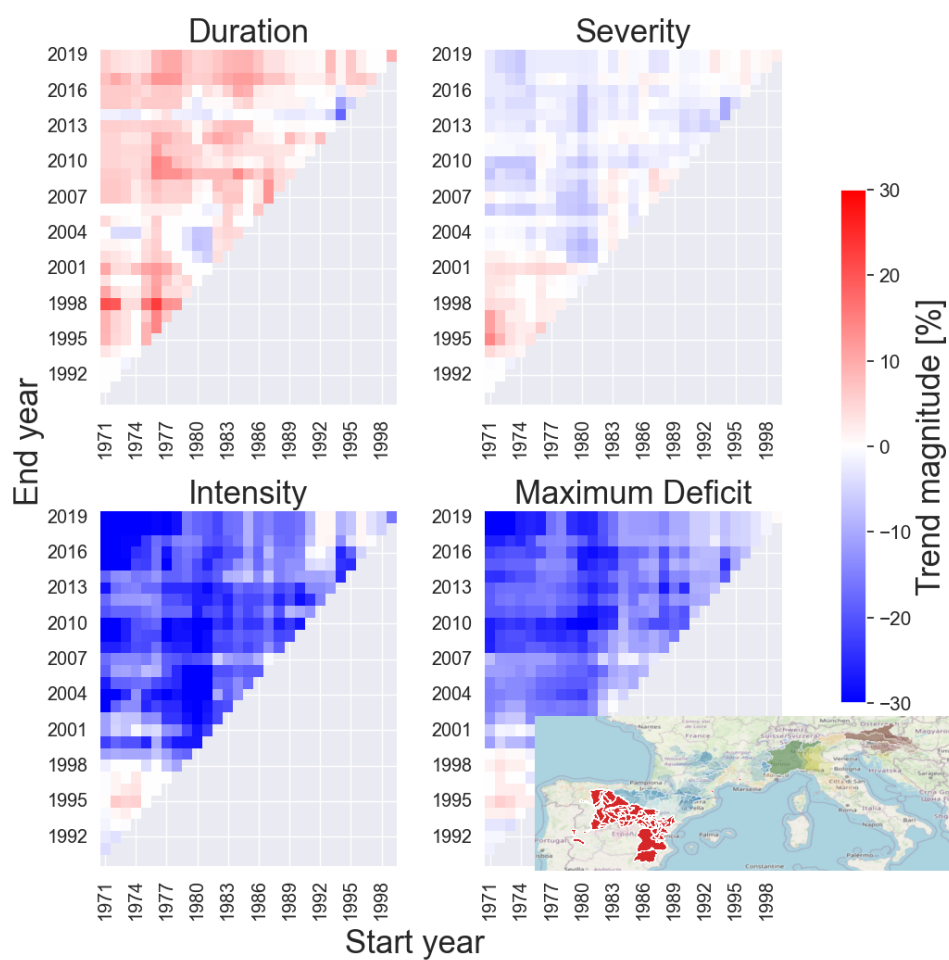


Figure A.6: Multi-temporal analysis of median trends, expressed as percentage, in fall drought characteristics (duration, severity, intensity and maximum deficit) for river basins of class 3. The heatmap illustrates the magnitude of trends for all combinations of time periods between 1970-2019, with the x-axis representing the start year and the y-axis representing the end year of each time period. Red indicates increasing trends, while blue represents decreasing trends.

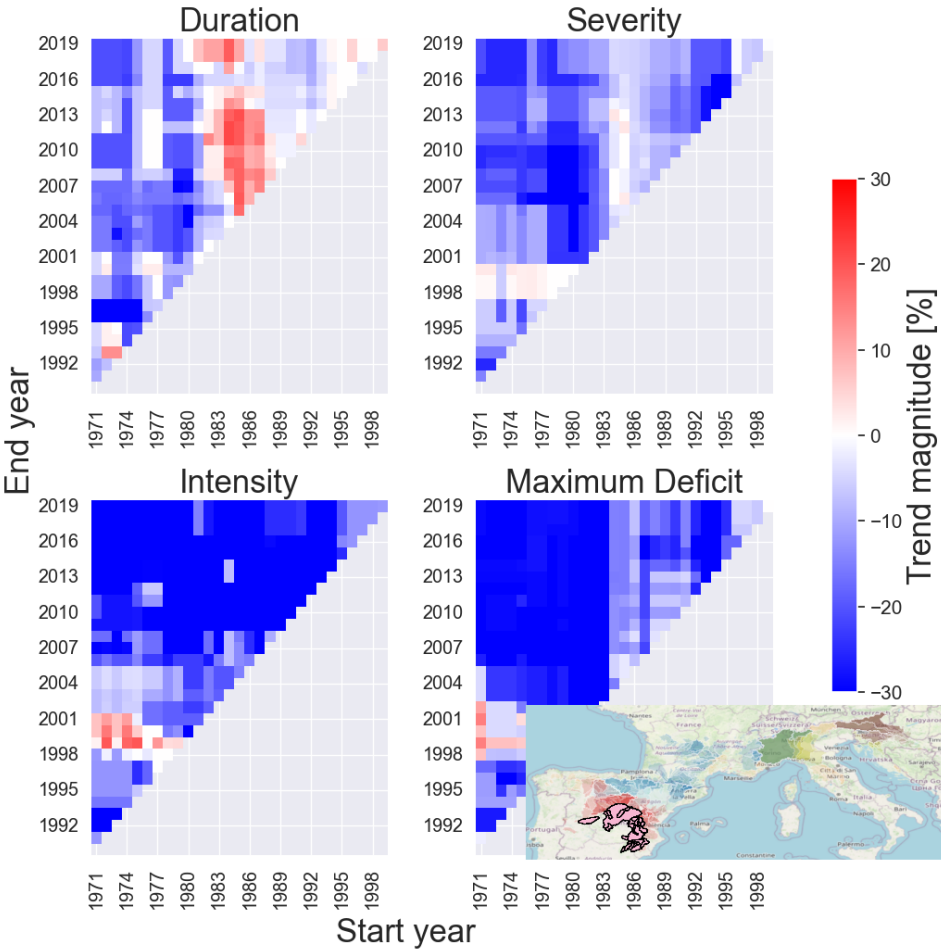


Figure A.7: Multi-temporal analysis of median trends, expressed as percentage, in fall drought characteristics (duration, severity, intensity and maximum deficit) for river basins of class 5. The heatmap illustrates the magnitude of trends for all combinations of time periods between 1970-2019, with the x-axis representing the start year and the y-axis representing the end year of each time period. Red indicates increasing trends, while blue represents decreasing trends.

B

Additional Figures

B.1. Trend Analysis

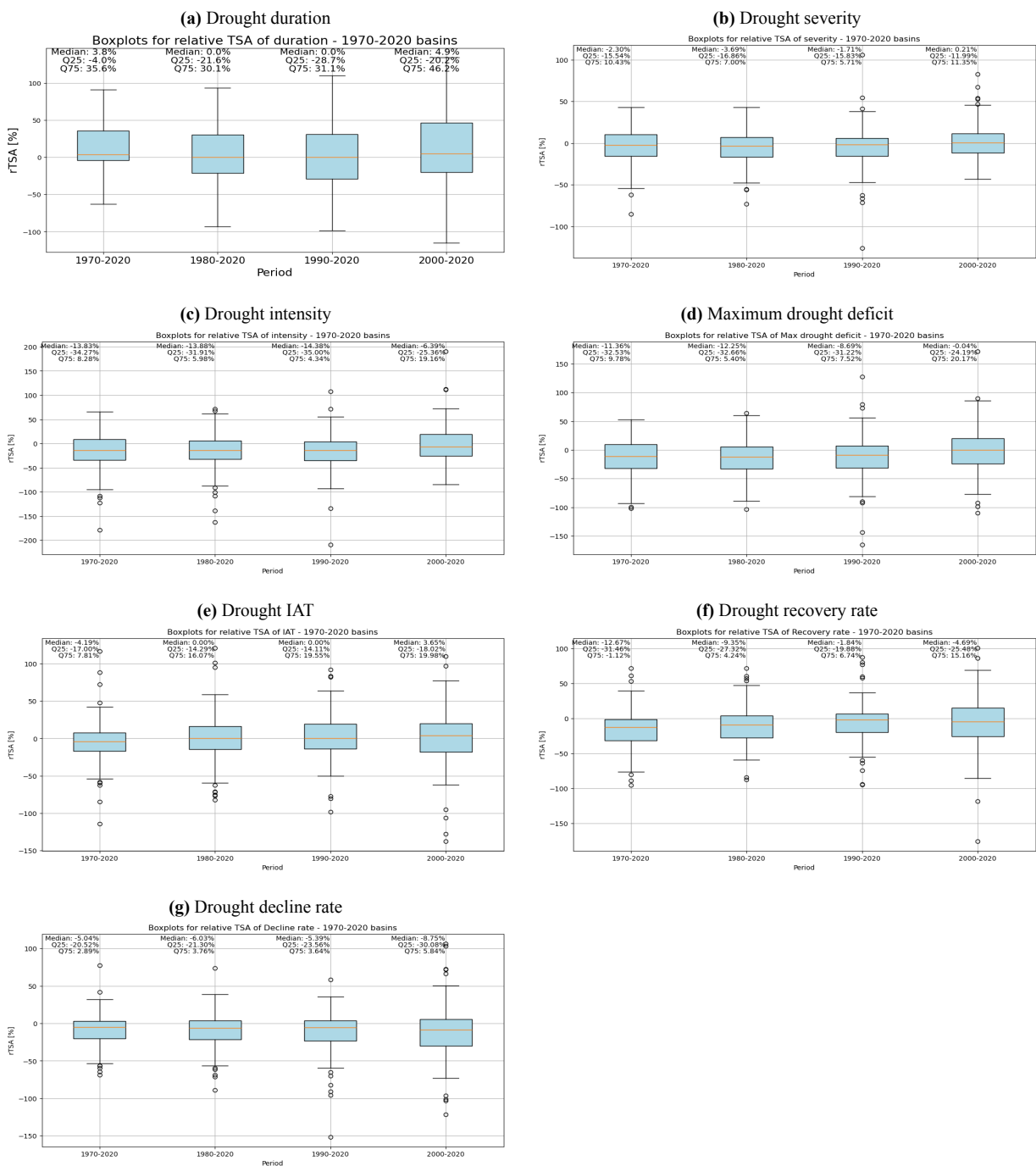


Figure B.1: Trend results for the basins with data in period 1. These were used as validation of the overall trends in the entire study area.

B.2. Multi-Temporal Analysis

B.2.1. Annual Trends

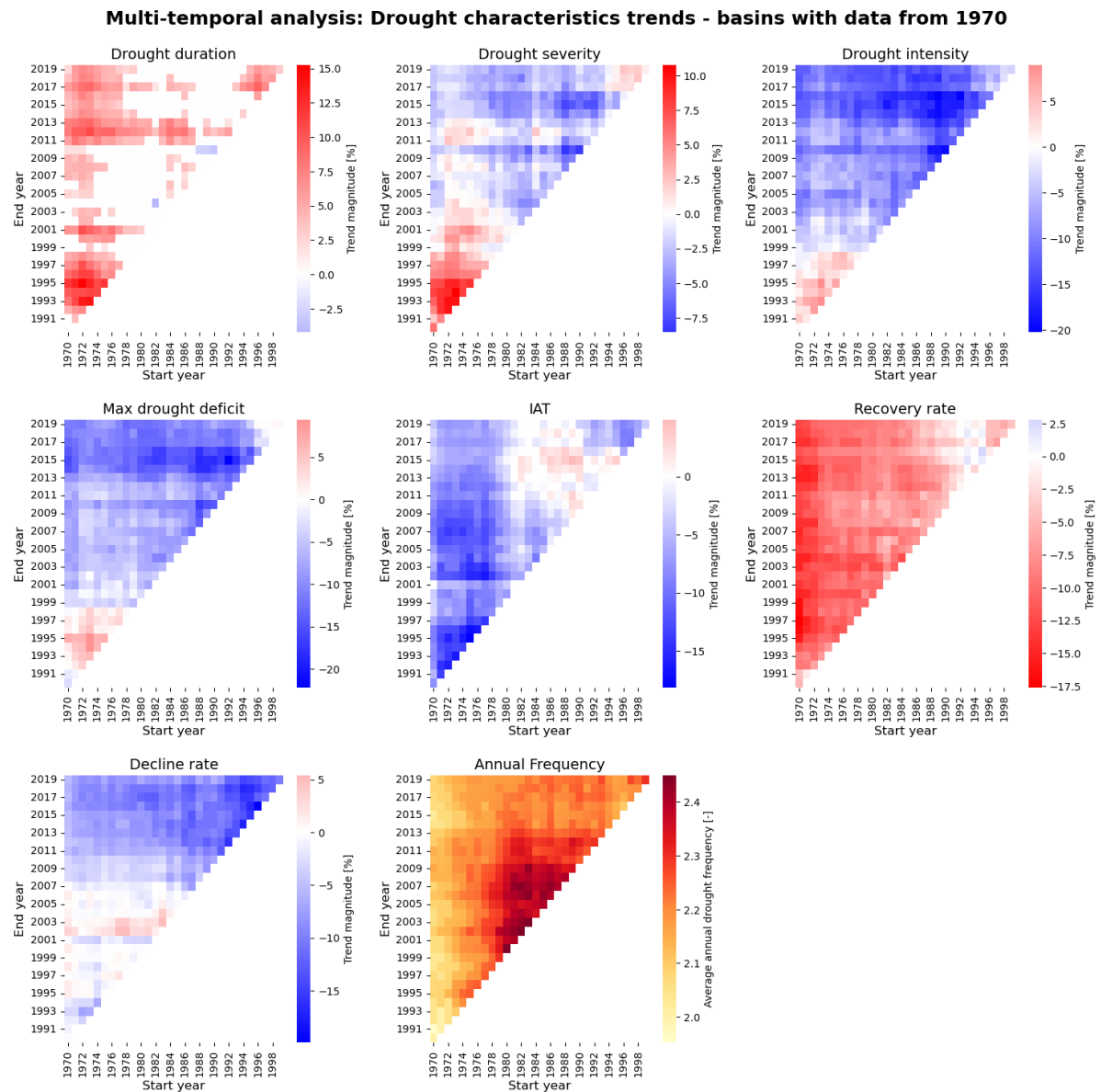


Figure B.2: Multi-temporal analysis of median trends, expressed as percentage, in annual drought characteristics for river basins of period 1 (1970-2019). The heatmap illustrates the magnitude of trends for all combinations of time periods between 1970-2019, with the x-axis representing the start year and the y-axis representing the end year of each time period. Warmer colors indicate increasing trends, while cooler colors represent decreasing trends.

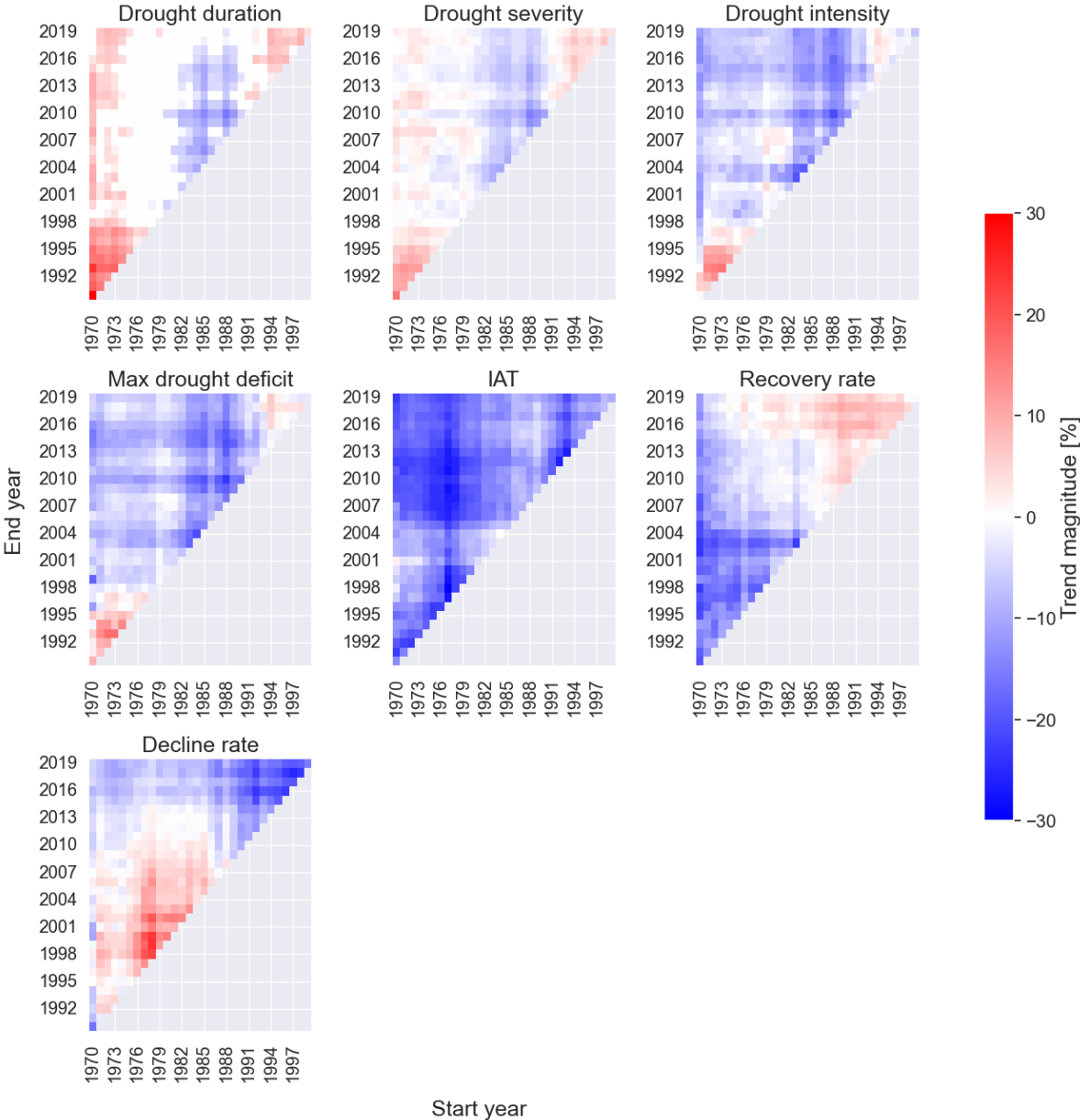


Figure B.3: Multi-temporal analysis of median trends, expressed as percentage, in annual drought characteristics for river basins of class 1. The heatmap illustrates the magnitude of trends for all combinations of time periods between 1970-2019, with the x-axis representing the start year and the y-axis representing the end year of each time period. Warmer colors indicate increasing trends, while cooler colors represent decreasing trends.

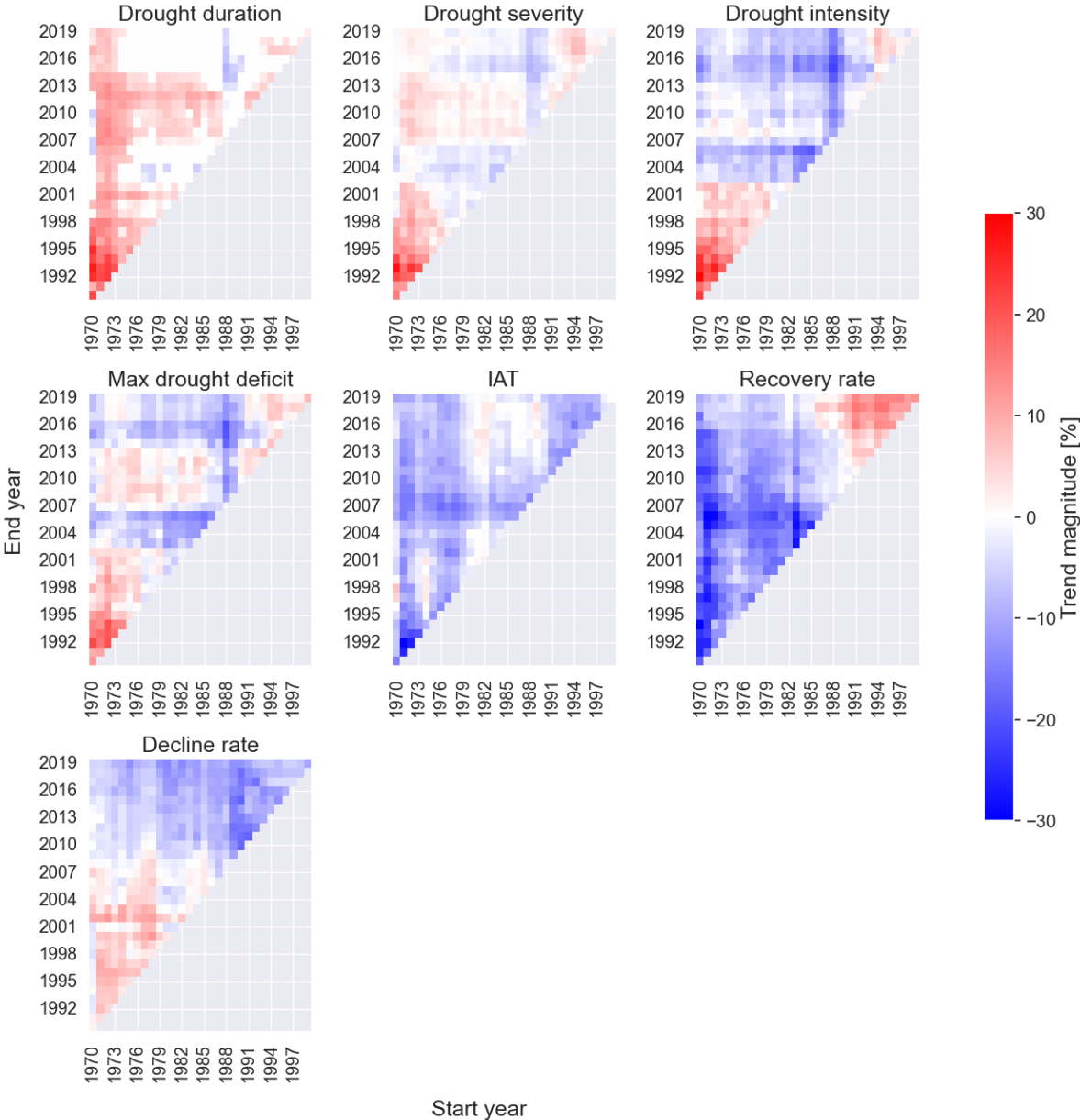


Figure B.4: Multi-temporal analysis of median trends, expressed as percentage, in annual drought characteristics for river basins of class 2. The heatmap illustrates the magnitude of trends for all combinations of time periods between 1970-2019, with the x-axis representing the start year and the y-axis representing the end year of each time period. Warmer colors indicate increasing trends, while cooler colors represent decreasing trends.

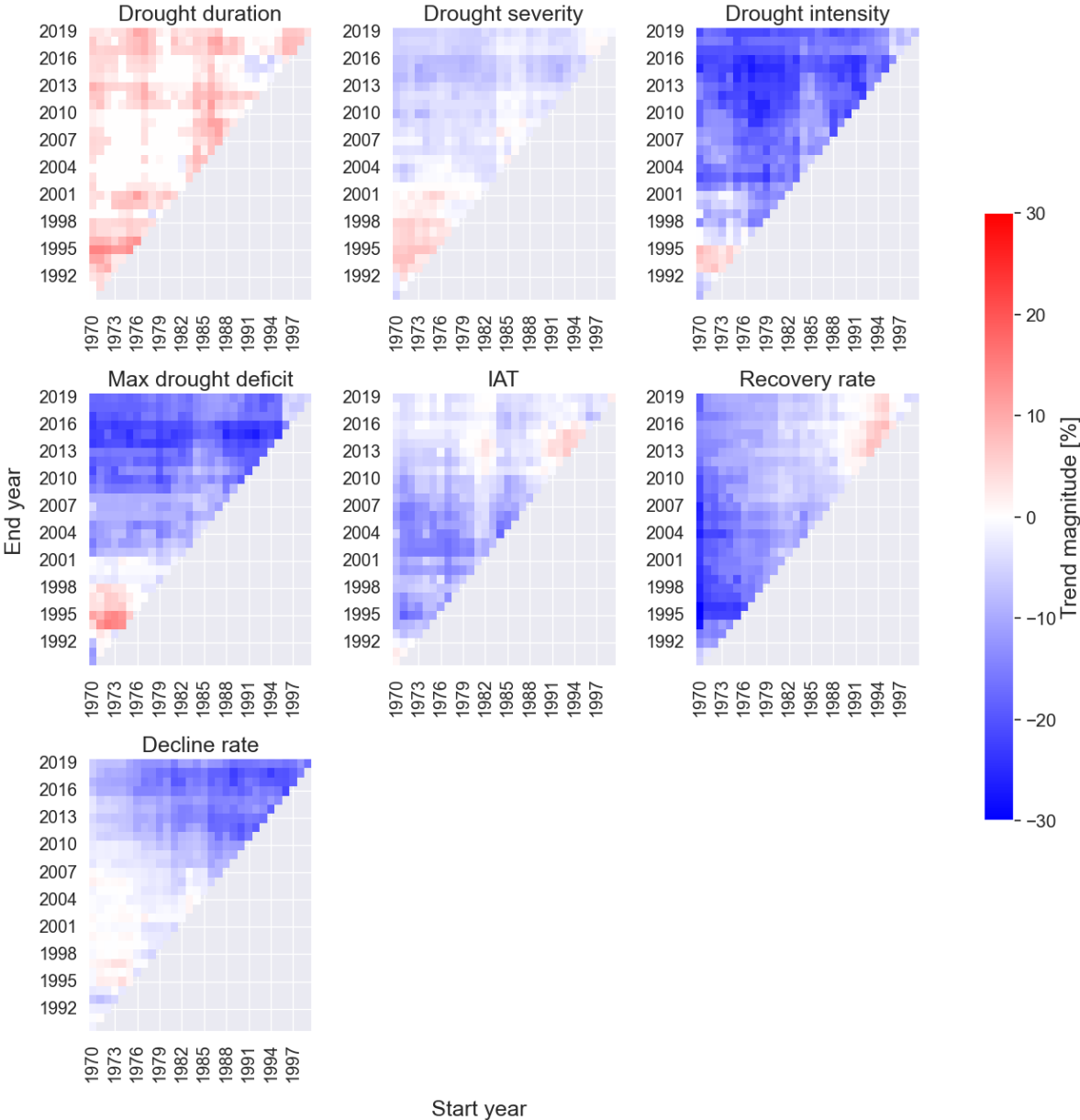


Figure B.5: Multi-temporal analysis of median trends, expressed as percentage, in annual drought characteristics for river basins of class 3. The heatmap illustrates the magnitude of trends for all combinations of time periods between 1970-2019, with the x-axis representing the start year and the y-axis representing the end year of each time period. Warmer colors indicate increasing trends, while cooler colors represent decreasing trends.

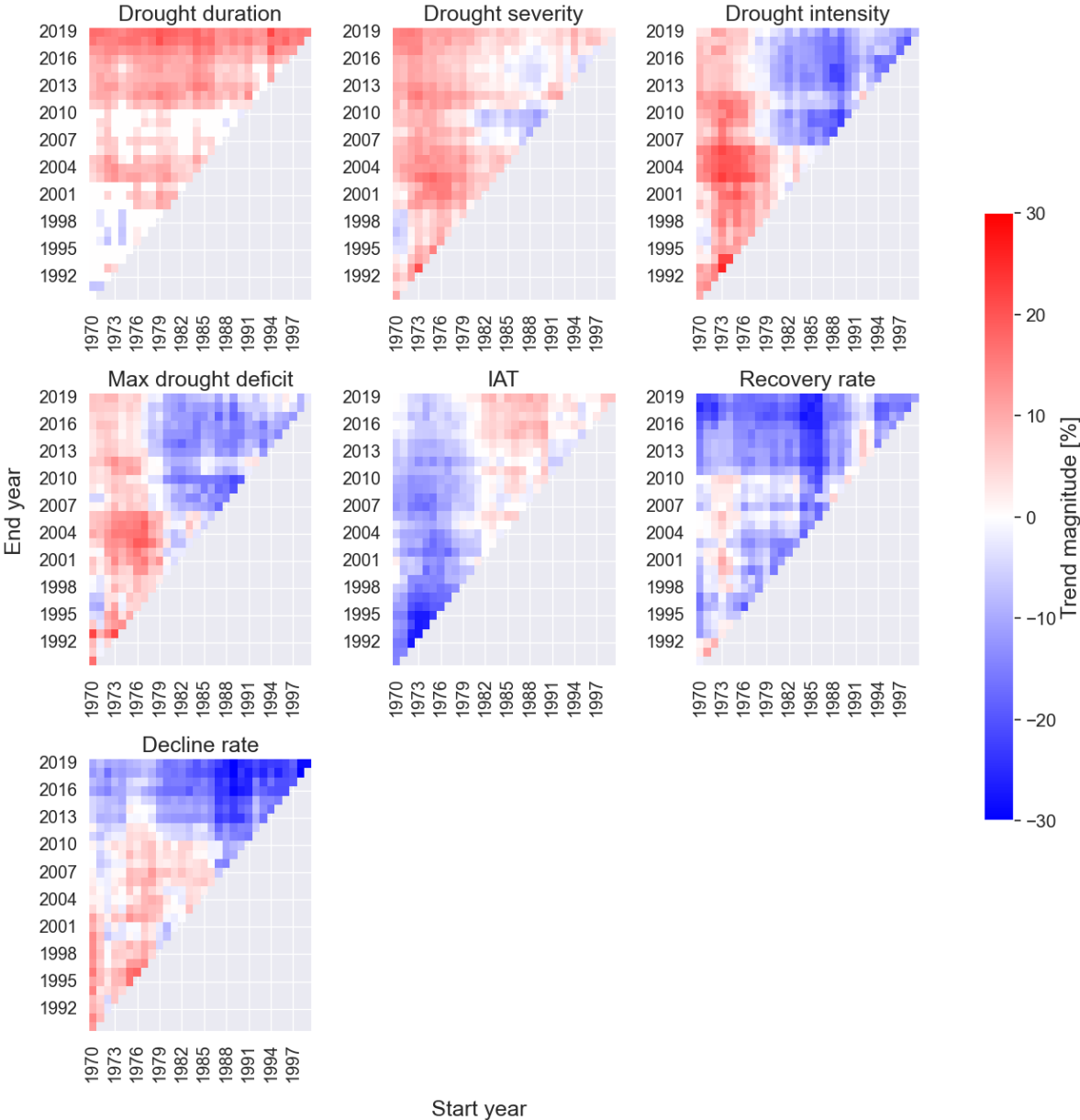


Figure B.6: Multi-temporal analysis of median trends, expressed as percentage, in annual drought characteristics for river basins of class 4. The heatmap illustrates the magnitude of trends for all combinations of time periods between 1970-2019, with the x-axis representing the start year and the y-axis representing the end year of each time period. Warmer colors indicate increasing trends, while cooler colors represent decreasing trends.

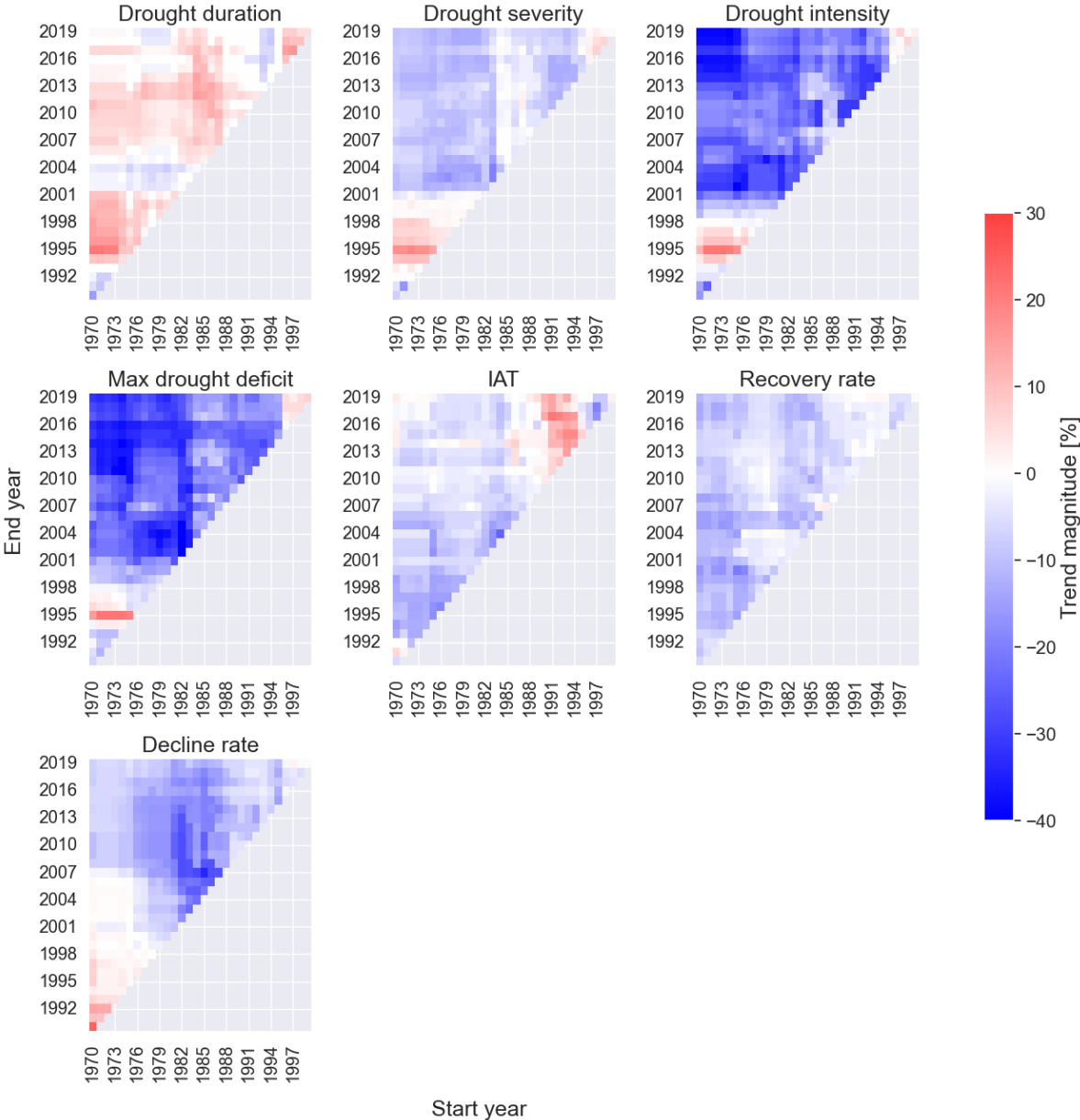


Figure B.7: Multi-temporal analysis of median trends, expressed as percentage, in annual drought characteristics for river basins of class 5. The heatmap illustrates the magnitude of trends for all combinations of time periods between 1970-2019, with the x-axis representing the start year and the y-axis representing the end year of each time period. Warmer colors indicate increasing trends, while cooler colors represent decreasing trends.

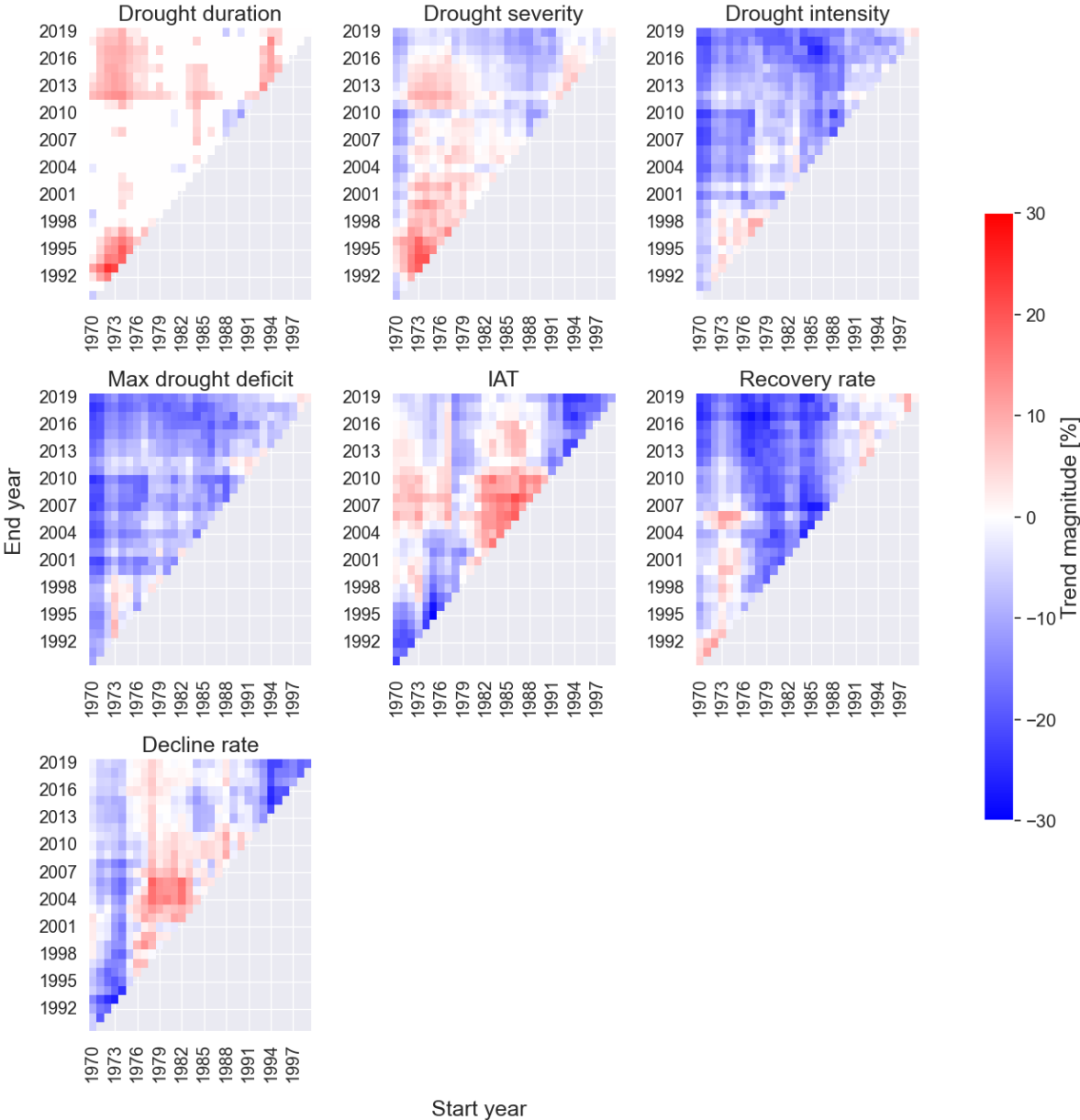


Figure B.8: Multi-temporal analysis of median trends, expressed as percentage, in annual drought characteristics for river basins of class 6. The heatmap illustrates the magnitude of trends for all combinations of time periods between 1970-2019, with the x-axis representing the start year and the y-axis representing the end year of each time period. Warmer colors indicate increasing trends, while cooler colors represent decreasing trends.

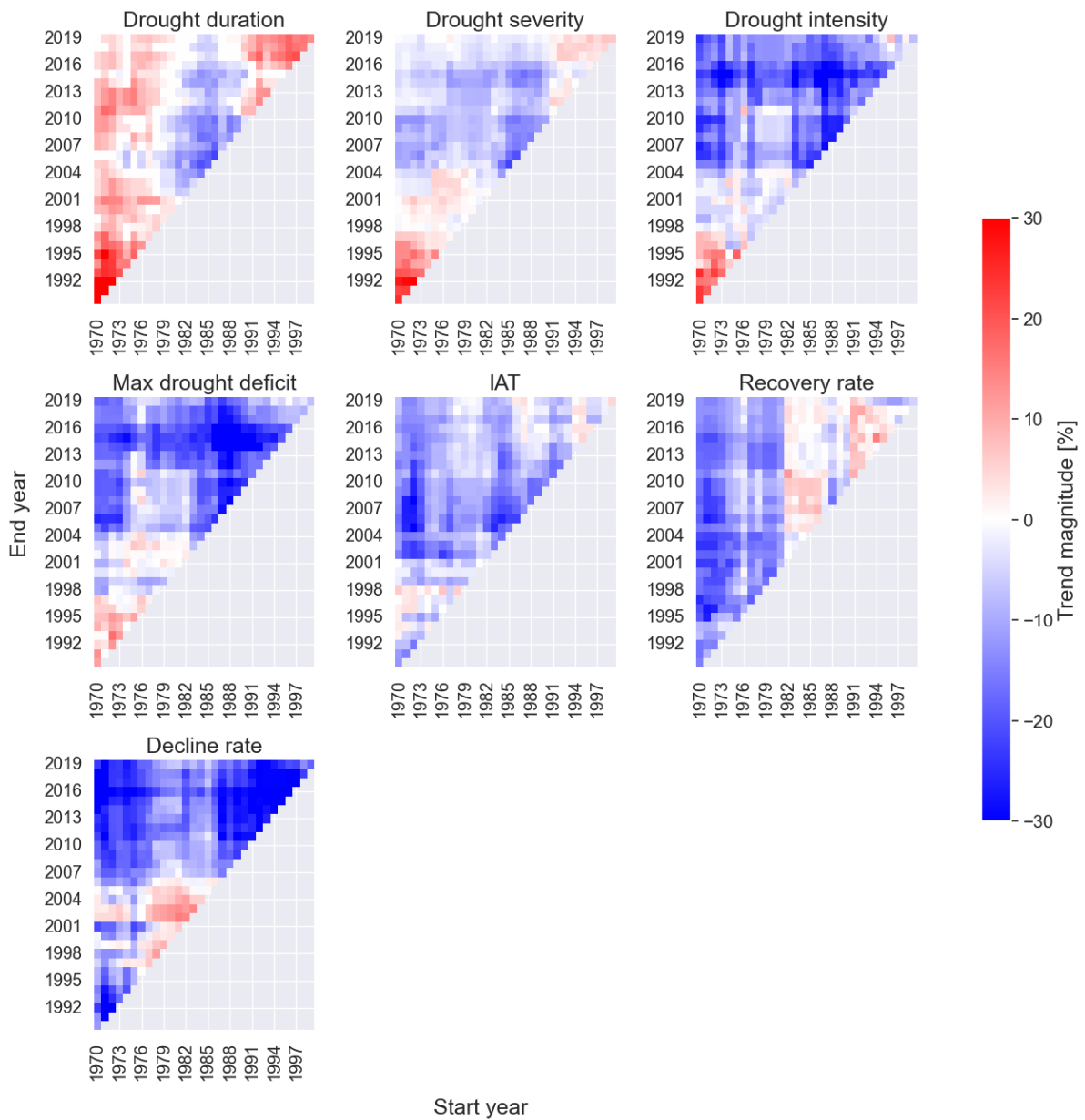


Figure B.9: Multi-temporal analysis of median trends, expressed as percentage, in annual drought characteristics for river basins of class 7. The heatmap illustrates the magnitude of trends for all combinations of time periods between 1970-2019, with the x-axis representing the start year and the y-axis representing the end year of each time period. Warmer colors indicate increasing trends, while cooler colors represent decreasing trends.

B.2.2. Annual-interval trends

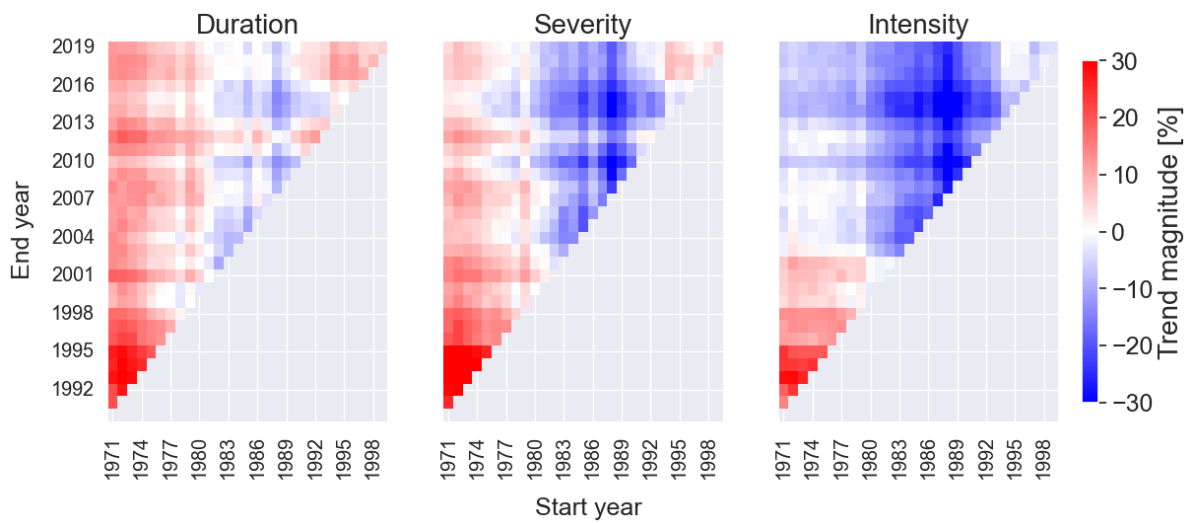


Figure B.10: Multi-temporal analysis of median trends, expressed as percentage, in mean annual drought characteristics for all river basins. The heatmap illustrates the magnitude of trends for all combinations of time periods between 1970-2019, with the x-axis representing the start year and the y-axis representing the end year of each time period. Warmer colors indicate increasing trends, while cooler colors represent decreasing trends.

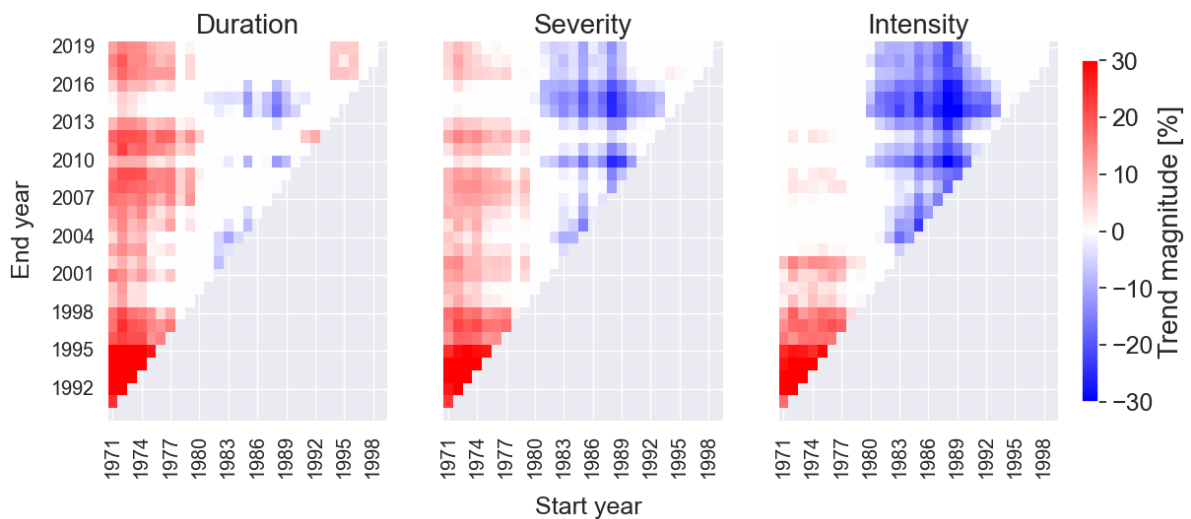


Figure B.11: Multi-temporal analysis of median trends, expressed as percentage, in mean annual drought characteristics for all river basins, including years with no drought events as a value of zero. The heatmap illustrates the magnitude of trends for all combinations of time periods between 1970-2019, with the x-axis representing the start year and the y-axis representing the end year of each time period. Warmer colors indicate increasing trends, while cooler colors represent decreasing trends.

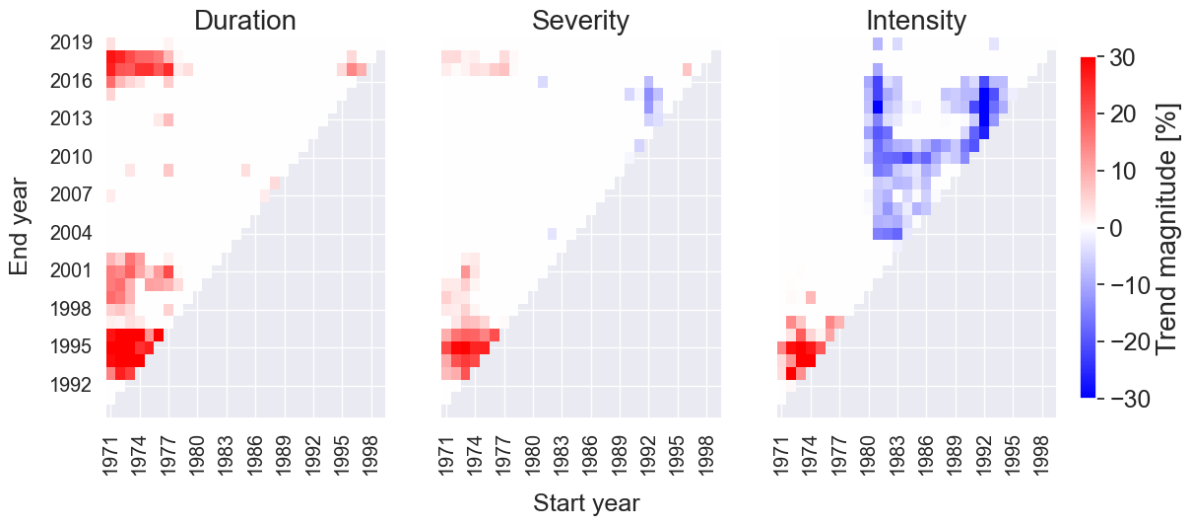


Figure B.12: Multi-temporal analysis of median trends, expressed as percentage, in mean annual drought characteristics for river basins of class 3, including years with no drought events as a value of zero. The heatmap illustrates the magnitude of trends for all combinations of time periods between 1970-2019, with the x-axis representing the start year and the y-axis representing the end year of each time period. Warmer colors indicate increasing trends, while cooler colors represent decreasing trends.

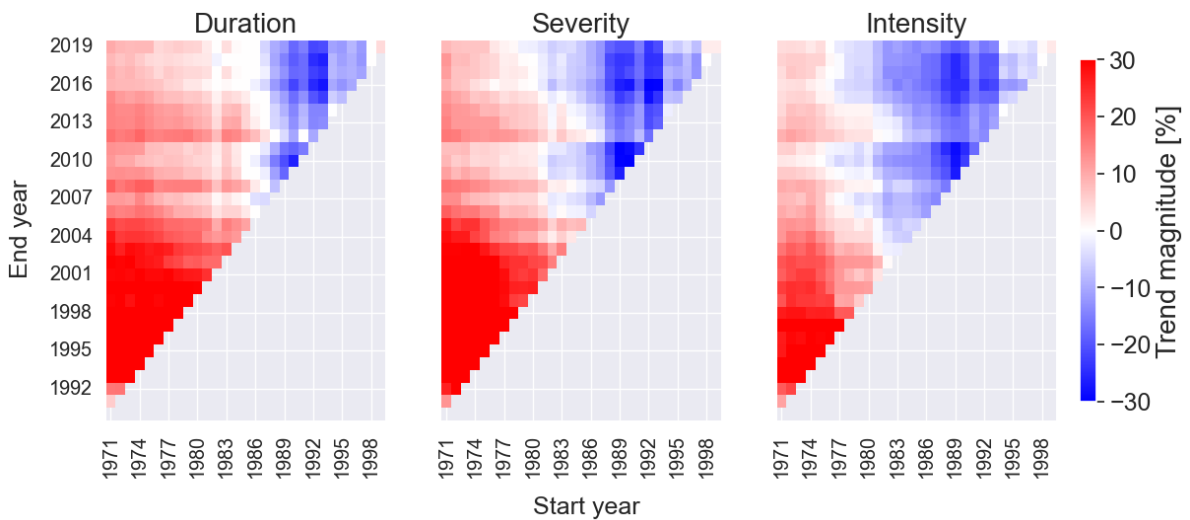


Figure B.13: Multi-temporal analysis of median trends, expressed as percentage, in mean winter drought characteristics for all river basins. The heatmap illustrates the magnitude of trends for all combinations of time periods between 1970-2019, with the x-axis representing the start year and the y-axis representing the end year of each time period. Warmer colors indicate increasing trends, while cooler colors represent decreasing trends.

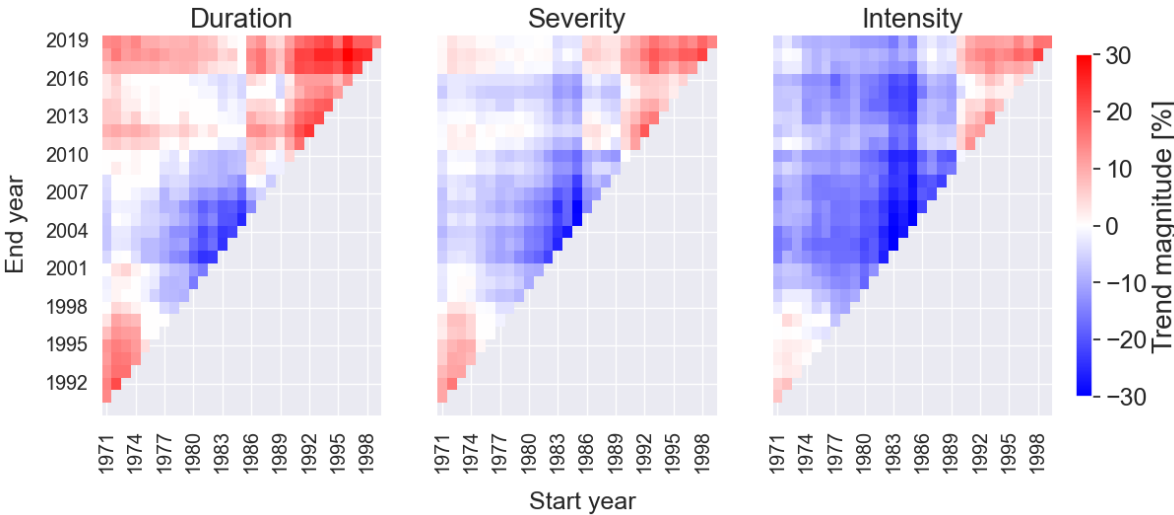
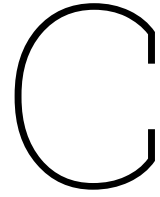


Figure B.14: Multi-temporal analysis of median trends, expressed as percentage, in mean summer drought characteristics for all river basins. The heatmap illustrates the magnitude of trends for all combinations of time periods between 1970-2019, with the x-axis representing the start year and the y-axis representing the end year of each time period. Warmer colors indicate increasing trends, while cooler colors represent decreasing trends.



Additional Tables

Table C.1: Number of river basins for each country in each study period

Time period	Spain	France	Italy	Slovenia	Croatia	Total
<i>Period 1</i>	106	0	0	0	35	141
<i>Period 2</i>	149	110	10	0	45	315
<i>Period 3</i>	150	129	14	11	56	361
<i>Period 4</i>	150	143	22	14	56	386

Table C.2: Climate classification boundaries based on Berghuijs and Woods (2016)'s framework.

Class boundary conditions	L	M	H	Units
\bar{P}	< 361	361 - 671	> 671	[mm/y]
\bar{T}	< 1.6	1.6 - 21.9	> 21.9	[°C]
δ_p	< 0.47	0.47 - 0.82	> 0.82	[-]
Δ_T	< 9.1	9.1 - 17.0	> 17.0	[°C]
s_d	< -0.12	-0.12 - 0.12	> 0.12	[year]